Cornwall FLOW Accelerator

WP4 – D1.1. WIND TURBINE BLADES DESIGN AND MANUFACTURING, CURRENT STATE-OF-THE ART LITERATURE REVIEW

Document Title		WP4 – D1.1. WIND TURBINE BLADES DESIGN AND MANUFACTURING, CURRENT STATE-OF-THE ART LITERATURE REVIEW	
Document Reference		CFAR-OC-020-31032022	
Date of Issue		31/03/2022	
Author		Oliver Nixon-Pearson, Peter Greaves, Dimitrios Mamalis, Lewis Stevenson	
Revision History	Date	Amended by	Reviewed By
First Draft	-		
Second Draft	-		
First Issue	31/03/2022		Mark Forrest
Rev 1			
Rev 2			
Rev 3			
Rev 4			

HM Government

European Union
European Regional Development Fund

CORNWALL FLOW ACCELERATOR

WP4 INNOVATION IN LOW CARBON DESIGN AND MANUFACTURABILITY – Wind Turbine Blades Design and Manufacturing, current State-of-the Art Literature Review

Authors: Oliver Nixon-Pearson, Peter Greaves, Dimitrios Mamalis, Lewis Stevenson.

Date: 31/03/2022

In partnership with:

DOCUMENT HISTORY

Revision	Date	Prepared by	Checked by	Approved by	Revision history
1	31/03/2022	Oliver Nixon-Pearson, Peter Greaves, Dimitrios Mamalis, Lewis Stevenson.	Mark Forrest	Mohammed Almoghayer	1

CONTENTS

1 Project Overview and Aims

The southwest offshore floating wind accelerator project aims to develop the south-west of England into an area which can lead in offshore floating wind turbine technology. The project aims to spearhead the industrialisation of floating offshore wind in the entire southwest region of England and will bring to the fore, Cornwall and Plymouth's world-renowned excellence in offshore renewables research and business. It will accelerate the region's readiness for large scale Floating Offshore Wind (FLOW) and will fast-track development of the region's capacity to build-out large-scale wind farms in the Celtic Sea from 2025 onwards. This puts the Southwest in a position to make a large contribution to the UK's offshore wind energy targets through development of a new floating wind industry that can create thousands of jobs with huge export potential. Also, this will generate many more R&D opportunities in the area. Floating platforms can access stronger winds in deeper waters than conventional fixed land-based turbines. The Celtic Sea (an area off the coast of Cornwall and West Wales to the south of Ireland) has some of the most prominent wind resources in Europe. By 2025, the region will be prepared for the first 500 MW FLOW farms. The Celtic Sea Zone will deploy up to 120 GW, of which up to 86.4 GW will be in the Southwest zone. The South-West region has world-leading floating wind research expertise and RD&I test facilities. The project will utilise these for new product and service development for industrial partners, building clear routes to market as well as de-risking initial investment. The region has an excellent port infrastructure, and this will be developed to fully exploit this growth market. The focus of this report aims to define the current state-of-the-art in offshore Horizontal Axis Wind Turbine (HAWT) blade manufacture, and to determine the best opportunities for low-carbon and environmentally friendly cost-effective processes for potential port development for blade production. Also, future blade concepts will be explored to determine feasibility.

The main scope of this project is for production of the next generation of turbine blades with reduced environmental impact, and with the next generation of recyclable materials in the manufacturing process. This report contains a desk-based benchmarking study into the opportunities for low carbon manufacture of turbine blades, which outlines the current state-of-the-art and explores some concepts for the immediate future of blade manufacturing in the Southwest of England. This will include a Lifecycle Assessment (LCA) of an up-to-date reference blade design which will act as the reference point for future estimates on costing and LCA.

2 Introduction

One of the major priorities in global energy policy is the development and growth of alternative energy, reducing the emission of greenhouse gases. Despite the higher initial costs, wind technology results in advantages for economies by generating local added value, and by creating a positive effect on the market through reducing electricity prices as the cost of wind is zero, and the producers of wind energy can provide cheaper energy than other forms of energy such as fossil fuel technologies [1]. This has forced manufacturers of wind turbines to develop higher capacity machines which significantly increase its electrical output, this has led to the trend of ever-increasing blade lengths. Wind turbine blade efficiency has focussed on increasing rated power of the system through larger blade lengths, obtaining greater energy from lower intensity winds, increasing the effectiveness of turbine integration and connection to the electrical grid infrastructure. Thus, turbine manufacturers need to increase their manufacturing capacity of production plants in each of the processes, along with maintaining efficiency factors, reducing costs, maintaining worker safety without impeding the final part quality.

Increased automation technologies in wind turbine manufacturing requires substantial initial financial investment (CAPEX), however it can simplify the manufacturing process, and ensure repeatability and reliability. Increased reliability and cost optimisation are key priorities for improving the competitiveness of the wind energy sector in an increasingly competitive international market.

The blades are the wind turbine component which captures the energy of the wind and transfers it into mechanical power (via torque) and subsequently into electricity generation. However, Betz law states that no more than 59.3% of the wind's kinetic energy can be captured [2]. The blades are thus a critical part of the overall performance, reliability, and cost of a wind turbine system. Longer blades increase the energy yield of a turbine system since they sweep a greater area. However, the blade needs to contain more material and has greater strength which comes at increased costs.

Current blade manufacture is labour intensive. However there have been technical advances associated with improving the facilitation of tasks and improving overall quality of the parts. Major areas which allow for systems development for blade manufacturing include:

- Automation of processes to shorten cycle times, improve accuracy, and repeatability.
- The use of high-performance materials with the support through collaborative relationships with key strategic suppliers.
- Precise novel tooling and assembly systems.
- Vacuum infusion technology advances, including low viscosity thermoplastic infusion, creating lighter stronger and more advanced composite structures.
- Metrology advancements, including inspection, testing and quality assurance tools. employing the most capable laser, ultrasonic, and other technologies to validate, verify, and ensure accuracy and quality to blades.

These advances in the manufacturing process, allow increasing the complexity of the geometry of the blade, enabling the exploitation the internal aerodynamic properties, and significantly increase energy output of the blades.

3   Review of Current Blade Manufacturing Processes

3.1   Manufacturing Process Overview

When blade manufacturing was in its early infancy in terms of development, wind turbine blades were often produced via wet-hand layup in open moulds. Glass fibres were laid down in the mould, where the resin reinforcement was applied by brush or paint rollers for impregnation. The shells were then adhesively bonded together with the spars. The disadvantages of wet-layup open moulding are high labour costs, relatively low part quality, environmental and health and safety issues [3]. Filament winding has been explored for use in wind turbine blades in the 1970s and again more recently for ENERCONs original segmented blade which used traditional construction, resin infused halves bonded together for the 44m outer segment and filament winding of an epoxy-impregnated glass fibre fabric for the 12m long inner segment. The automated wrapping process reduces material cost and production time whilst giving a higher-quality product due to the reliability and repeatability of the process, as well as better working ergonomics. What is produced through filament winding is the inner segment load-bearing core or blank. In a second step, a prefabricated aerodynamic trailing edge with ENERCON's signature integrated spoiler becomes bonded onto the blank to complete the inner blade segment [4].
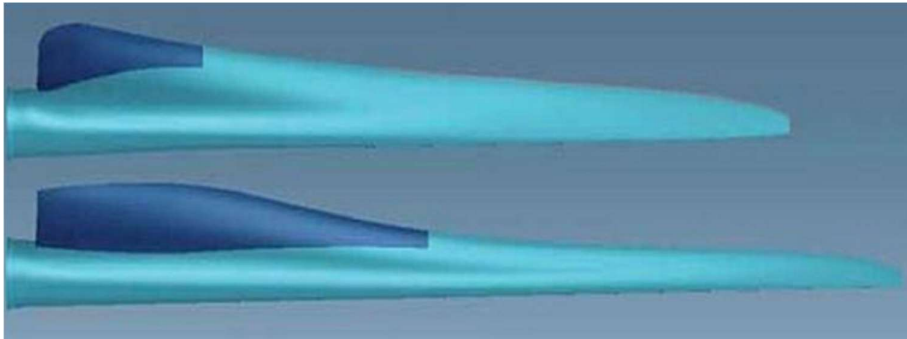
Figure 1. ENERCON Filament Wound Blade Concept [4].

Improvements in the manufacture of wind blades came about with the introduction of vacuum technologies, to include vacuum infusion and prepregs (preimpregnated fibres). Prepregs are tapes of fibres which are pre-impregnated with the uncured resin material system by the manufacturer. These are then subsequently laid up in stacks in which the sequence depends on the load case of the laminate and is then cured either in an oven or an autoclave. Prepregs tend to be used by Vestas. Whereas the other manufacturers typically use vacuum infusion of dry preforms. The most widely used technology to date in the production of wind turbine blades is vacuum infusion, especially for producing longer blades.

The blades are some of the most critical components of the turbine – not only are they key to improving energy production, but catastrophic failure of a blade can lead to failure of other parts of the turbine structure and so it is to be avoided at all costs. Extreme wind or operational loads can cause sudden damage, whilst regular loads over their service life can cause material degradation and fatigue, which can limit their effectiveness and safety.

The blade structure and materials define the types of manufacturing processes which can be used, so they are summarised here. The primary function of a wind turbine blade is to capture the wind and transfer the load to the shaft, which creates a bending moment on the root bearing, and a torque on the main shaft. A blade is a large cantilever beam, which is primarily loaded in two ways. Flapwise, or out-of-plane, bending loads arise from aerodynamic forces and edgewise, or in-plane, bending arises from the blade self-weight.

The blade structure is designed to resist these loads whilst having a form which is as close as possible to the optimal aerodynamic shape. The suction side and pressure side shells are large aerodynamic panels designed to "catch the wind" and transfer the loads to the spar caps. They are comprised of a lightweight core material sandwiched between triaxial fabric.

They are typically moulded in two "blade shell" tools, and adhesively bonded to each other along their leading and trailing edge, and to the spar caps in the middle. Shell skins are lightweight triaxial glass fibre skins, of low thickness; they therefore need to be stabilised using a lightweight core (typically made from balsa wood or PVC foam) to prevent buckling. The shells are bonded together at the leading and trailing edges.
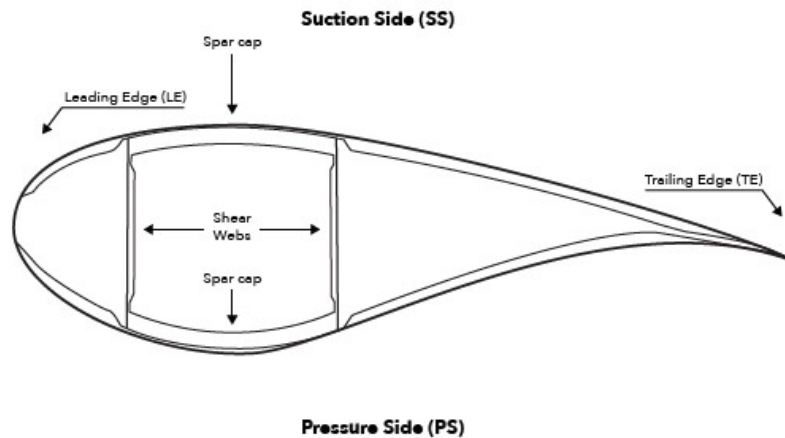
Figure 2. Terminology and parts of a wind turbine blade

The spar caps are generally made of uniaxial material (often carbon fibre instead of glass for modern offshore blades) placed at the thickest part of the section to maximise their contribution to the bending stiffness. The shear webs transfer the forces between the spar caps and are typically made of biaxial glass fabric with a core material (again made from balsa wood or PVC foam).

The entire exterior of the blade is coated in a general coating to protect the composite structure from the environmental conditions of UV degradation and moisture ingress and provide an aerodynamic surface. This general coating is typically a gelcoat applied in mould but can also be a filler and topcoat. Additionally, on the leading edge close to the tip a rain erosion resistant material is applied. This blade manufacturing process is shown in figure 3.
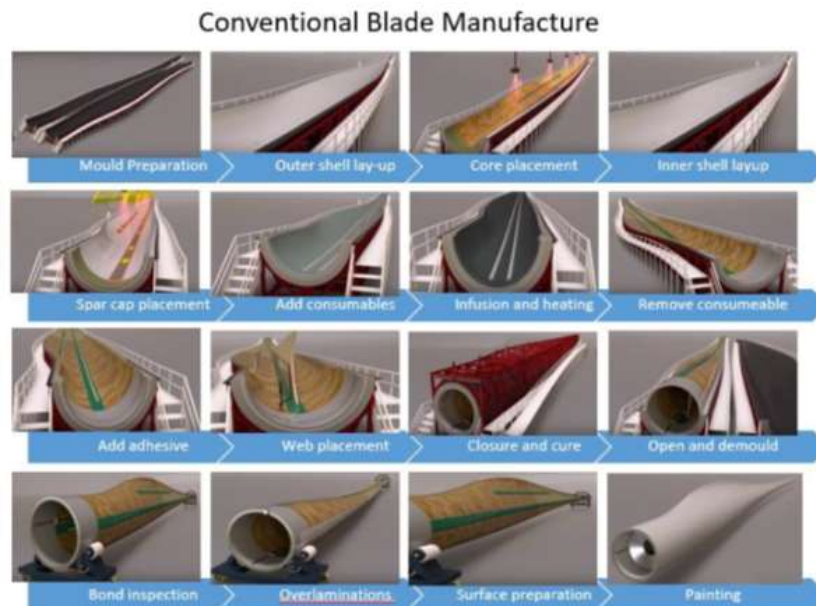
Figure 3 - Conventional blade manufacturing process comparison [5]

3.2 Review of Current Blade Manufacturing and State-of-the-Art

This section aims to provide more detail into the traditional manufacturing methods outlined in section 3.1. This also sets the scene for the introduction of the conventional blade factory descriptions given in later sections.

3.2.1 Vacuum Infusion

In resin infusion, dry fibres are placed into closed moulds and sealed, in which resin is injected into the cavity or bag under pressure. After the resin has filled the areas between the fibres, the component is then cured. Resin infusion can be separated into two techniques: Resin Transfer Moulding (RTM) where the liquid resin saturates the dry fibre preform in a closed mould, and Vacuum Assisted Resin transfer moulding (VARTM), which uses a partial vacuum line as the driving force which draws the resin in to the dry preform until complete saturation is achieved. The vacuum also provides the compaction required during processing. Currently VARTM is the most common manufacturing method for wind turbine rotor blades. It is a variation of RTM in which the top part of the mould tool is replaced with a vacuum bag, and thus a single sided mould is required. Layers of dry preform are laid up along the length of the blade in the moulds along with any sandwich core components. This step is crucial in the manufacture of wind blades since both production time and part quality are dependent on this process. crucial in the manufacture of wind blades since both production time and part quality are dependent on this injection process.

In the early stages of the manufacturing process, the reinforcement or preform is prepared which includes the cutting of the glass fibre mats, and the preparation of the core kit, usually made from either balsa wood or foam for the sandwich areas in the blade. The next step involves the draping of the preforms into the one-sided mould, where the reinforcement in stacked and positioned in the mould. The process is referred to as draping, where during the insertion into the mould, the material deforms and adapts to the curvature of the mould. Draping is important as it can introduce wrinkling in the preform which can give rise to defects resulting in knockdown in mechanical performance. Also, the manufacturing properties can be altered due to draping. During layup pre-cut material is used however in some instances material can be drawn directly from the roll to minimise layup time and to minimise the material distortion. Once the layup of core, and preform is complete, the preparation for injection begins by applying a peel ply, which allows separation of the inlet tubes and bagging material after infusion and cure. Once the peel ply is laid down, the resin inlets are positioned, the resin inlets are connected to resin containers. Many resin inlets are applied throughout the mould. In theory, this manufacturing method is well suited for upscaling as more resin inlets and vacuum points can be added, however thicker stacks of preform can result in a greater propensity for wrinkling defect formation as well as plies being more able to move or slip relative to one another. The thickness is higher at the root section and can be 50-60 cm in the consolidated state [3].The lastly the preform is covered by a foil and then the vacuum bag and then made airtight using tacky tape (sealant tapes) around the perimeter. The air is then evacuated from the bag causing the preform to compress, to allow the pull of full vacuum. After the pull of full vacuum has been achieved, the resin inlets are sequentially opened allowing wet-out infusion and saturation of the preforms. Once full saturation of the preforms has occurred, then the part is left for several hours for the curing process to fully finish. The last step in the cycle involves the demoulding of the part after curing [6]. The infusion process is usually more cost effective than the prepreg process, however the prepreg process has less variable mechanical properties than for infusion.

3.3 Current State-of-the-Art in Mould Production

3.3.1 Mould Design

Since wind turbine blades are manufactured separately in mould halves, where the pressure and suction sides are fabricated separately by layup of dry reinforcement and core materials followed by infusion. The two halves are glued together. The adhesive is applied to the inner face of the lower blade half prior to the lowering of the upper half onto it. A complete tool pair for a 40 m blade can weigh around 17 tonnes, where a quarter of this weight arises from the composite materials, and the rest from the rigid steel frames which provide the backing structure. In reality mould sets rarely turn out 300-400 blades that they're specified for, since newer designs render them obsolete prior to reaching this point and then need to be replaced with new tooling [7]. Metallic moulds, which are still sometimes used by manufacturers of smaller blades tend to be regarded as heavy and unwieldy for the size requirements for larger blades. Composite materials are much lighter and have lower thermal conductivities, they therefore have a similar coefficient of thermal expansion to that of the blade shell materials, whereas metallic blade moulds can cause manufacturing difficulties due to locked in thermal stresses and other manufacturing effects such as spring in, due to the mismatch between the thermal expansion coefficients of the mould and the blade materials. Composite moulds can be made to the desired shape with less material wastage. They can be perceived as being less durable than for metallic moulds, however blade design improvements and obsolescence would mean that this isn't a significant consideration.

Early blade mould pairs were produced with their steel backing frames, microprocessor-controlled heating systems, three-phase electrical systems, resin distribution systems, and vacuum solutions, and thus set the scene for the future where the provision of complete integrated blade manufacturing systems with full associated services became the norm. Earlier mould designs using the complete integrated approach were developed and fabricated by Solent Composite Systems (SCS) which began as a division within SP Systems (now Gurit), to produce 23 and 31 m blades in the first instance.

A typical blade is fabricated by moulding the two half shells in a mould pair, where spar caps, web stiffeners along with ribs and other details are installed into one of the mould shell halves with the application of adhesive to the exposed bonding edges. The other half shell is turned and lowered onto the first which still lies inside the mould tool where the adhesive is left to cure sealing the two halves along with all its internal details together. Thus, these types of blades require a main set of mould tools for the shells as well as other moulds needed to produce the web stiffeners and spar caps. Blade edges and root ends may also require further moulds. The moulds are normally supplied as a complete solution along with all the relevant associated services.

Each of the mould halves are backed with a mild steel frame. For longer relatively narrow moulds, the steel backing structure is required for the mould to maintain the shapes which are getting ever more complicated due to twisting and pre-bending. For a typical 40 m mould truss structure should not sag greater than 5-10 mm when supported at the ends. At the hinge and lifting points where higher loads are expected, extra strength and reinforcements are required. The structures are usually designed to be close to the ground to minimise the height and reduce the access requirements during blade production.

The mould pairs are linked via hinges and open in a clamshell fashion where the last part of the travel of the upper tool is vertically downwards towards the contact points to preserve the glue lines until the point of contact. Each half mould is fabricated out of resin infused glass and or carbon fibres and

are situated within the tool corresponding to the parts of the blade where these materials are to be moulded. Both woven and non-woven (zero crimp) fabrics are used rather than stitched. Resins are usually epoxy, however vinyl esters can also be suitable. Some blade producers require the use of gel-coat as the inner mould surface whilst others don't. Gelcoats can be seen to provide a better surface finish with reduced voids, however others see this as another interface which introduces another point of failure.

3.3.2 Plug Fabrication

The traditional method of blade production requires the generation of a plug, which is a full-scale impression of the blade and is one of the most time and labour-intensive processes in the production of wind blades. The process of fabricating the plug for the main shell begins with the polystyrene foam blank which is used for the manufacture of the plug. Plugs are made in sections which vary between 6-8 m long and can be joined and separated when required and provides a certain degree of flexibility where changes are made to the blade design.

The blank is first machined to the approximate final shape of the blade, then either a tooling paste or over-lamination is applied. Over lamination can be more cost effective however difficulties can arise when accurate tolerances on the surface profile are required. Then the next step is to machine the outer surface using CNC milling to fine tolerances required for the blade. Where required the milled surface is sanded and polished to a flawless surface finish. The plug is then ready for the application of the release system and lamination of the mould. Fabric layers are applied to the plug where the heating elements are included on the back surface along with layers of metal foil to distribute the heat effectively.

Uncured blade laminate properties vary considerably throughout the length. At the root section large exotherms can be expected during the in-mould cure cycle, and at the ends towards the tip this effect is negligeable. For this reason, moulds contain zonal heating facilitated by an electrical heating system. Rarely, and in only a few cases, where a higher production rate is required, active cooling is used as well as heating in which a hot/cold air system is used.

At a later stage in the mould laminate preparation, the resin feed lines are laid into the mould system. Locators which ensure that the mould halves line up correctly upon closure are then added in, likewise for vacuum lines and compressed air pipes. Tooling systems tend to be plug and play and supplied as a complete solution by the respective tooling manufacturers.

Then the entire laminate is vacuum bagged and prepared for infusion where the infused tool has an initial cure which is slightly above ambient temperature for 24 hours, followed by a post cure at around 50-60C. Having relatively low and long curing temperatures prevents internal stresses due to thermal gradients. The next step is the lamination of stiffeners to the blade mould, this enables the loads to be evenly distributed in blade demoulding operations. The final stage is the addition of the steel backing structure. A full mould set also usually requires tooling for the spar caps and webs. Spar caps can have complex tooling and are also laminated onto plugs.

3.3.3 IntegralBlade Process

In 2012, a feature was published which showed the latest iteration of a turbine blade at the time [8]. The blade was 75 m long and had been manufactured using Siemens patented technology which involves glass reinforced epoxy infused and manufactured in one piece using a half-shell closed mould

process. Siemens claimed that if the blade were to be produced using traditional technologies, it would be 25-50% heavier. The glass reinforcement is laid out in a patented mould arrangement with a closed-out mould and an expanding inner mould with the epoxy resin injected under a vacuum with the blade curing at elevated temperatures in the mould. The blade is removed from the outer mould whilst the inner mould collapses away and is pulled out from it resulting in a seamless blade without bonded joints required to bond the halves of the blade together. It was stated that the process is efficient in terms of labour requirements and also only requires one mould set for the manufacturing cycle. Having no adhesive joints means that in addition to weight savings, there is likely to be performance enhancement due to fewer weak points which can act as crack initiation zones or water ingress points.

3.3.4 Innoblade Process

The Innoblade process refers to the modular design developed by Gamesa back in 2013 for the G128 onshore turbine which was the first segmented composite blade, and the longest for the onshore market at the time. The aims were to increase power generation and ease the installation costs associated with longer blade designs since power generation and costs are the major drivers in wind turbine development (figure 4). If no change is design, materials, and method of construction are assumed, then power generated increases with blade length in proportion to the square of the rotor diameter, however blade mass increases with the cube of the blade length. This results in longer heavier blades which drastically increase transport costs along with installation costs (where transport costs can be more of a logistical issue when designing for onshore blades), with the additional mass cascading the cost increases throughout the rest of the system. The turbine generates up to 5 MW power whilst maintaining blade weight and installation costs.
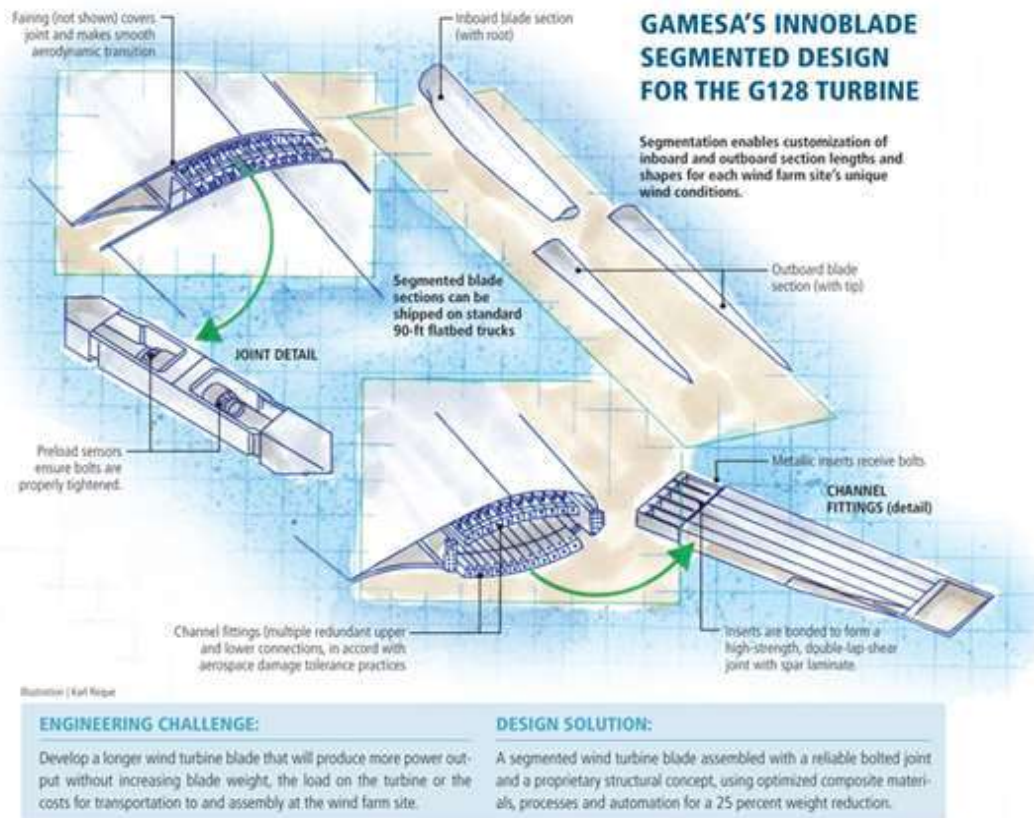
Figure 4. Gamesa's Innoblade Segmented Blade Design

A segmented wind turbine blade was designed and patented by Gamesa in 2005, where it was refined to increase the annual energy production, noise, and costs, as part of the large turbine design project UpWind. A 42.5m/139-ft in-house blade design was evaluated with different aerodynamic profiles for efficient energy production, including aeroelastic analysis. Gamesa developed a trade-off matrix for various blade joint alternatives, studied their effects on modal shapes and pursued integration of a control system that would mitigate the increased load of longer blades.

In parallel to UpWind, more than 150 Gamesa engineers completed the majority of the G128 turbine development in-house, obtaining multiple patents for the innovations required. There were strict limits on weight and aerodynamic performance, so a joint needed to be developed without modifying the blade aerodynamics. Starting with an optimized geometry supplied by Gamesa's aerodynamics department, the team began prototyping a composite blade structure.

Gamesa tackled the issue of where to divide the blade for the joint through many iterations between the aerodynamics and the structures teams. The UpWind research project had shown that there were many possible joint positions without impacting the modal shapes and natural frequencies of the blade. However, Gamesa had chosen to locate the join around the middle of the blade such that the lengths were minimised for transport. The original concept evolved into a modular system featuring root (inner sections), and tip sections in customisable lengths to suit the specific wind conditions of each installation. For onshore turbines especially, blade-specific trucks are required for rotors beyond 100 m. These trucks are more expensive, for larger rotos many ships, trucks and shipping terminals may not be able to handle blade sizes over 100 m at all. Therefore, the Innoblade design enables easier transport to onshore windfarms in more remote locations.

With a basic configuration established, Gamesa still faced challenges in how the joint would be manufactured at the site. The design allowed for considerable mass in the joint of the blade. Typically for mechanical joints similar technologies could be used to existing root connections, however the UpWind findings indicated that that channel fittings had performed better than spar lugs or T-bolts.

These channel fittings were bonded to a pultruded carbon fibre-reinforced profile embedded within the spar cap laminates, which widened at the joint to accommodate multiple fittings. A simple bolted joint between each set of two fittings connected the two blade segments.

The final G128 design used many insert and bolt connections within the joint and it was designed according to aircraft industry regulations for fail-safe performance and damage tolerance. Thus, if any inserts failed, the remaining must work. There are around 15 connections in the upper section of the joint and likewise for the lower section.

The inserts are metallic and are bonded into the blade laminate in such a way that they form a double lap-shear joint, long considered by the aerospace industry to be one of the strongest options for adhesively bonded joints in composite structures. The bonded metallic inserts enable the two segments to be bolted together, with all the loads in the blade transferred through the joint. It is thus highly critical that the joint functions as if the blade were a single part, therefore an automated process was used for assembly. To ensure quality and repeatability, the process used automation for the manufacture and installation of the inserts. The time required for blade assembly is approximately four hours. After the bolts are secured, a metallic external fairing covers and protects the joint's metal components and provides a smooth transition across the joint. Gamesa claims its joint and assembly design achieves low cost by enabling transport via standard equipment used for 2-MW turbines. The joint adds ~10 percent to blade cost, but the increase is more than offset by transport savings [9].

A trade-off between many parameters was required for a successful joint design. Both metallic and composite joint designs were considered. Gamesa used prepreg in the spar laminate around the join area to reach the required load capacity. The G128 used both glass and carbon fibre with balsa core, the weight of the completed blade was around 15 tonnes. They considered many materials and combined many different processes including resin infusion, prepreg technologies, and pultrusion. Gamesa completed a large test and validation programme for the G128 segmented blade to include 600 different component tests at 100 of the certified labs across the US, Japan and Europe, with 190 functional tests which were carried out at the Wind Turbine Test Laboratory (LEA, Navarra Spain). There were a total of around 300,000 hours of test and validation engineering with the G128 currently long into their service lives.

3.4 Review of Current Blade Structures and Materials

This section aims to discuss the materials used in the wind turbine blade, here we limit the scope to the fibre reinforcements, resins, and the sandwich structures. The various properties of these will influence the manufacturing process. A literature review of the current state of the art, and other materials that have potential for use in wind turbine blades will be carried out. This will consider near term material changes (e.g., projects exploring thermoplastics. This review will also include current and emerging adhesives that could meet the performance requirements for novel turbine blades.

3.4.1 Fibres

Typically both glass and carbon fibres are used in the manufacture of blades, and can be used as a prepreg (where resin has already been infused into the fibres upon material production), or via dry layup of fibres followed by an infusion process. The composite stiffness is typically determined by the stiffness of the fibres. The principle reinforcement used in the manufacture of wind turbine blades is E-glass (a borosilicate glass, or also known as Electric glass due to the high electrical resistance). By increasing the volume content of the fibres, the mechanical properties increase in proportion. However beyond around 65% fibre volume fraction, there is a greater propensity for dry areas to be more prominent which can negatively affect the fatigue performance [10]. There have been efforts to determine whether improvements can be made to the strength of fibres. Typically E-glass (Electrical) is used in the case of wind turbine blades. However the higher strength fibres show promising prospects when it comes to composite material improvements however they are more seldom used in parctice in wind blade applications. Such fibres include S-glass ('S' means Strength) and R-glass (where 'R' stands for Reinforcement) where the glass fibres have undergone modifications for strength and temperature resistance, and also basalt and aramid fibres. S-glass shows around 40% improvement in tensile and flexural strengths, with around a 10-20% improvement in compressive strength and flexural modulus [1]. However S-glass is much more expensive than traditional E-glass, with S2-glass developed as a commercial iteration of S-glass. Both S- and S2-glass have the same composition, however the major differences are the fibre sizing (fibre surface treatment) and the material certification [3]. S2-glass is approximately $20/kg whereas for E-glass it is approximately $2-3/kg, therefore around 10 times more expensive.

Therefore in the context of substantially improving turbine blade life from 25 to 40 years it may make financial sense to incorporate superior materials if repair costs are reduced over the course of its useful life, thus cost calculations must take into consideration the likely numbers of repairs. Carbon fibres have higher stiffness and lower density than glass, thus allowing for stiffer, lighter blades. However carbon fibres are more expensive than glass, have lower impact strength, lower damage tolerance, and are relatively sensitive to fibre defects (misalignment and wrinkling) leading to knockdowns in

mechanical performance. Carbon fibres tend to be used in the spar caps of large blades produced by Vestas and Siemens Gamesa.

Another alternative is the use of Basalt fibres. Basalt tends to have applications in thermal insulation, for example in car exhausts, however in addition to its thermal properties the combination of strength, impact resistance, and chemical inertness make it an attractive candidate for composite applications. Basalt fibres are have around 30% greater strength, 15-20% greater stiffness, and have around 8-10% less weight than for standard E-glass [3]. A preliminary study by the Aachen Center for Integrative Lightweight Construction and the Institut für Textiltechnik der RWTH (Aachen, Germany), have shown a 35% greater specific energy absorption capacity of a basalt hybrid yarn woven fabric (HYWF) with polyamide 6 resin compared to glass HYWF/polyamide 6, and 17 percent higher compared to carbon HYWF/polyamide 6 [11]. Basalt bridges the cost and performance gap between glass and carbon fibres. The appeal of basalts recyclability, combined with its good mechanical properties should afford it many market opportunities, however basalt fibre producers need to determine reliable sources with consistent composition and properties. The main parameter affecting the material performance is the chemical composition, so finding a reliably consistent source of basalt is important as well as the standardisation of properties for mass production.

3.4.2 Matrices

Composites in the wind blade industry commonly utilise thermosets in the form of epoxies, vinylesters and polyesters. However thermoplastics are used less frequently. Thermoset based composites represent a greater market share for reinforced polymers materials. The main advantages of thermosets are the potential for room temperature curing, and lower viscosity required for infusion of longer blades. DSM Composites Resins (Switzerland), have shown that it is feasible to use unsaturated polyester resins in the production of blades greater than 45 m length, due to faster cycle times and improved energy efficiency in manufacture. They state that their newly developed polyesters are able to meet the durability requirements needed for large blades [3].

Thermoplastics are a potentially interesting alternative to the thermosetting matrix systems. The main disadvantages of these are the higher processing temperatures and hence the greater energy consumption required, and the greater viscosities which give rise to difficulties in producing parts greater than around 2m length and 5 mm thickness. Generally the melt viscosity of thermoplastic matrices is of the order of 10^2-10^3 Pa s, whereas thermosets, when used to infuse dry preforms using their contituent monomers, have viscosities of around 0.1-10 Pa s making infusion much easier than in the case for thermoplastics. However the major advantage of using thermoplastics is that the melting temperature is lower than that of the temperature by which decomposition occurs. This means that components fabricated from thermoplastics can be reshaped when melted. While the fracture toughness of thermoplastics is greater than that of thermosets, the fatigue behaviour is generally not as good with either carbon and glass fibres [12]. However one of the advantages of thermoplastics is the larger strains to failure.

The manufacture of wind turbine blades has been traditionally based on thermoset matrices such as epoxies, however thermoplastics could offer recyclability along with other advantages. Thermoplastics can be deformed when heated and so can be easily repaired or reworked whereas thermosets remain rigid. As a result thermoplastics are more easilty recycled for other uses. Since blade manufacturing accounts for a significant quantity of composite material this recyclability and reformability will be beneficial. Thermoplastics can also remove some of the barriers associated with cure cycle delays since

their polymer chains do not cross link and so don't require long cure cycles, however an exception would be for the themoplastic Elium resin produced by Arkema. Parts may also be co-consolidated or joined by heating. Reinforced thermoplastics can have greater strength to weight compared to thermosets, and so can be a useful strategy for reduction in weight. Thermoplastics typically have good strength and stiffness to weight, along with generous elongation at failure. Thermoplastics may also have greater weatherability and hence improved resistance to rain compared with thermosets. Thermoplastics can have better crack resistance due to the cracking being more ductile than for thermosets. However thermoplastics have poorer fatigue performance compared with thermosets due to the poorer interfacial bonding between fibre and matrix. The standard coupling agents used to improve the interface between carbon and glass fibres with the matrix tend to also not work as well with thermoplastics. Likewise for hot-wet properties of thermoplastics, which can further reduce the bond strength between fibres and matrix. Thermoplastics tend to be highly viscous which can render them unsuitable for infusion of large amounts of dry preform as is necessary for wind blade production. However there are new thermoplastic materials coming to the fore which tackles this issue. A research team at the University of Delft in the Netherlands have investigated a polyamide resin system which has an infusion viscosity of 10 mPa s which is an order of manitude lower than that of thermoset resins. They used anionic PA6 (APA6) which polymerises similarly to a thermoset whist retaining some of the properties of a thermoplastic, making it able to conserve mechanical properties and higher fatigue resistance owing to the degree of polymerisation.

Other examples of novel matrices used in wind blades are Polyurethanes (PU). Covestro has produced polyurethane raw materials for use when producing wind blades for the Chinese market, which is the worlds largest. This represents the first commercial use of PU resins in the blades market. Their claims are that PU shows better mechanical properties than epoxies with the advantage of improved blade production efficiency and hence infusion speed. According to Covestro, the polyurethane infusion resin was developed to meet the ever increasing demand for longer blade designs. Turbine blades are typically made out of glass reinforced epoxy produced by vacuum infusion. The successful use of polyurethane resin for manufacturing large-scale rotor blades for wind turbines suggests that the material itself features superior mechanical properties and good fatigue damage resistance as well as benefits arising from the production process in the factory, hence a faster curing process with more favourable processing parameters which can deliver shorter blade production cycles with lower energy expenditure [13].

Other material improvements have been made in the field of nano-materials. More generally there has been effort in determining the improvements of composite materials using nano-reinforcements in the matrix. Minor amounts around the level of 0.5% by weight of carbon nanotubes or clay can potentially increase the fatigue, shear or compressive strength as well as fracture toughness of composites between 30-80% [14]. Loos et al. have investigated the effect of carbon nanotubes on the fatigue performance of composites, and had shown that the inclusion of a small amount of carbon nanotubes increased the fatigue life of the epoxy matrix in the high cycle low amplitude fatigue regime by 1550% under tension-tension fatigue loads with the key mechanisms identified as crack bridging and pullout [15]. Essentially carbon nanotubes are able to reduce and supress the extent of crack initiation by the bridging of the crack interface. Thus CNTs could offer notable material improvements when applied to wind turbine blades. The extent of improvements are a function of matrix physico-chemistry, matrix–filler and filler–co-filler interactions, CNT morphology (aspect ratio, number/type of defects) and the filler density, distribution, and homogeneity.

Industrial scale manufacture of any CNT-based material for turbine blades is a trade-off between properties and economics. New CNT-based nanomaterials are expensive and costly. Also, there is a greater degree of batch-to-batch variation on production when compared to glass or carbon fibres for

example. Thus, CNTs are still finding their way into the global wind energy industry. On the other hand, market prices of CNTs are continuously declining. Some examples of prices of industrial grade CNTs are as follows: 95 €/kg (Nanocyl NC7000™ MWCNTs), 100 $/kg (MWCNTs, Jiangsu XFNANO Materials Tech Co. Ltd), 600 $/kg (Cheaptubes™ MWCNTs). However, carbon nanotubes vary between producers due to the numerous critical parameters from contamination levels to inter-batch differences in number of crystallographic defects to dispersion of geometrical parameters (length, diameters, etc.). Some effort towards standardization of carbon nanomaterials is required and would merit further consideration [16].

Another material development strategy in the wind industry is the use of novel self-healing polymer composites. As wind turbine blades undergo fatigue loads, the material performance degrades with time. This is due to the crack initiation and subcritical crack growth. Self-healing is a concept where these subcritical cracks can self-repair soon after formation. Amano et al. [17] demonstrated a new method for supplying the monomer more uniformly throughout a fibre reinforced composite by varying the vascular tube layouts for greater accessibility for the healing agent to damage. The vascular network arrangement coupled with the DMA data can be used to uniformly supply the healing agent required for self-healing in polymer matrix composites fabricated using VARTM.

3.4.3 Sandwich Core Materials

The term sandwich composite refers to a structure which consists of two or more thin face-sheets, in this context these are usually composites laminates. These are then separated by a relatively thick lightweight compliant core material (figure 5).
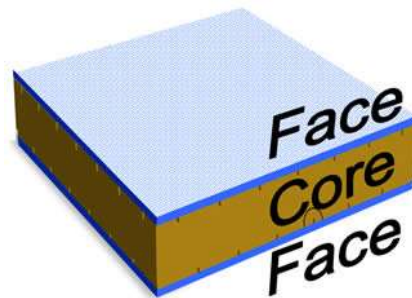

Figure 5. Sandwich Core Concept

This strategy is a good method of obtaining very light structures with high buckling resistance, high strengths and bending stiffnesses. Figure 6 shows the approximate location of sandwich cores in box beam wind turbine design.

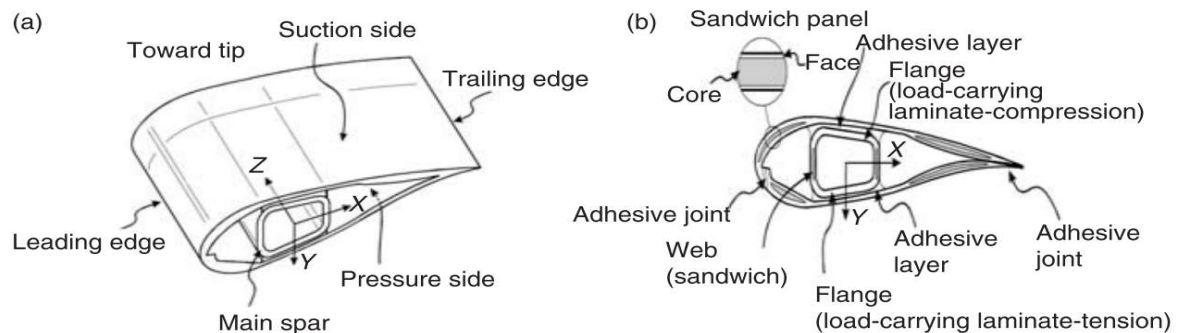

Figure 6. Sandwich Core Schematic

Since there is a shift in priority towards more sustainability and recyclability, this must be considered upon implementation of any novel core material choice therefore the major criteria for sandwich core material design are:

- Properties: weight, stiffness, strength, damage tolerance, heat resistance
- Cost: material, excess resin uptake, finishing options, ease of processing, life cycle cost.
- Sustainability: CO_2 footprint, recyclability, life cycle analysis.

The last several years have seen the emergence of four sandwich core material types which are most widely used in the wind blade industry. Namely end-grain balsa, styrene acrylonitrile (SAN) foam, polyvinyl chloride (PVC) foam, and polyethylene terephthalate (PET) foam. End grain balsa wood is a popular option since it has good mechanical properties, it is inexpensive and come from renewable and sustainable sources since the balsa tree is fast-growing. Balsa, although it can be used throughout the blade, is commonly used in the first 10 m from the root due to higher strength and stiffness owing to its end grain structure. However, when used throughout the blade balsa can incur a weight penalty due to its relatively higher density. One of the pitfalls with balsa is the uptake of resin on infusion due to its end-grain structure. All core systems irrespective of the material they are fabricated from, require scoring or for the core system to be segmented. This generates hinges enabling the core system to conform to curved surfaces in the blade structure. Therefore, this scoring system creates resin channels in the regions where each of the core segments are angled away from one another. So, although the kerfs between the core segments enable greater distribution of resin throughout the structure when they're filled through the infusion process, they also add significant weight to the structure. Therefore, any further developments which can reduce this resin uptake can reduce costs, since one of the major issues in blade production in resin pricing. However, one of the advantages of this phenomenon is an additional increase in torsional rigidity and buckling resistance.

Cores fabricated from SAN or PVC tend to be less dense that that of balsa, however they tend to be more expensive. SAN and PVC provide structural support in areas that benefit from weight saving but where strength and stiffness are not as dominant. The thickness of SAN and PVC foams would need to be increased by roughly a factor of 2 to match the physical properties of balsa. However, in any infusion process, careful consideration of the resin flow is required to ensure wetout. This can be achieved by machining out flow channels in the surface of the core to facilitate this resin transport, and ensures resin flows evenly on both faces of the core. One of the disadvantages of PVC is its tendency to outgas when prepregs are used as skins, this can cause delaminations at the interface between the skin and the core which originate from the voids generated from the outgassing. Outgassing occurs when gases which are trapped, dissolved or absorbed in a material are released.

In the last decade PET has come to the fore in sandwich core technology in wind blade fabrication. PET is an excellent material choice for use in sandwich panel construction and has many advantages including its recyclability and circular nature, density control and consistency in mechanical properties, no outgassing upon using prepregs, thermo-cuttability for example when using a hot wire, it is thermoformable and can be performed to conform to mould curvatures and can be remelted and fused with face sheet laminates. However thermal preforming is not routinely used in the manufacture of blades. PET requires a marginally higher density than SAN or PVC in order to afford similar mechanical properties. PET cores thus tend to be used in the shells at the tip section around the last 10 m of the blade. Regardless of the material, a good quality blade requires tight quality control of any raw materials. The core material needs to be machined precisely so that when inserted into the mould, the have shapes and thicknesses within the specification, whilst also having minimal gaps between them, the tolerances are 2 mm. Hence prevents the gaps from becoming resin traps and prevents "race

tracking" of the resin during infusion. It also makes the blade's finished weight more consistent and predictable and enables the blade manufacturer to more closely calculate resin requirements [18].

The Diab Group, who are a leader in sandwich composite solutions, has utilised SABIC's new LNP™ COLORCOMP™ formulation, which uses nanotechnology to reduce weight and improve mechanical properties of sandwich structures with PET foams to form a use case in wind turbine blades. The compound produced by SABIC is used over standard nucleators for production of Diab's Divinycell PY PET foam core series. This compound improves the foaming process by improved nucleation for a wide variety of foam densities and thus reduces the foam's cell size by a factor of up to 2, whilst maintaining the same density and decreasing the cell size dispersity, it thus enables the final part to be lighter and more efficient in use. Also, this solution can reduce resin uptake on infusion leading to weight savings. Smaller foam cell sizes and narrower size distribution can also potentially generate improvements in shear strength and strain properties that are currently not possible with conventional technologies or lower-density foams. These improvements to the core foam material can help designers create new, longer blades that address increasingly stringent standards for precision, weight, and consistent quality, and contribute to greater overall energy generation [19].

3.4.4   Bonding Materials

A wind turbine blade generally consists of two shells bonded together with a structural adhesive. It is important to understand the load distribution for a given blade design. The trend is towards longer larger blades, and thus require material improvements and durability in bonding adhesives since these adhesives are used to bond leading and trailing edges along with bonding the shear webs to spar caps. Blades are the most severely loaded parts of a wind turbine where the bonded joints play a significant role in the structural integrity of the blade. The bond-line thickness can reach up to 30 mm along a 70 m blade where the geometry of the bond-line varies along the length depending on tolerances.

Curing of adhesive bond lines is also a critical and time-consuming operation in blade manufacturing. Where significant variation in adhesive thicknesses can lead variations in thermal histories across the adhesive bonds which arise due to the exothermic nature of the cure process. Thus, thicker bond lines are more likely to result in larger exotherms leading to performance variations along the length of the bond lines. There needs to be a fine balance between the competing factors of bond line cure time reductions and avoiding adhesive overheating[20]. The adhesive needs to exhibit low shrinkage during curing and show high stress and fatigue resistance. It must be able to withstand high centrifugal forces and a large temperature range. Also, the adhesive must maintain bond strength for a blade's lifetime. Epoxy adhesives meet these requirements. They possess high strength, excellent adhesion, dimensional stability and high temperature and moisture resistance. Also, they are highly compatible with the epoxy-based laminates systems which currently dominates the wind blade sector. Dow Chemicals makes the claim that their new Airstone ® 770E 2-part epoxy resin system has greater durability and fatigue performance than conventional adhesive systems.

3.5   Structural Applications

The design of a modern wind turbine blade is a balancing act between aerodynamic and stiffness considerations. The outer geometry of a blade is typically formed by the assembly of two half shells to give it an aerodynamic shape. Each half shell is a sandwich construction of fibre-reinforced polymer composite skins on either side of a low-density core material, as discussed typically lightweight thermoplastic foam or balsa wood. For the transfer of shear loads and to provide additional stiffness, the reinforcing sections such as a box spar or structural webs are fitted on the inside of the hollow

blade. In general, all the different parts are manufactured separately, and then bonded together using adhesives to form the final blade assembly. Figures 7 and 8 show a general schematic regarding the locations of the material constituents. To summarise, sandwich core materials typically use balsa, PET, or PVC, the skins tend to be fabricated from either prepregs, or dry preform with an infusion resin using a VARTM or one of its related processes. Epoxies are used for both the leading and trailing edge joints, and for coating solutions. Turbine blades are a combination of monolithic and sandwich structures. Generally, the flapwise bending load is carried by the main spar or an equivalent structure which consists of spar caps and internal webs and stiffeners, with the edgewise loads being carried by the shells.

3.5.1   Basic Overview of Blade Structures

3.5.1.1   Spars

The main spar usually extends from the root of the blade to a position near the tip. The primary function of the main spar is to withstand the bending loads from the bladewise bending moments. For some of the larger blades these are made using hybrid glass/carbon composites. The main spar lay-up usually includes UD-layers to provide the bending stiffness as well as some off-axis or angle-ply layers to provide buckling resistance on the suction side when loaded in compression.

3.5.1.2   Webs

The function of the webs is to carry the flap-wise shear forces, and they are usually made as composite sandwich plates with polymeric or balsa core and with thin composite face sheets which are usually fabricated as composite sandwich plates with polymeric or balsa core with biaxial laminate thin composite face sheets with orientation ±45° relative to the blade length. The sandwich design is used for optimal resistance against in-plane shear buckling.

3.5.1.3   Shells

The composite sandwich laminates around the leading and trailing edges provide the buckling resistance for the edgewise loading which becomes much more prominent as the manufacturers are trending towards larger blade lengths. Gravitational loads will become more pronounced with greater blade lengths. As discussed there has been recent advances in sandwich core materials for their uses in the blade shells and webs, for example affording greater control over nucleation of the cells in the foam structure of PET to better utilise the mechanical properties and reduce the mass required in blade shells. This in turn could enable greater usage of PET throughout the blade instead of its current utilisation near the blade tip section. This is also an attractive proposition since this increases the propensity of the blade to be better recycled at the end of life as well as to extend the working life of the blade which amortises the initial capital cost of the blade.
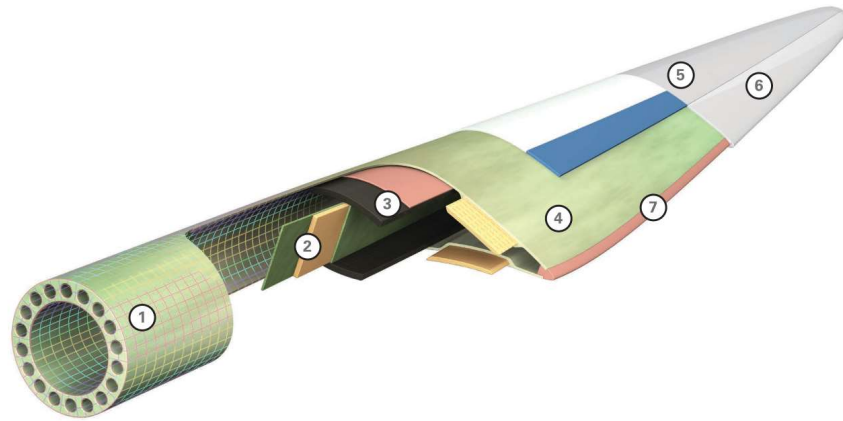
		PET	PVC	Balsa	Prepregs	Dry Preform Systems	Epoxy Adhesives	Film Adhesives	Coating, Filling and Fairing
1	Root	✔		✔	✔	✔		✔	
2	Shear Web	✔	✔	✔	✔	✔			
3	Spar Cap				✔	✔			
4	Shell	✔	✔	✔	✔	✔			
5	Blade Surface								✔
6	Over-lamination					✔			
7	LE/TE Bonding						✔		

Figure 7 General blade schematic with the various material components [20].
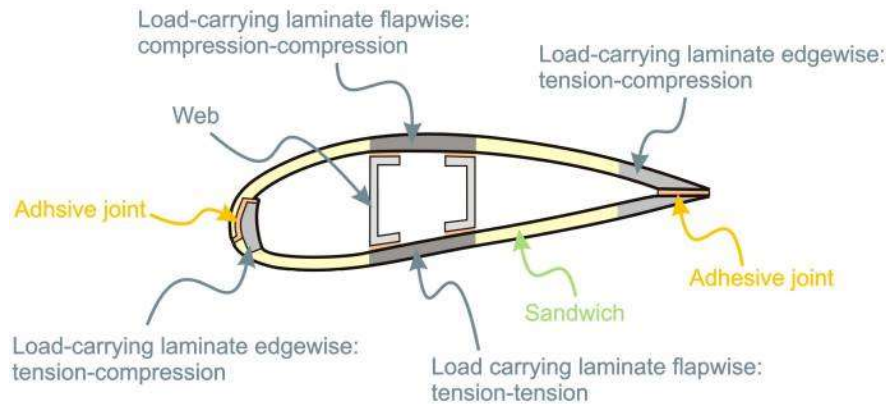
Figure 8.Overview of blade structure.

4 Optimised Reference Blade Design

4.1 Reference Blade Overview

Upscaling of wind turbines is an effective lever for reducing the levelised cost of energy (LCoE). However, in order for the research community to contribute to the ensuing challenges, realistic reference models are needed that keep up with the rapid pace of technology development. A number of reference turbines have been developed over the years, including the NREL 5MW [21], the DTU 10MW [22], and the IEA 3.4MW [23]. More recently, NREL and DTU developed and publicised a 15MW reference wind turbine, as part of the IEA Wind Task 37 [24], sized in line with several recently announced multi-MW turbines (GE Haliade-X, Vestas V236-15MW and Siemens-Gamesa SG 14–222 DD). The 15MW turbine was designed using NREL's WISDEM [25] tool, and all relevant data is published according to the WindIO ontology on GitHub.

The IEA 15MW blade was identified as a suitable reference blade for this project. However, through refined analyses of the baseline turbine, structural and aeroelastic stability issues have been identified. In particular, a fictitiously high structural damping (6%) is required for stable aero-servo-elastic simulations. Furthermore, the ultimate load envelopes—when applied to a finite element (FE) model of the blade—result in significant strength and buckling failures. Whilst small discrepancies between models and aeroelastic codes are common [26], using a baseline blade with significant failures has been deemed unsuitable for this project because it will lead to an unrealistic bill of materials for the blade.

Given the aforementioned pitfalls of the original design, the aim of this work is to develop an updated blade model for the existing 15MW turbine platform that is feasible and representative of the current state-of-the-art. Two optimisation processes of increasing complexity are employed for the task. The first, a 'frozen-loads' approach demonstrated by various authors [27]–[29], generates a mass-optimal internal blade structure given a fixed planform. The second is an integrated aero-structural optimisation that designs aerodynamic, structural, and operational parameters to minimise LCoE. Both methods are performed using the multi-disciplinary analysis and optimisation (MDAO) tool known as ATOM (Aeroelastic Turbine Optimisation Methods) [29]–[31], co-developed under the Wind Blade

Research Hub (WBRH) by the Offshore Renewable Energy Catapult and Bristol University. Finally, the structural feasibility of the optimised designs is assessed using FE shell analyses.

The methods used in this work are described in Section 4.2, followed by the analyses of the baseline 15MW turbine in Section 4.3. Section 4.4 then presents the optimisation results, and the FE analyses are discussed in Section 4.5. Further modifications of the blade design which were necessary to satisfy buckling requirements are described in Section 4.6, and the finalised blade design is presented in Section 4.7.

4.2 Methods

4.2.1 Load simulations

Two aero-servo-elastic simulations methods are employed in this work. The first is used for the baseline analysis and frozen-loads optimisation, and couples blade-element-momentum theory and a dynamic blade model based on modal reduction (15 blade modes) in a fixed-point iteration scheme. Dynamic control is provided by a simple PI controller with gain schedules found in the relevant ROSCO controller [32]. The first method employs a reduced set of IEC design load cases (DLCs) [33]—1.1, 1.3, 2.3, and 6.1—as these have been found to offer a good estimate of ultimate blade loads without excessive computational effort.

The second analysis method uses an aeroelastic piecewise linearised model of the rotor [34] for the aero-structural optimisation. A further reduced set of DLCs is used, consisting of 11, 600s simulations from DLC 1.1 and 1.3. Whilst such a reduced set may not capture all extreme/fatigue loads, a compromise between accuracy and computational time is required.

4.2.2 Optimisation

The optimisation problem formulations are now described. However, a number of features/modifications common to both processes are first explained. The nacelle, tower and foundations are assumed identical to the baseline. Conversely, the material properties used for the blade, defined in Table , are modified based on in-house data—in particular the strength values are more realistic. Blade structural damping is also set to 0.5%.

Several changes to the blade structural configuration are described as follows:

- Shear webs are extended closer to the blade root and tip—to avoid stress concentrations.
- Spar caps contain UD glass and carbon layers, allowing the optimiser to control the ratio.
- Skins contain independent glass UD and BIAX layers, as opposed to TRIAX in the baseline.
- Sandwich core thickness may vary independently, depending on the optimisation.
- Root bolt diameter is optimised. Whilst not modelled in the beam/aeroelastic model, root connection mass is considered in the cost model. A bolt stress constraint is applied, based on a scaling law from in-house data, which enables a realistic blade mass and root chord.

Frozen-loads optimisation

The 'frozen-loads' process used here is as described in Scott et al. [29]. The blade planform is fixed to that of the baseline and design variables (DVs) describing only the internal structure (defined in Table) are optimised. The objective is to minimise an augmented mass metric that accounts for the added

cost of carbon [29]. Optimisation constraints include strength, buckling, fatigue, aeroelastic stability, tower clearance, and ply taper rates, as described in [29], [35]. Additions in this work include a finite strip buckling constraint [36] and a root bolt constraint. Load envelopes are computed as in Section 4.2.1.

Aero-structural optimisation

The aero-structural optimisation process uses a monolithic architecture to minimise LCoE, using the INNWIND cost model [37]. The architecture performs 600s DLC simulations and assesses a comprehensive set of constraints at every design evaluation. This architecture enables the optimiser full control over all aeroelastic effects and allows for innovative design features to emerge from the design process. Due to space constraints, the reader is referred to Samuel Scott's thesis for full details [35]. DVs for this process are listed in table 4.2, and constraints are the same as for the frozen-loads process with the addition of a tip speed constraint (< 95ms−2) to limit noise and erosion.

Table 4.1 - Material properties used for optimisation

Material	E_{11} (GPa)	E_{22} (GPa)	G_{12} (GPa)	υ_{12} (-)	ρ (kg/m³)	X_t (MPa)	X_c (MPa)	Y_t (MPa)	Y_c (MPa)	S (MPa)
UD glass	43.2	12.6	4.42	0.29	1926	777	648	48.6	157	90.3
BIAX glass	13.4	13.4	12.1	0.53	1910	300	185	300	185	144
UD carbon	129.2	7.62	3.81	0.32	1548	1954	967	46.6	158	55
Foam	0.13	0.13	0.05	0.32	130	2.1	1.56	2.1	1.56	1.25

Table 4.2 - List of design variables. Number of DVs in brackets indicates the frozen-loads process

Name	# DVs	Normalised location of spline control points along the blade arc-length. 0:Root - 1:Tip	Comments
Aero **Blade radius**	1	NA	-
Chord	6	[0 0.25 0.4 0.7 0.9 0.98]	Root/tip fixed
Thick.-to-chord	5	[0.1 0.33 0.567 0.8 1]	Root/tip fixed
Twist	6	[0 0.25 0.45 0.7 0.95 1]	-
Pitch axis	3	[0.2 0.5 1]	Dist. ref. axis to LE
Prebend	3	[0.35 0.6 1]	Root fixed
Cone angle	1	NA	-
Tilt angle	1	NA	-
Structural **Shell skin**	10	[0 0.02 0.05 0.1 0.25 0.4 0.6 0.8 0.9 0.95]	Glass BIAX
Root reinf.	10	[0 0.02 0.05 0.1 0.25 0.4 0.6 0.8 0.9 0.95]	Glass UD
LE reinf.	5	[0.1 0.25 0.4 0.6 0.8]	Glass UD
TE reinf.	5	[0.1 0.25 0.4 0.6 0.8]	Glass UD
Spar cap glass	8	[0.05 0.1 0.25 0.4 0.6 0.8 0.9 0.95]	Glass UD
Spar cap carbon	16	[0.05 0.1 0.25 0.4 0.6 0.8 0.9 0.95]	Carbon UD

LE core	7 (14)	[0.1 0.25 0.4 0.6 0.8 0.9 0.95]	Foam
TE core	7 (14)	[0.1 0.25 0.4 0.6 0.8 0.9 0.95]	Foam
Web 1 & 2 skin	8	[0.04 0.1 0.25 0.4 0.6 0.8 0.9 0.96]	Glass BIAX
Web 1 & 2 core	8	[0.04 0.1 0.25 0.4 0.6 0.8 0.9 0.96]	Foam
Spar cap geom.	8	[0 0.98]	
Root bolt diam.	1	[0]	
Control **Tip-speed ratio**	1	NA	Region II
Total	120 (107)		

4.2.3 FE modelling

To assess the blade designs, shell FE models are generated using ORE Catapult's in-house meshing tool—BladeMesher—which reads the WindIO yaml file from ATOM, and creates an ANSYS APDL input deck. The elements used are SHELL281, 8-node quadratic. Note that elliptical cut-outs at the web run-outs are included to avoid stress concentrations.

Loads are applied as shear forces to 100 artificial nodes equally spaced along the blade reference line, which are tied to the blade spar caps using RBE3 elements. Accordingly, for each of the 12 resolved load directions, a shear force distribution is generated from the load envelopes using a least-squares method which aims to minimise the difference between the current and target internal moment distributions. Fully-fixed constraints are applied at the root nodes.

Linear static and eigen-buckling analyses are performed on the resulting FE models, in order to offer an equal comparison between the baseline and optimised designs; note that non-linear analyses would be preferable but do not converge for the baseline blade. Furthermore, pre-stress effects are included to enable the eigen-buckling analysis.

Lastly, strength is assessed using the Puck criterion [38], for which an in-house APDL implementation has been developed, to ensure consistency with the original criterion.

4.3 Analysis of the baseline

Analyses of the baseline turbine consist of aero-servo-elastic simulations to obtain a load envelope, followed by FE simulations to assess strength and buckling failures. It is found that a structural damping coefficient of 6% is required to avoid aeroelastic instability during simulations. This value of damping is significantly higher than those found experimentally for other large blades ($\approx 0.5\%$ or lower [39]), hence, the damping is reduced for the optimisations in this work. Note that, when instabilities are observed for the baseline, edge-twist motions typically dominate the divergent oscillations.

Load envelopes are displayed in Figure 9, indicating the magnitude and relative contributions from each load case. The load envelopes are then applied to the FE model as described in the previous

section, with strength failure indices (FIs) shown in figure 10 for the flapMAX load case (note contours are clipped at 2 for clarity). In general, there are some small compressive fibre failures (FF) on the suction-side (SS) spar cap, whist the pressure-side (PS) spar cap is relatively underutilised—likely due to the forced equality in the spar cap DVs. However, interfibre failures (IFF) for this blade are significant (greater than 10 in some localised spots), and failures can be found in the skins, webs, and LE/TE reinforcement. The significant IFFs can be attributed to the fact that WISDEM currently only performs a low-fidelity check on longitudinal strains, and omits any transverse, shear, or inter-fibre checks. Furthermore, the baseline blade exhibits extremely low buckling resistance as stated in Table (for some load cases less than 3% of the design loads). Critical buckling failures near the tip are likely due to low spar cap thickness, and elsewhere on the blade due to insufficient core material in the panels. Lastly, the tower clearance constraint is satisfied but far from optimal, and fatigue failures (as computed in ATOM) are significant. These failures motivate the optimisations conducted in this work to generate a realistic baseline from which to work.
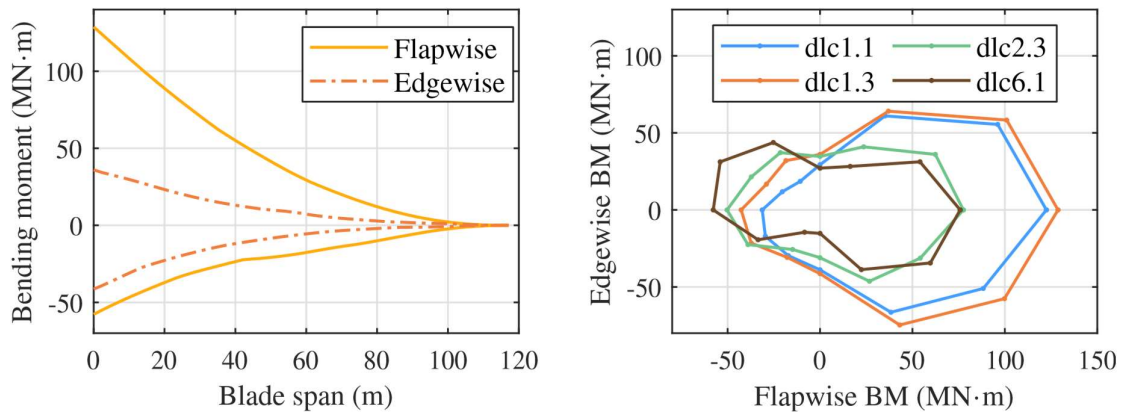
Figure 9 - Blade spanwise, and root clock-face, load envelopes for the baseline. Loads quoted in the element coordinate system, safety factors included.
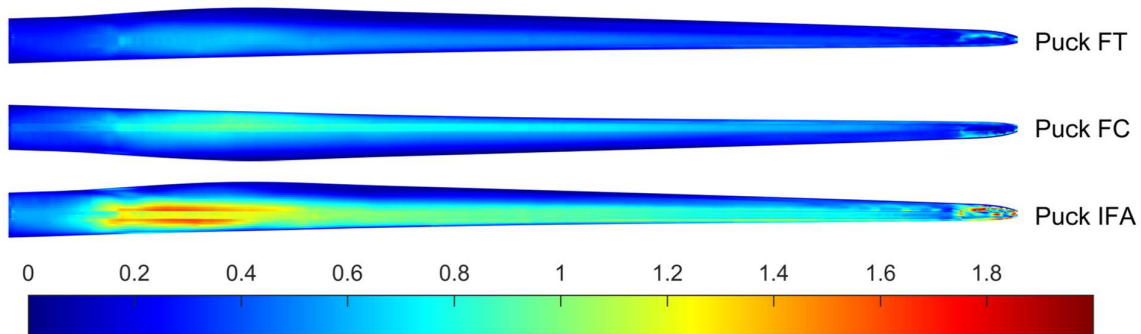
Figure 10 - Strength failure indices for the baseline—flapMAX load case. Contours clipped at 2. FT = fibre tension, FC = fibre compression, IFA = inter-fibre mode A.

4.4   Optimisation results

Global metrics for the optimised designs are shown in Table . It is noted that due to space constraints, discussion is limited to global metrics and key features in the resulting designs. The reader is referred to [15] for exhaustive discussion on auxiliary topics such as gradients (Chapter 4), convergence

(Chapter 7), and detailed analysis of bend-twist coupling solutions (Chapters 6 and 8); albeit for a 20MW system.

It can be seen that the frozen-loads design displays an increase in LCoE due to the higher blade mass. As demonstrated in 4.3, the planform of the baseline design produces high loads relative to the structures ability to withstand those loads. Therefore, fixing the planform and only designing an internal structure inherently requires more material to ensure feasibility. In contrast, the aero-structural optimised design offers a significant LCoE reduction, due to improvements in energy yield and reductions in blade mass. Optimising LCoE entails a balancing act between maximising AEP and minimising costs—these typically being in opposition. However, using a monolithic architecture as done here allows for the AEP-cost balance to be finely tuned, and even for features such as passive load alleviation to 'ease' the balance by enabling more power for the same loads (and cost), or vice-versa.

Table 4.3 - Comparison of design metrics. All % differences are relative to baseline.

Metric	Baseline	Frozen-loads		Aero-struct	
		Val.	%	Val.	%
LCoE (AC/MWh)	93.32	94.19	0.93%	91.19	-2.29%
AEP (GWh)	78.29	78.24	-0.07%	79.47	1.49%
Blade mass (tn)	71.08	95.72	34.7%	63.05	-11.3%
Specific power (W/m^2)	329	329	0%	304	-7.67%
Capacity factor (%)	0.596	0.596	-0.06%	0.605	1.49%
Blade arc length (m)	117.15	117.15	0%	122.23	4.34%
Solidity (%)	3.14	3.14	0%	3.24	3.48%
Cone (°)	4	4	0%	4.56	13.9%
Tilt (°)	6	6	0%	2.4	-60.3%
Tip prebend (m)	-4	-4	0%	-4.81	20.29%
Rated wind speed (m/s)	10.67	10.69	0.16%	10.56	-1%
Max. tip speed (m/s)	91.47	90.71	-0.83%	94.68	3.51%
TSR (-)	8.56	8.48	-0.99%	8.97	4.77%
1st blade freq.	0.488	0.333	-31.6%	0.449	-8.09%
2nd blade freq.	0.689	0.555	-19.5%	0.673	-2.31%
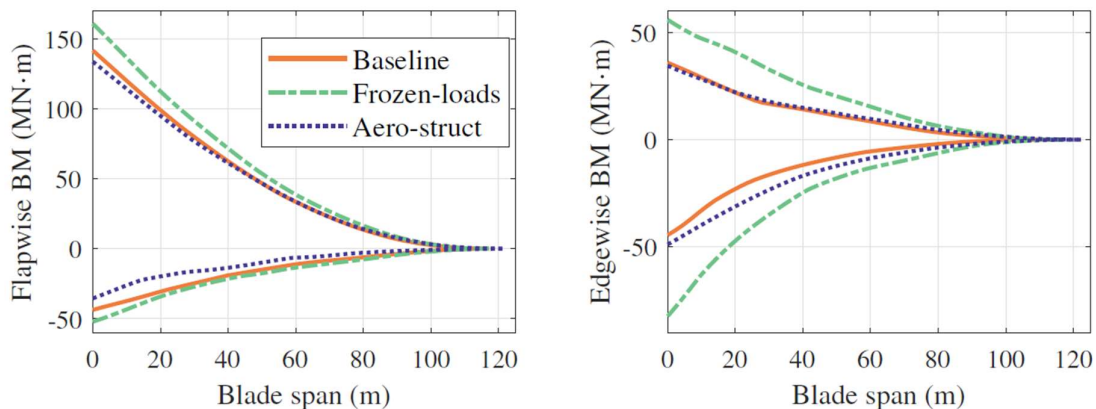
Figure 11 - Spanwise load envelopes for the baseline and optimised blades. From piecewise linear simulations and reduced set of DLCs.

Relative to the baseline, the aero-structurally optimised blade is 4.3% longer yet offers a small reduction in ultimate loads (see Figure 11). Accordingly, greater section thickness and chord near the root (see Figure 12) are employed to add stiffness, hence more efficiently satisfying the failure constraints. The aforementioned load reductions are the result of a smaller chord near the tip, less aerodynamic aerofoils, and a strong nose-down bend-twist response ($\approx 7°$ at rated). This bend-twist response can be explained using figure 13, in which a simple blade planform is plotted, including the spar cap locations, flexural axis (FA) (computed as in [40]), aerodynamic centre (AC), and mass centre. The optimiser's choice to move the spar caps (and hence the FA) toward the LE, as well as for a short distance between LE and the straight pitching axis, results in the AC being rearward of the FA. Thus, a nose-down twisting moment is generated upon any downwind flapwise aerodynamic force. Importantly, this bend-twist response is induced without the use of sweep or fibre steering, i.e. the methods most commonly applied in recent literature, as these come with associated drawbacks such as increased torsional loads, reductions in stiffness, and manufacturing/transport difficulties [41]. Note the kink in the planforms LE near the root is due to the optimiser sharply varying the pitch axis DV outboard from the enforced region of root tangency. Whilst the kink is far smoother when plotted with equal x-y axis scaling, a smoothness constraint would also avoid this.
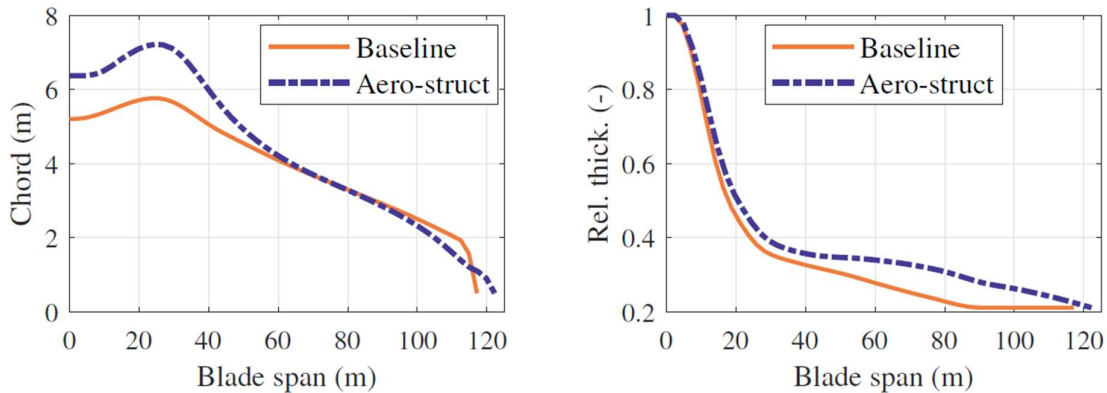
Figure 12 - Chord and relative thickness distributions
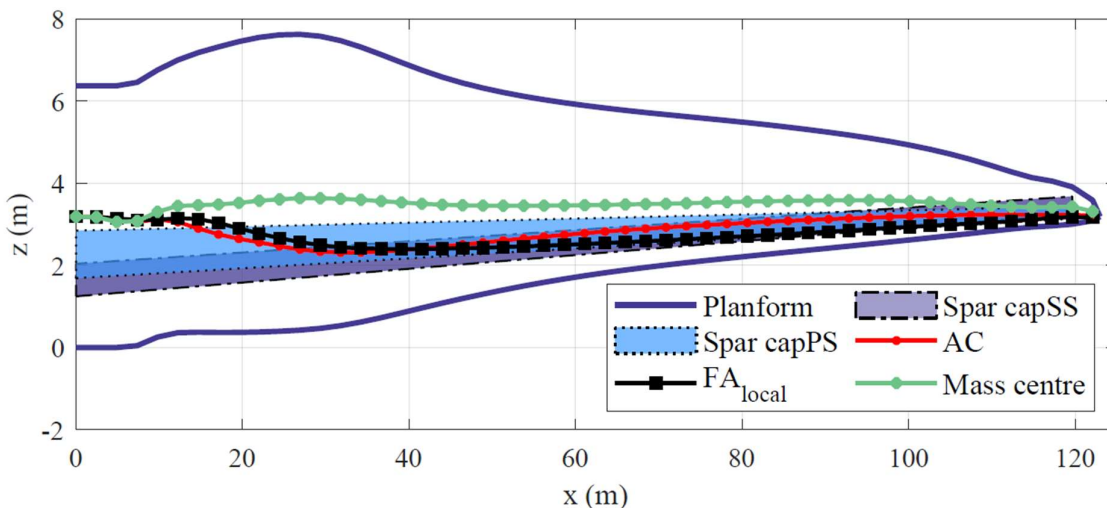
Figure 13 - Planform showing aerodynamic centre, flexural axis, mass centre and spar cap locations.

4.5 FE shell analysis of optimised blades

This section now presents the results, and insights gained, from FE shell modelling of the optimised blades. Strength FIs for the frozen-loads and aero-structural optimised blades are plotted in 14 and 15, respectively, for the Flap max load case.
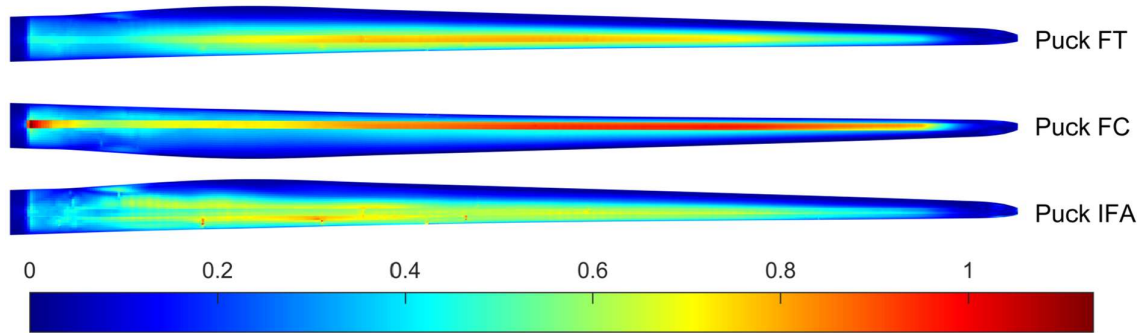
Figure 14 - Contour plot of failure indices for the frozen-loads blade for maximum flapwise load case
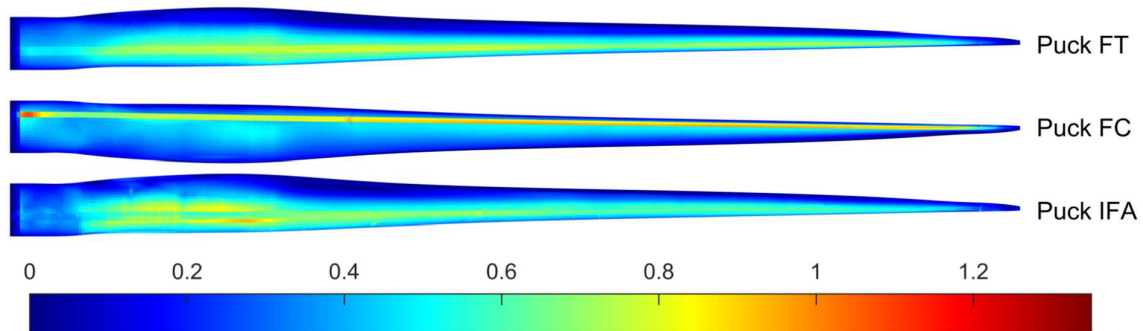
Figure 15 - Contour plot of failure indices for the aero-structural blade for maximum flapwise load case

In addition, the maximum FIs from all load cases are plotted with respect to the blade span in figure 15. As can be seen, both designs resolve the strength failure issues found with the baseline, although for the frozen-loads design feasibility comes at the expense of increased blade mass.
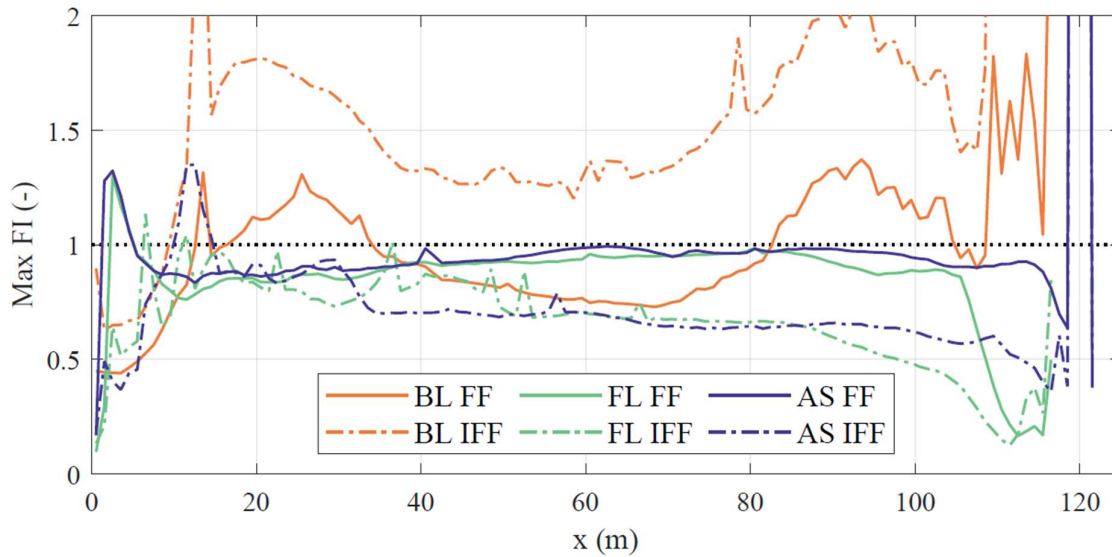
Figure 16 - Comparison of maximum FIs. BL = baseline, FL = frozen-loads, AS = aero-struct.

For both models, a major strength driver is fibre compression on the SS spar cap. It can be seen that both blades have FI close to 1 for much of the spar cap, indicating this key structural element is both well-utilised and adequately predicted by the lower fidelity model. This is confirmed by the maximum FF indices in figure 16. The PS spar caps are less utilised from a strength perspective (FIs ≈ 0.8 for fibre tension) due to the higher tensile strength of carbon and the typically smaller upwind flapwise loads. Thus, the PS caps are more stiffness driven. IFF is predominantly design driving on the PS of the blades, with IFF mode A (matrix tension + shear) being the most critical as the matrix is weakest in tension. The most design driving region for IFF is along the region boundaries between spar cap and sandwich panels. Given the low-fidelity representation of the blade used in ATOM, there is a simple step change in thickness at this boundary, as opposed to a thickness taper, or, as might be found in a real blade, staggered ply drops and tapered core material. Thus, stress concentrations arise along this boundary which could likely be mitigated to some extent by a higher fidelity representation.

Table 4.4 - Location of critical buckling mode and buckling RFs for the three blades

|	1 (Flap Max)		4 (Edge Max)		7 (Flap Min)		10 (Edge Min)	
	Loc. (m)	RF	Loc. (m)	RF	Loc. (m)	RF	Loc. (m)	RF
Baseline	110	0.03	103	0.04	112	0.03	115	0.47
Frozen-loads	11.3	1.21	12.7	1.39	78.8	1.08	7.7	1.43
Aero-struct	7.13	0.74	7.51	1.03	7.51	1.01	31.8	1.07

Table .4 defines the location and buckling reserve factors for the critical buckling mode, for each of the four main load directions. Whilst the buckling resistance of the optimised designs significantly improves on the baseline, these values would not be acceptable in practice for not meeting the target reserve factor (RF) of 1.62. Results indicate that the lower fidelity buckling checks in ATOM are not conservative, which is unsurprising given the known limitations of panel methods and the finite-strip method when applied to a full wind turbine blade. Improving buckling predictions within an optimisation context is an active area of research for both the University of Bristol and ORE Catapult, but for this project the decision was taken to section the blade and optimise the core thicknesses in each section individually as described in Section 4.6. This requires a higher safety factor of 1.81, meaning that core material usage may be increased.

Overall, strength FIs in the main load-bearing components are predicted well by ATOM, especially when considering the significant reduction in computational effort compared to a shell model. This work indicates that the areas typically predicted poorly are localised stress concentrations, such as web terminations, or step changes in material at region boundaries. It is likely, however, that the required modifications to achieve feasibility in the higher fidelity model, and crucially the resulting difference in aeroelastic properties, would be minimal. This is an important point for preliminary system-design tools, as whilst they can produce innovative aeroelastic synergies, it is crucial that such properties be retained when moving to more detailed design phases.

4.6 FE Optimisation of core thickness

As shown in Table , the blades as optimised by ATOM did not achieve the required buckling reserve factors. To resolve this issue, a further optimisation of core material thickness was conducted using ANSYS APDL.

The blade was divided up into sections with length of 1.5 x the local chord length. Rigid regions were applied to each end of the sections as shown in Figure 17, with the displacements constrained but rotations free (essentially this is like a rigid diaphragm placed across each end of the section). The design loads for the end of each segment (forces and moments) were applied to the tip end of the segment and the displacements and rotations of the root end were set to 0. Each of the 12 load directions was considered, and the minimum buckling factor was found for each load direction. The code also determines the mass of the blade section. An example result from the blade section between 46 and 54m is shown in Figure 18 (note that the buckling reserve factor indicated by FACT is 1.81005, indicating that the optimiser has successfully minimised the mass as far as possible whilst still satisfying the buckling constraint.

This model was utilised in an optimisation routine based on the GCMMA (Globally convergent method of moving asymptotes) algorithm [42]. The objective was to minimise the mass of the blade sections whilst keeping the buckling reserve factor for all 12 load directions above 1.81, the safety factor required if linear eigen-buckling analyses are performed on blade sections.

The core thickness optimisation results in the distribution shown in Figure 19. The results for the trailing edge panels on both the suction and pressure side look sensible, but for both the pressure and suction side of the leading edge panels there is a massive increase in core thickness required to satisfy the minimum buckling reserve factor of 1.81. Table shows which load case is causing the minimum buckling reserve factors to drop below 1.81 – it is predominantly those cases close to flapwise maximum and also cases around edgewise maximum.

Reducing the material to the same thickness as it was before the rapid change in thickness results in the blade not having a sufficiently high buckling reserve factor (as low as 1.55) so we must conclude that these sandwich core thicknesses are necessary for the blade to withstand the design load cases with the outer laminates using the current thicknesses. Other potential issues are the resolution of the mesh, which was quite low because the model was being used in an optimisation context.
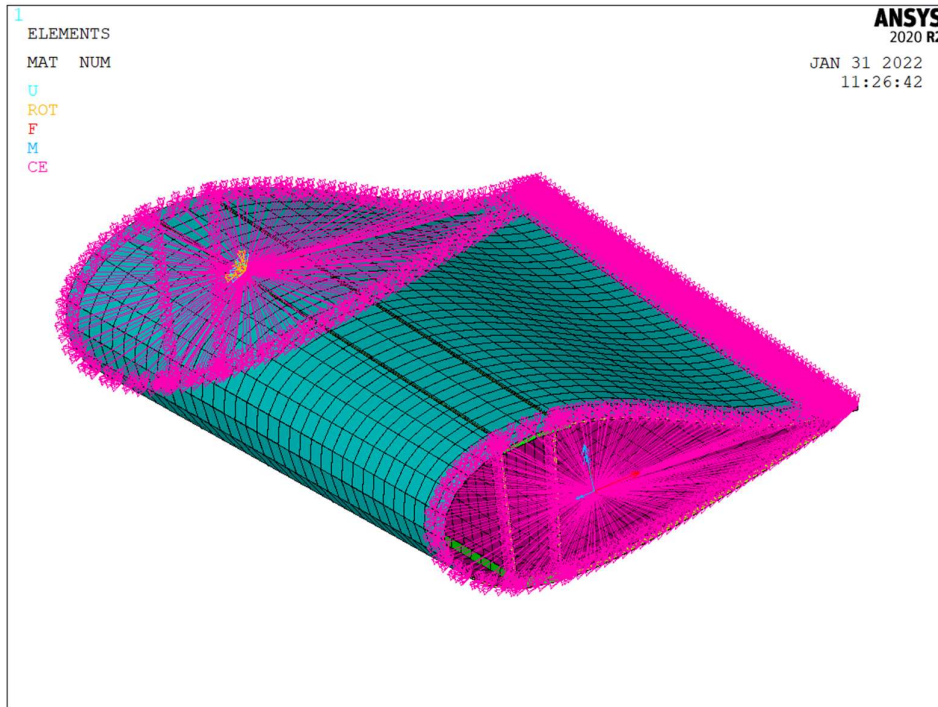
Figure 17 - Boundary conditions for core thickness optimisation (46 - 54m section)
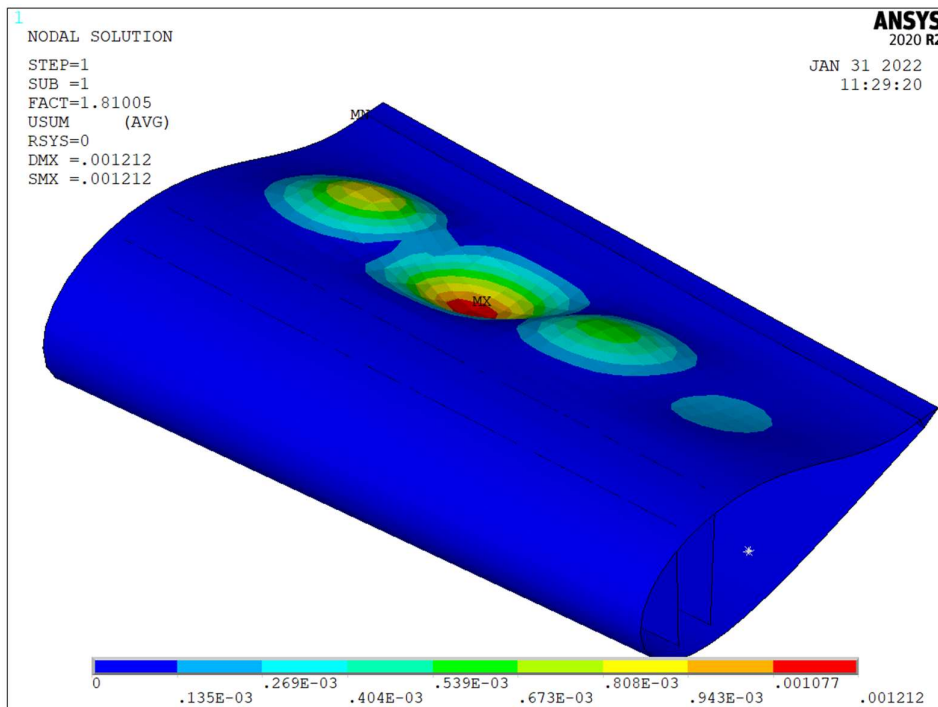
Figure 18 - Buckling reserve factor for minimum flapwise moment (46 – 54m section)

Table 4.5 - Tabulated minimum buckling reserve factor for each load case

Section start (m)	BRF LC 1 (Flap Max)	BRF LC 2	BRF LC 3	BRF LC 4 (Edge Max)	BRF LC 5	BRF LC 6	BRF LC 7 (Flap Min)	BRF LC 8	BRF LC 9	BRF LC 10 (Edge Min)	BRF LC 11	BRF LC 12
0.00	1.82	1.81	1.88	2.40	1.81	1.81	3.38	3.38	4.31	2.29	1.89	1.81	1.82
15.93	1.84	1.82	1.81	2.87	1.83	1.81	2.87	2.87	4.92	2.13	1.86	1.82	1.84
26.26	1.88	1.85	1.81	1.86	1.84	1.81	2.84	2.22	2.11	1.87	1.81	1.81	1.88
37.07	1.83	1.81	1.83	1.98	1.81	2.58	3.07	2.77	2.77	1.93	1.82	1.82	1.83
46.60	1.82	1.81	1.91	1.82	1.81	1.81	3.10	4.42	4.42	1.96	1.82	1.82	1.82
54.44	1.83	1.83	1.93	1.81	1.81	1.94	3.05	3.62	4.81	2.09	1.94	1.83	1.83
61.29	1.81	1.81	1.93	1.81	1.81	1.89	2.92	2.42	3.15	2.04	1.88	1.82	1.81
67.49	1.81	1.81	1.99	1.81	1.81	1.83	2.71	2.71	3.38	1.85	1.85	1.81	1.81
73.21	1.81	1.81	1.90	1.88	1.88	1.81	3.05	2.71	3.36	1.83	1.83	1.81	1.81
78.55	1.81	1.81	1.90	2.20	1.81	1.81	2.76	2.76	3.26	1.83	1.83	1.81	1.81
83.56	1.81	1.81	1.87	2.56	1.81	1.81	2.28	2.62	3.06	1.81	1.81	1.81	1.81
88.25	1.81	1.91	1.81	2.35	1.81	1.81	2.12	3.03	3.98	1.81	1.81	1.81	1.81
92.63	1.82	1.82	1.81	2.54	1.81	1.81	2.02	2.76	4.06	1.81	1.81	1.81	1.82
96.70	1.82	1.82	1.84	2.45	2.45	1.92	1.88	2.29	4.75	1.98	1.98	1.98	1.82
100.45	1.84	1.82	1.90	2.42	2.42	1.88	2.14	3.75	4.67	1.94	1.94	1.94	1.84
103.88	1.85	1.83	1.84	2.84	2.38	1.86	2.16	3.79	3.79	1.97	1.97	1.97	1.85
106.98	1.88	1.84	2.03	2.95	2.45	1.89	2.30	2.59	3.22	2.15	2.15	2.15	1.88
109.74	1.82	1.82	1.91	2.74	2.22	1.81	2.10	2.27	2.91	1.84	1.84	1.84	1.82
112.15	1.90	1.96	2.00	1.90	1.99	1.90	1.99	2.24	2.99	1.89	1.89	1.85	1.90
114.26	1.99	2.26	3.10	2.12	2.10	1.86	1.81	1.81	2.24	1.92	1.92	1.89	1.99
116.12	2.89	2.97	4.20	6.01	2.47	1.81	1.81	1.81	2.26	3.14	3.14	2.89	2.89
117.84	1.82	1.83	2.41	8.80	2.84	1.81	1.81	1.81	2.14	2.16	2.16	1.82	1.82
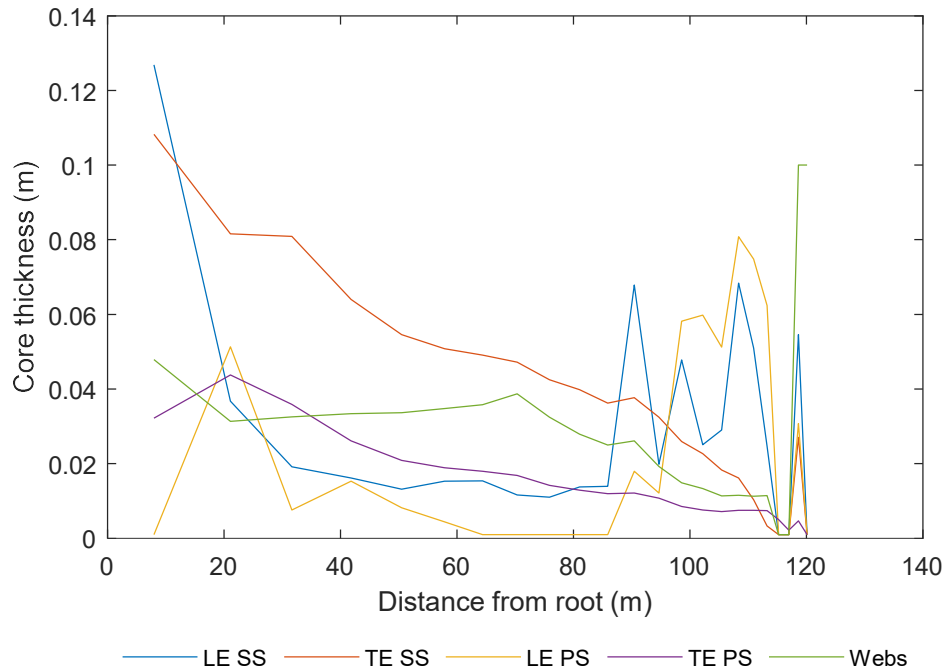
Figure 19 - Core thickness distribution

With the buckling constraints satisfied, the blade bill of materials can be estimated.

4.7   Finalised Blade Design

The NREL blade cost model has been used to estimate what a factory manufacturing the baseline blade would look like. It is assumed the factory will be manufacturing 300 blades per year and that the cycle time is 48 hours.

4.7.1   Bill of Materials

The bill of materials for the finalised blade design is shown below in Table and the breakdown is shown in figure 20. The total blade mass of 69.5t is in line with upscaling of current blade designs.

As core materials are being considered in more detail in this project, the breakdown of core material thickness by area for each component is shown in Table .
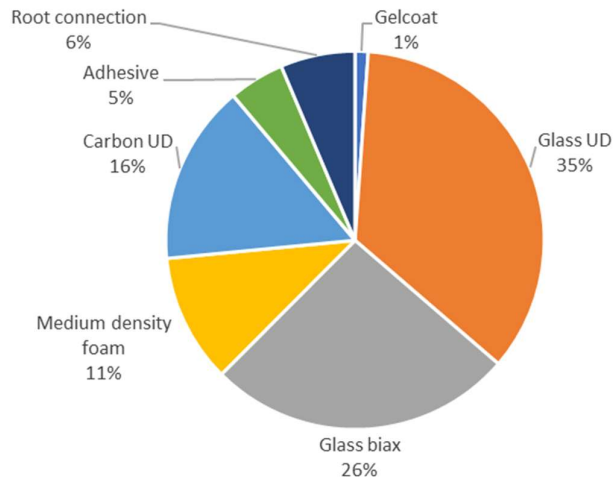
Figure 20 - Baseline blade mass breakdown

Table 4.6 - Bill of materials for baseline blade design

Component	Total Mass (kg)	Fibre Mass (kg)	Fibre Mass with waste (kg)	Resin Mass (kg)	Resin mass with waste (kg)
Shell					
Gelcoat	777.9			777.9	972.4
Glass UD	20550.8	14591.1	15320.7	5959.7	7151.6
Glass biax	13900.1	9869.0	11349.4	4031.0	4837.2
Medium density foam	5414.4		6497.3		
Spar Caps					
Carbon UD	10704.5	7814.3	8205.0	2890.2	3468.2
Glass UD	3927.6	2788.6	2928.0	1139.0	1366.8
Web 1					
Glass biax	2071.1	1470.5	1691.1	600.6	720.7
Medium density foam	1073.8		1288.6		
Web 2					
Glass biax	2218.9	1575.4	1811.7	643.5	772.2
Medium density foam	1158.5	822.6	1390.2		
Adhesive	3311.5			3311.5	3973.8
Root connection	4432.6				
Total	69541.8	38931.5	50481.9	19353.4	23263.0

Table 4.7 - Breakdown of core material requirement by thickness

Thickness (mm)	Shell (m²)	Web 1 (m²)	Web 2 (m²)
0 - 10	46.3	0.0	0.0
10 - 20	183.1	10.7	12.3
20 - 30	66.1	10.9	12.6

30 - 40	177.0	123.0	129.4
40 - 50	89.4	78.2	85.9
50 - 60	61.1	0.0	0.0
60 - 70	35.5	0.0	0.0
70 - 80	0.0	0.0	0.0
80 - 90	96.8	0.0	0.0
90 - 100	0.0	0.0	0.0
100 - 110	72.6	0.0	0.0
110 - 120	0.0	0.0	0.0
120 - 130	45.6	0.0	0.0

4.7.2 Consumables

A wide variety of consumable materials are used as part of the vacuum infusion process. For the reference blade used in this work, mass estimates have been obtained from the cost of consumables and their price per kg (sometimes this has been estimated) as detailed in the NREL cost model.

Table 4.8 - Cost and estimated mass of consumables from the NREL cost model as applied to the reference blade

Consumable	Cost ($)	Cost with waste ($)	Material	Mass estimate (kg)
Peel ply	4028	4632	Polyester fabric	229.3
Nonsand tape	231	266	Polyurethane	119.5
Chopped strand mat	10	10	Glass fibre	4.6
Tackifier bulk	265	278	Epoxy	40.99
Tackifier cans	185	194	Epoxy	28.6
Release agent	847	889	PTFE	54.96
Flow medium/vacuum bagging	939	1080	Nylon	263.14
Tubing 3/8	140	154	PVC	34.8
Tubing 1/2	140	154	PVC	48.21
Tubing 5/8	299	329	PVC	62.4
Tubing 3/4	379	416	PVC	76.49
Tubing 7/8	379	416	PVC	113.7
Tacky tape	7361	7729	Poly(isobutylene)	48.05
Masking Tape	220	242	Paper/acrylic	50.98
Chop Fibers	76	84	glass	39.09
White Lightning	76	83		27.61
Hardener	25	27	epoxy	0.794
Putty	185	203	Polyaspartic ester	33.83
Putty Catalyst	49	53	Polyaspartic ester	33.83

4.7.3 Other Inputs Required for Blade Life Cycle Assessment LCA

The other main materials input for the reference blade is the materials used to make the mould tooling for the blade. This has been estimated using documentation on the mould tooling for the 83.5m blade

of ORE Catapult's Levenmouth Demonstration Turbine and the number of moulds required to hit 300 blades per year.

The weight of the blade moulds has been estimated using a cubic law, where the mass is estimated as $M = M_{Ref} \times \left(L/L_{Ref}\right)^3$ because it is assumed that the weight will be related to the volume of material. This formula has been checked against the mass quoted in [43] for a 40m blade of 16-18t, and yields a shell mould mass of 16.9t which gives some confidence that the relationship holds true. The above reference also states that 75% of the mould mass is the steel backing frame, with the remaining 25% accounted for by the GFRP mould surface.

Table 4.9 - Estimated mass of mould tooling for factory producing 300 baseline blades/year

Component	Number of processes	Reference Mould mass (kg)	Estimated Mould mass (kg)	Total Mould Mass (kg)	Steel Mass (kg)	GFRP Mass (kg)
Spar	3	78100	243597	730790	548092	182697
Shells	3	154000	480331	1440994	1080745	360248
Web 1	2	15006	46804	93608	70206	23402
Web 2	2	12230	38146	76292	57219	19073
Root	3	9372	29232	87695	65771	21924
				Total	1822033	607344

In addition to the mass of the moulds themselves, hinges are used to close the shell moulds. There are 5 hinges, each of which have a mass of 11t for the 83.5m reference blade case. Using the same relationship as above we can conclude that the hinges per mould will have a mass of 171t, for a total of 514t. They are predominantly made of steel but differ from the steel framework because they are a complex mechanical part.

Finally, a master plug will need to be made to create the moulds. There are two ways to do this:

- Create a volume of polyurethane blocks by gluing them together as shown in Figure 21 and then machine it to the shape of the blade. This is then covered in a layer of GFRP and a further layer of tooling paste, which is then machined to the final shape. To estimate the mass of materials used to create a plug in this way we have assumed $0.8m^3$ of foam block will be required for $1m^2$ of blade shell surface and $0.4m^3$ for the spar caps and webs.
- A more cost effective but labour-intensive method is to assemble wooden profiles shaped to the blade profile at intervals. These ribs are then connected by stringers which are overlaminated with a layer of composite, a layer of foam and then 3 further layers of composites. Finally, a layer of tooling paste is added which is machined back to create the final shape. The structure is assembled on a steel frame for transportation and handling. This structure is shown in Figure 22.
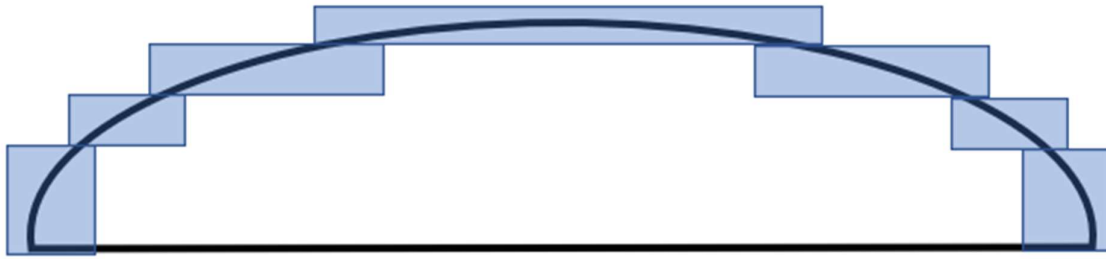
Figure 21 - Foam block plug manufacture
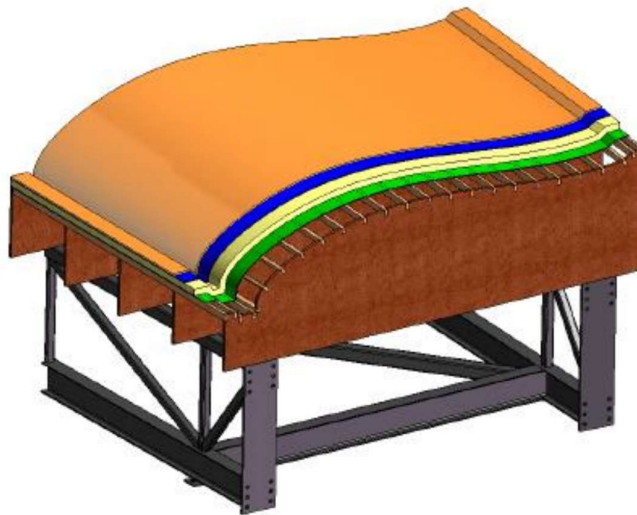
Figure 22 - Method used to estimate the volume of polyurethane blocks required to create the plug

Estimated masses of materials for the plugs are manufactured using these two techniques are shown in Table . The calculation assumes that the polyurethane blocks have a density of 100kg/m³, the tooling paste has a density of 630kg/m³ and a thickness of 8mm and the composite backing has a thickness of 4mm, a density of 1915kg/m³ and a fibre volume fraction of 0.53.

Table 4.10 - Estimated material breakdown for mould plug manufactured using foam block backing

	Shell	Web 1	Web 2	Spar PS	Spar SS	Total
Area of mould (m²)	1262	212	208	111	111	
Polyurethane volume (m³)	1010	85	83	45	45	
Polyurethane mass (kg)	100983	8464	8302	4457	4453	126659
Composite glass fibre mass (kg)	6092	1021	1002	538	537	9189
Composite resin mass (kg)	3578	600	588	316	316	5397
Tooling paste mass (kg)	6362	1067	1046	562	561	9597
Total mass (kg)	117014	11152	10938	5872	5867	150842

For the second plug manufacturing technique we can use the same technique used to obtain the mould masses and scale from the mass of the plugs for the Levenmouth demonstration turbine (30700kg, resulting in a shell mould plug mass of 95754kg for the 122m blade). The cross-sectional areas of 488 points along the length of the blade were determined, corresponding to one slice every 250mm. The total area was 3800m^2, and it was assumed that any wastage arising from imperfect nesting of the wooden profiles was offset by nesting larger profiles within smaller ones and having a slightly hollow structure. Assuming a plywood density of 630k/m^3 and a thickness of 12mm for each sheet and keeping the other components the same, the mass of wood comes out as 29300kg for the shell mould. The mass of steel is then estimated by subtracting the rest of the components from the estimated plug mass.

Table 4.11 - Estimated material breakdown for mould plug manufactured plywood and steel backing

	Shell	Web 1	Web 2	Spar PS	Spar SS	Total
Area of mould (m^2)	1262	212	208	111	111	
Steel mass (kg)	79723	6438	6315	3390	3387	99253
Plywood mass (kg)	29300	2792	2739	1470	1469	37770
Composite glass fibre mass (kg)	6092	1021	1002	538	537	9189
Composite resin mass (kg)	3578	600	588	316	316	5397
Tooling paste mass (kg)	6362	1067	1046	562	561	9597
Total mass (kg)	95754	9126	8950	4805	4801	123436

Whilst there are several estimates inherent in this breakdown, we can see that the mass of steel is relatively low compared to the actual mould tools. Furthermore, only one plug for each component is created so the mass totals are relatively insignificant.

4.7.4 Energy Usage During Manufacture

The total energy usage by process in the blade manufacturing is shown in table 4.12. The total is obtained from the floor area required for each process, a base rate of 250kWh/m^2/year for basic factory usage and an extra amount for the infusion and postcure steps related to the heating time and mass of blade component being heated. Taking the total, and dividing by the cost of energy used in the NREL model (0.08 $/kWh) we can obtain a total energy usage/blade manufactured as 89300 kWh, or 89.3 MWh.

Table 4.12 - Utility costs during blade manufacture

Process	Utility Costs ($/blade)
Material cutting	140.28
Spars infusion	329.99
Shells infusion	3318.98
Web 1 infusion	228.62
Web 2 infusion	226.22
Root infusion	2144.72

Assembly	0.00
Demould	0.00
Trim	19.42
Overlay	44.53
Postcure	303.93
Root cut and drill	31.40
Install root bolts	25.17
Surface preparation	198.46
Paint	37.64
Surface finishing	52.99
Weight/balance	13.14
Inspection	17.18
Shipping	12.32
Total	7145.00

4.8   Conclusions

This project required the use of a reference blade to use in manufacturing simulation, cost modelling and Life Cycle Assessment (LCA) exercises. Initially, the IEA 15MW turbine was selected as the reference turbine. However, it was found to require an unrealistically high value of structural damping to avoid aeroelastic instability. Furthermore, inter-fibre, buckling, and fatigue failures are significant; whilst the all-carbon spar caps are underutilised indicating that the material has been used inefficiently.

This motivated two attempts to improve on the initial blade design to develop a structurally and dynamically feasible blade design for the IEA 15MW wind turbine.

The first design attempted to retain the original blade geometry and control schedules and used a frozen-loads internal structure optimisation to minimise blade mass. The mass of this blade was not deemed to be acceptable for this project as it is not inline with upscaling of current blades. There are several reasons for this – the blade is very aerodynamically efficient at the expense of structural efficiency, meaning that extra material must be used. Also, the root diameter is extremely small for a blade of this size so very large root bolts must be utilised to satisfy the stress constraint which leads to an excessively high root connection mass. The frozen-loads design results in an LCoE increase of 0.93% due to the mass penalty of satisfying the feasibility constraints.

The second design applied a monolithic aero-structural optimisation architecture to minimise LCoE with aerodynamic, structural, and control DVs. In contrast to the frozen loads design, the aero-structural design offers an LCoE reduction of 2.29% due to improved AEP and reduced blade mass. Subsequent FE shell analyses of the optimal blades indicate that strength failures are well predicted and the structural material well utilised by the optimiser. However, buckling reserve factors do not satisfy the required target values, indicating the low-fidelity buckling checks in ATOM are not conservative. This necessitated the use of a further optimisation step in which the core material thickness in individual sections of blade was altered until the blade met the design requirements.

5 Key Considerations for Low Carbon Manufacturing Opportunities

5.1 Background to Life Cycle Assessment

Life cycle assessment (LCA) is a tool that has been developed to analyse and quantify the environmental burdens connected with the production, use and disposal of a material or product and is arguably the best way of quantifying this information [44]. The foundation underpinning any LCA is data about a process. In order to perform an LCA study, it is first necessary to determine the goal and scope (i.e., what is the purpose behind conducting the LCA and what is being included in the study). The scope must define what the system boundaries are in the study and the functional unit must be declared. For many purposes, the system boundary can be defined as 'cradle to gate', that is the manufacture of a specific product in a factory to the point at which it leaves the facility (modules A1-A3 in EN 15804). The 'cradle to gate' section of an LCA generally gives an accurate representation of results, because this stage of a product life cycle involves the fewest assumptions and the data gathering process is relatively straightforward. A complete LCA can be completed which investigates a products entire life cycle known as 'cradle to grave' however, this generally will include a list of assumptions, which depending on the industry can range in size and accuracy. This is why within a 'cradle to grave' LCA, if the focus is on a specific component, there may be a snippet of results which give a 'cradle to gate' set of results which are of more relevance to the study along with it also having limited assumptions and a higher accuracy. A life cycle assessment is not static but a dynamic process and there are ongoing programmes dealing with improving various aspects of this methodology [45]. It is important that the correct decisions are made regarding the choice of materials for the built environment and LCA can be used as a means for informing those choices. This requires that LCA is used correctly and that the decision support tools allow for comparability between products [46], [47]. The purpose of the LCA may be simply to report the environmental burdens associated with a product or process i.e., referred to as an **attributional LCA**, or it may examine the consequences of changing various parameters or assuming different scenarios which is called **consequential LCA**. Another important consideration when studying the environmental impacts associated with a product or process is the timescale involved and it is important that this is also defined at this stage. It is also a requirement to specify what allocation procedures were used during the analysis. In contrast with other wind turbine components such as steel towers, concrete foundations and the high value metals used in generator linings, whose end-of-life is properly described in life cycle assessment (LCA) studies in literature, composite blades have proven to be the sustainability blind spot of wind energy systems. The reason for this is that end-of-life management of composite wind blades is a complex engineering problem which depends on the actual design of the blade, its material composition, the availability of recycling technology, legislation, and requisite infrastructure, as well as the economics of the process itself—including the logistics of transportation, dismantling, etc.

5.1.1 Life cycle impact assessment

Once the Life Cycle Impact assessment (LCI) phase has been completed; this phase of the analysis requires the assembly of all the information about the process, it is then necessary to quantify the environmental burdens, during the life cycle impact assessment phase. At this stage there are several further complications/parameters that must be considered. The biggest problem is deciding how to report and describe the environmental impacts. There is still discussion as to which process is the best to properly report the environmental burdens, but a consensus has been developing over the past

decade or so. The principle is to aggregate the environmental implications associated with the flows to and from nature into a small (but nonetheless meaningful) set of indicators. This methodology has essentially distilled down into two main approaches, referred to as **midpoint** and **endpoint** indicators [48]–[50]. In the midpoint approach, the environmental burdens are grouped into similar environmental impact categories (e.g., global warming potential, ozone layer depletion, freshwater eutrophication, etc.). The endpoint approach seeks to model the chain of cause and effect to the point of the evaluation of damage, which makes for simpler reporting with fewer indicators, but has a higher level of uncertainty.

Characteristically, the environmental impacts are calculated using a variety of models (over 150) which attempt to determine the impacts of processes upon the environment.

Examples of such models include:

• **Midpoint:** TRACI, CML, EDIP, Ecopoints

• **Endpoint:** Eco-indicator [51], LIME2

• combined midpoint and endpoint: ReCiPe [48], IMPACT2002+ [50]

5.1.2 Embodied Energy

The embodied energy of a material or product used in a structure or product is often defined as the primary energy used in the manufacturing process, which includes all the energy used in the production, as well as the primary energy used in the transport of materials and goods required for the production process. This definition relates to the initial embodied energy, which is related to the cradle to factory gate stage (modules A1-A3, EN 15804) of the product life cycle. In some definitions, the transport to construction site (A4) and the energy used on site for the erection or installation of the product (A5) is also included. The units used are generally MJ per unit mass, or volume, or per defined functional unit, although some workers report this as kWh (=3.6 MJ). Transport of materials to site can have a major impact on the embodied energy of the construction materials.

The embodied energy is invariably reported according to the cumulative energy demand (CED) method, which states that the embodied energy is assessed as the primary energy used for the manufacture, use and disposal of an economic good (product or service), or which may be attributed to it with justification. The method distinguishes between non-renewable and renewable energy use. The cumulative energy demand (CED) represents the primary energy used (both direct and indirect) during the life cycle of a product [52]. This includes the energy consumed during the extraction, manufacturing and the disposal of the product and raw and auxiliary materials. Indeed, there are different methods for determining the primary energy demand exist. For example, the lower or higher heating values of primary energy sources may be used, the use of renewable energy resources may not be included, or it may be reported separately. Fay and Treloar (1998) define primary energy as 'the energy required from nature (e.g., coal) embodied in the energy consumed by the purchaser (for example, electricity) and the energy sued by the consumer as 'delivered energy' [53]. This means that a process using 1 MJ of electricity in one region of the world may have a different embodied energy compared to an identical process using 1 MJ of electrical energy in another part, because the grid mix in the two regions is different. Dixit et al. (2012) noted that some research workers do not include renewable energy in their definition of embodied energy and found that the use of different

information sources and the failure to distinguish between primary or secondary energy could lead to errors as high as 40% when reporting embodied energy [54]. They stated that there is a need to develop a common methodology to accurately determine the embodied energy associated with buildings and that there is a need to develop a complete and robust database of embodied energy information. Thus, there is the widely used University of Bath Inventory of Carbon and Energy database [55]. However, this (and others) may not necessarily be the most reliable sources of information. For example, the Bath ICE database has been shown to inaccurately report data for harvested wood products [44]. Cabeza et al. (2013) [56] and Jiao et al. (2012) [57] note that there is a relationship between embodied energy and GWP for primary production, for some building components and that there is a link between embodied energy and cost of buildings, which is related to the energy intensity per unit GDP for that country. It is necessary to define the meaning of primary energy, since it is not always clear that the primary energy has been used when the embodied energy is reported. The primary energy is defined as the energy measured at the natural resource level, i.e., the energy found in nature that has not been subjected to any conversion process through human intervention. This is the energy used to produce the end-use energy which includes the energy used in the extraction, transformation, and distribution to the user [53]. Measurements of embodied energy are only consistent if they are based upon primary energy but if delivered energy is used, the results are misleading. Unfortunately, there is a lack of clarity and incomparability in the reporting of embodied energy [54], [58]. The difference in energy intensity reported for onsite energy use and for primary energy for different composite manufacturing processes is illustrated in table 5.1.

Table 5.1: Energy Intensity of Forming (MJ/kg) [59]–[62]

Process	Primary energy	Onsite energy
Autoclave moulding	66.8	22.3
Hand lay-up	57.7	19.2
Spray up	44.8	14.9
RTM	38.4	12.8
VARI	30.6	10.2
Cold press	35.4	11.8
Preform matching die	-	10.1
SMC	-	3.5
Filament winding	8.1	2.7
Pultrusion	9.3	3.1
Compression moulding	34.3	11.4
Injection moulding	33.7	11.2
Prepreg	120.1	40.0
Sheet moulding	10.5	3.5

The current standards do not provide complete guidance and do not address important issues regarding embodied energy reporting. For example, EN 15804 standard does not mention embodied energy, although it does require the reporting of energy inputs as primary energy and requires the reporting of the following categories describing resource use:

• Use of renewable primary energy excluding renewable primary energy resources used as raw materials

• Use of non-renewable primary energy excluding non-renewable primary energy resources used as raw materials

It is important to distinguish between **embodied energy**, which is associated with the production of a good or service and the **inherent (or embedded) energy**, which is a physical property of the material. The terms embodied and embedded are sometimes confused in the literature. As noted previously, the embodied energy of a material is the primary energy that is associated with the extraction, processing, and transportation of that material from the cradle to the factory gate. In contrast, the embedded energy of a material is a property of that material and can be directly measured. For example, the inherent energy in a wood product can be recovered at the end of its life cycle by incineration, whereas the inherent energy of concrete is zero. The inherent (embedded) energy is reported in EN 15804 in the following categories:

• Use of renewable primary energy resources used as raw materials

• Use of non-renewable primary energy resources used as raw materials

However, different LCA practitioners report data for these categories in different ways. In addition, the inherent energy is reported as primary energy in these categories, which does not necessarily represent the true value of the recoverable energy.

5.2   LCA of Composites

5.2.1   Composite manufacture

A review of the currently available data has been given previously. There is additionally data for prepreg production given by Suzuki and Takahashi (2005) [62] as can be seen in Table 5.2. This gives the impact associated with the production process and does not include the materials. The EuCIA EcoCalculator [51] tool can also be used to calculate impacts for composite production using the following processes: Pultrusion, Resin infusion (RI), Resin transfer moulding (RTM), SMC compounding, SMC compression moulding, Thermoplastic compounding, Long Fibre Thermoplastics compounding, Thermoplastic injection moulding. However, at the time of writing, the Eco calculator tool does not include these processes: Centrifugal casting, Filament winding, Spray-up, Pre-forming, Pre-preg autoclaving, BMC compounding BMC injection moulding.

Table 5.2: Energy Intensity of Prepreg Production [62]

Process	EE (MJ/kg)
Resin blending	0.1
Resin coating	1.4
Resin impregnation	2.1
Prepreg winding	0.2
Atmosphere control	20.8
Raw material storage	11.5
Prepreg storage	3.4
Release paper production	0.5

Note that the EuCIA EcoCalculator [51] tool was interrogated to determine the impacts that are assigned to different processing technologies. This was evaluated by setting the imaginary composite composition to **0.5 kg of glass fibre rovings and 0.5 kg of unspecified polyester resin** and including different processes, with the results shown in Table 5.3. The columns labelled 'difference' give the impacts associated with the process only.

Table 5.3: Environmental impacts associated with processing

Process	EE (MJ/kg)	Difference (MJ/kg)	GWP (kg CO_2e/kg)	Difference (kg CO_2e/kg)
Resin infusion	78.12	18.41	4.23	1.25
RTM	66.10	6.39	3.31	0.33
Pultrusion	68.66	8.95	3.55	0.57
No process	59.71	0.00	2.98	0.00

The values obtained for the embodied energy associated with the processes are considerably less than those reported in table 5.4. The reasons for this are not known at present. A search of the literature for LCA of composite manufacturing has revealed the data shown in Table 15.

Table 5.4. Embodied energy and GWP of composite manufacture

Composite	EE (MJ/kg)	GWP (kg CO_2e/kg)	Reference
CF-EP	200	11.2	Rydh and Sun (2005) [63]
CF-EP	-	26.7-34.5	Bachmann et al. (2017) [64]
CF-EP	315.0	10.10	Kara and Manmek (2009) [65]
GF-PE	169.69	-	Song et al. (2009) [59]
GF-UP	11.0	1.11	Kara and Manmek (2009) [65]
GF-PE	12.0	0.60	Kara and Manmek (2009) [65]
GF-PE+VE	26.1	0.79	Kara and Manmek (2009) [65]
GF-VE	26.0	1.23	Kara and Manmek (2009) [65]
GF-VE	14.0	0.57	Kara and Manmek (2009) [65]
GF-PE-SMC*	-	1.99	Witik et al. (2011) [66]
CF-SRIM*	-	48.06	Witik et al. (2011) [66]

CF=carbon fibre, GF=glass fibre, EP=epoxy, UP=unsaturated polyester, VE=vinyl ester, SMC=sheet moulding compound, SRIM=structural reaction injection moulding, *vehicle bulkhead manufacture

The data supplied in the report of Kara and Manmek (2009) [65], gives EE and GWP values for GF reinforced composites that appear to be quite low, given the values reported for resins and composites

reported elsewhere in this report. The data that they reported was obtained by working with five composite manufacturers in Australia and are the cradle to factory gate analyses including transportation of raw materials. Further work will be conducted to examine the impacts associated with composite manufacture.

5.3 LCA of Resins

5.3.1 Epoxy resins

The most common commercially used epoxy resins are bis-A epoxy (bisphenol-A diglycidyl ether epoxy) and novalac epoxy (epoxylated phenol-formaldehyde novalac). Bisphenol-A is synthesised by the condensation reaction of acetone with two molecules of phenol. The products of the cumene process (acetone and phenol, derived from the reaction of benzene with propylene) can be used to produce bisphenol A.

Table 5.5. LCA data for epoxy resins

Material	EE (MJ/kg)	GWP (kg CO_2e/kg)	Reference
Epoxy	76-137	4.7-8.1	Bachmann et al. (2017) [20]
Epoxy	76.0	-	Suzuki and Takahashi (2005) [62]
Epoxy	137.1	8.1	Plastics Europe (2005)
Bisphenol-A	80.1	2.54	Plastics Europe (2011)
Epoxy	77.4	-	US DoE (2016) [61]
Epoxy	76-80	-	Song et al. (2009) [59]
Epoxy	137.1	5.7	Rankine (2006) [67]
EP Curing Agent-Ethylenediamine	124.6	6.3	Eu CIA (2014) [51]
EP Curing Agent-Phthalic Anhydride	78.2	2.7	Eu CIA (2014)
EP Resin	135.0	6.8	Eu CIA (2014)

5.3.2 Polyester Resin

Polyester resins are generally manufactured by the reaction of saturated or unsaturated dibasic acids, or acid anhydrides (see Appendix A) with di-functional alcohols (Appendix B). The unsaturated polyester backbone is formed by a condensation reaction of the two components. Once the polyester backbone is formed it is dissolved in a reactive diluent, for which styrene is usually used, but acrylates or methacrylates can be used in speciality resins. The resin is cured by reaction of the unsaturated polyester chains with styrene in a free-radical process, using a peroxide (e.g., methyl ethyl ketone peroxide, MEKP) initiator, plus a reducing agent (typically a cobalt salt). By varying the ratio of saturated to unsaturated di-acids, it is possible to control the cross-link density and hence the rigidity of the thermoset polymer. Over 2 million tonnes of polyester resins are manufactured per year globally. Fillers are very often added at up to 40-50% weight to reduce cost and the vapour permeability of the resin. Flake glass, or silane treated micaceous iron oxide are often preferred as

fillers. The ester linkages in the polyester backbone are susceptible to hydrolysis when water penetration occurs.

Table 5.6. LCA data for polyester resins

Material	EE (MJ/kg)	GWP (kg CO_2e/kg)	Reference
Unsaturated polyester	62.8	-	Suzuki and Takahashi (2005) [62]
Unsaturated polyester	63-78	-	Song et al. (2009) [59]
Unsaturated polyester	110	-	Wang et al. (2013) [68]
Unsaturated polyester	87.8	3.79	EuCIA [51]
UP DCPD based	77.0	2.93	EuCIA [51]
UP DCPD based	90.2	3.06	Rietveld and Hegger (2014)
UP isophthalic acid based	91.7	4.13	EuCIA [51]
UP isophthalic acid-based	86.9	4.15	Rietveld and Hegger (2014)
UP orthophthalic based	94.6	4.19	EuCIA [51]
UP orthophthalic based	92.5	4.32	Rietveld and Hegger (2014)
UP maleic based	87.9	3.93	EuCIA [51]
UP maleic based	76.9	3.11	Rietveld and Hegger (2014)
Polyester	103.8	-	Bath ICE database

5.3.3 Vinyl ester resins

Vinyl ester resins are produced by the reaction between an epoxy resin and an unsaturated carboxylic acid and are more expensive than polyester resins. Vinyl esters are more damage-tolerant compared with polyesters and are more resistant to water penetration, they exhibit less shrinking on curing and exhibit better bonding to core materials so de-lamination is less of an issue. The reduced number of ester linkages in the backbone makes the cured resin less susceptible to hydrolysis compared to a polyester resin.

Table 5.7: LCA data for vinyl ester resins

Material	EE (MJ/kg)	GWP (kg CO_2e/kg)	Reference
VE Resin (BPA epoxy based)	121.5	5.97	Eu CIA [51]
Bisphenol-A VE	119.3	5.87	Rietveld and Hegger (2014)

5.4 LCA of Reinforcement

5.4.1 LCA of Glass Fibre

The most common type of glass fibre used for composites is E-glass, which is an alumina-borosilicate glass with low levels of alkali oxides. However, E-glass fibres are susceptible to chloride ion attack and are unsuitable for marine applications. Other types of glass fibres produced are R-glass, A-glass, AR-glass, T-glass, ECR-glass and C-glass. R-glass fibres are used for higher strength applications such as building or aerospace applications (these are referred to as S-glass fibres in the US). C-glass and T-glass fibres are used for thermal insulation products. In the first stage of glass manufacture the different ingredients are accurately weighed into a mixing vessel where they are combined in the batch house. After mixing, the ingredients are transferred to a furnace where they are heated to temperatures around 1400oC. Differences in energy intensity (reported as MJ per kg fibre) and Global Warming Potential (kg CO2e per kg fibre) are illustrated in table 5.8.

Table 5.8: LCA data for glass fibre production

EE (MJ/kg)	GWP (kg CO_2e/kg)	Reference
19.9	-	US DoE (2016) [61]
13-32	-	Song et al. (2009) [59]
45.6	2.5	Bachmann et al. (2017) [64]
21.1	-	Bachmann et al. (2017) [64]
13-32	-	Bachmann et al. (2017) [64]
45	-	Bachmann et al. (2017) [64]
10.3	-	Bachmann et al. (2017) [64]
31.6	2.16	EuCIA [51]
28	1.54	Bath ICE database

GlassFibreEurope, the European Glass Fibre Producers Association have published the results of an LCA study of glass fibre production. The impact was mainly associated with the glass melting stage of the production process (17.1-20.5 MJ/kg and 1.03-1.44 kgCO2e/kg).

Table 5.9: LCA data from the GlassFibreEurope study (GEF 2016)

Fibre type	EE (MJ/kg)	GWP (kg CO_2e/kg)
Dry chopped strands	27.6	1.42
Wet chopped strands	24.4	1.23
Rovings	24.5	1.29
Assembled rovings	33.9	2.09
Mats	40.5	1.78

5.5   LCA of Carbon Fibre

About 90% of carbon fibres are made from poly(acrylonitrile) (PAN) fibre precursors, with the remainder made from rayon of pitch. Before the fibres are carbonised, they are pre-heated at 200-300°C in air for 30-120 minutes. After this stabilisation process, they are carbonised by heating at

1,000-3,000oC in an inert atmosphere for several minutes. After carbonisation, the fibres may then be surface treated to improve bonding properties.

Table 5.10: LCA data for carbon fibre production

EE(MJ/kg)	GWP (kg CO_2e/kg)	Reference
436	-	Suzuki and Takahashi (2005)
247	-	Suzuki and Takahashi (2005)
704	31.0	Das (2011)
183-286	-	Song et al. (2009)
478.5	29.7	Bacnmann et al. (2017)
285.9	20.5	Bacnmann et al. (2017)
286	22.4	Bacnmann et al. (2017)
1122	53	Bacnmann et al. (2017)
286-704	24.4-31	Bacnmann et al. (2017)
198-594	-	Pimenta and Pinho (2011) quoting Carberry (2009)

5.6 Recyclability – approaches supply chain review

5.6.1 Composite material recycling technology

In recent years, a few significant events took place that added immensely to the sociotechnical push for developing sustainable composite recycling solutions, namely (1) a ban on composite landfilling in Germany in 2009 [69], (2) the first major wave of composite wind turbines reaching their End-Of-Life (EoL) and being decommissioned in 2019–2020 [70], (3) the acceleration of aircraft decommissioning due to the COVID-19 pandemic (mass decommissioning of aircrafts expected in the 2020s decade) [71], and (4) the increase of composites in mass production cars, thanks to the development of high volume technologies based on thermoplastic composites [69], [72]. Stella Job reported already back in 2014 to Reinforced Plastics journal that a barrier to the increased use of glass fibre reinforced (GFRP) and carbon fibre reinforced polymer (CFRP) composites is the lack of recycling facilities [73]. The increased use of CFRPs and GFRPs in the industry coupled with landfill disposal restrictions and bans has resulted in a need to develop effective recycling technologies for composites [74]. It is only logical to conclude, that such sociotechnical pressure will only grow in the upcoming years as other EU countries are to follow Germany by banning landfill options [69], by the growth of the composite markets, increase in composite production rates and composite structure installations (see Figure 23), and by the ever-growing number of expired wind turbines waiting to be incinerated or recycled. The latter is especially certain, as the decommissioning intensity will follow the historical increasing-by-year number of installed wind turbines [69]. Therefore, the key drivers to develop the outmost sustainable composite recycling technologies are without a doubt crucial to the survival and viability of the composite industry, and it is expected that such trend will become more and more prominent in the current decade of 2020s.
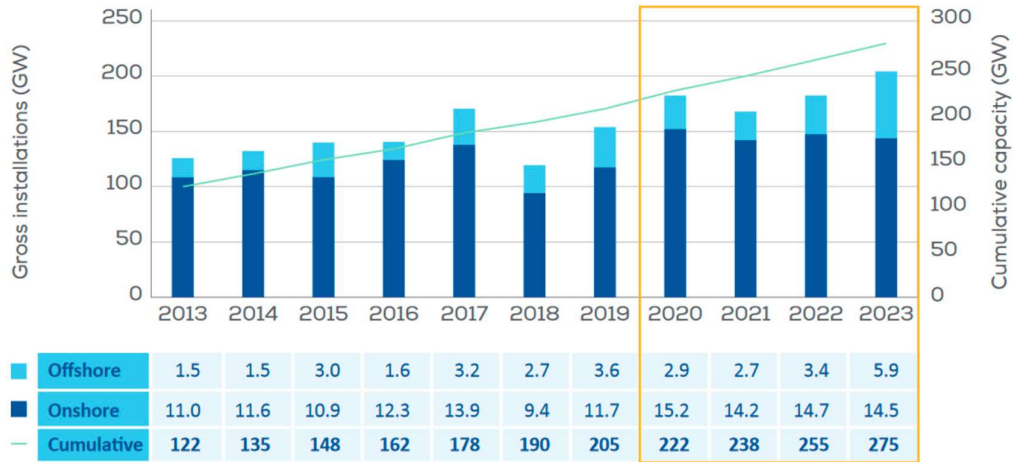
Figure 23. Gross annual wind turbine installations in Europe[69].

	2013	2014	2015	2016	2017	2018	2019	2020	2021	2022	2023
Offshore	1.5	1.5	3.0	1.6	3.2	2.7	3.6	2.9	2.7	3.4	5.9
Onshore	11.0	11.6	10.9	12.3	13.9	9.4	11.7	15.2	14.2	14.7	14.5
Cumulative	122	135	148	162	178	190	205	222	238	255	275

5.6.2 Wind Energy

In wind energy, composites are employed in blades, thanks to their high specific strength. It was reported by Global Wind Energy Council (GWEC), that there are more than a third of a million utility scale wind turbines installed around the world, most of which are designed for service life of 20–25 years. Turbines from the first major wave of wind power in 1990s are reaching the end of their life expectancy nowadays and in the decade of 2020s [75]. Therefore, the looming issue of recycling of the expired FRP blades, about two gigawatts worth of turbines were already expected to be refitted in 2019 and 2020 [70]. For instance, Denmark was one of the major players in the early wind energy adoption and is becoming one of the first countries to face the bulk disposal challenge [75]. For sustainability purposes, some EU countries have banned disposal in landfills of composite blades [69], so new EoL solutions for composites are required to emerge and develop in this industry. Disposing of composite wind turbine blades in an environmentally friendly way is a year-by-year growing problem [70]. With the increase in the application of renewable energy, wind turbine blade waste has a high tendency to increase [1]. According to Amaechi et al. and Liu et al. [72], [76] the usage of blade material waste is expected to grow from 1,000,000 t in 2020 up to 2,000,000 t in 2030, doubling in the current 2020s decade's time. It is predicted that a quarter of this EoL waste will be in Europe [77].

Most turbine rotors have three blades, ranging in size from 12 m (early wind turbines) up to 80 m in length—and some even larger—today. Many of these rotor blades will soon turn into the EoL items [75]. A longer blade examples include Siemens Gamesa Renewable Energy (SGRE)—14 MW wind turbines with 108 m long IntegralBlades and a rotor diameter of 222 m. Recycling will become an even more pressing matter in the 2020s—today around 85 to 90% of wind turbines' total mass can be recycled, and there are about 2.5 million t of composite material are currently in use in the wind energy sector, globally. According to WindEurope, there will be around 14,000 blades (about 40,000–60,000 t) planned for decommissioning by 2023. Recycling these old blades is a top priority for the wind industry [69]. This challenge requires both logistical and technological solutions for disassembling, collection, transportation, waste management and reintegration of the composite materials and/or structures into the value chain [69]. The recycling of composite materials will therefore play an especially important role in the 2020s and further in the future, not only for the wind energy, but also

for aerospace, automotive, construction and marine sectors to reduce environmental impacts and to meet the demand. Another very recent potential driver—presented in November 2020—which could affect the composite industry is a recent plan of a "Green Industrial Revolution"—UK's vision to completely ban sales of new gasoline and diesel cars in the UK by the end of 2020s, creating up to 250,000 jobs in energy, transport, and technology [78]. It will very likely have a major impact on the automotive and energy sectors, also affecting the composite industry.

5.6.3   Current Industrial End-of-Life Solutions for Composite Materials

For many composite structures, for example wind turbines, the EoL is approaching. The question arises naturally: What to do with "spent" composite materials? This leads us to three major current options: (1) Landfill, (2) Incineration or (3) Recycling [79]. The question of how to dispose of EoL composite parts is growing in importance. "Can EoL thermoset composite parts and production waste be recycled?" According to Amanda Jacob, the frequency of these questions is growing with every year, indicating that the composites industry and its customers are no longer content with the traditional disposal routes of landfill and incineration [80]. There are also geopolitical drivers behind this trend, traditional disposal routes such as landfill and incineration are becoming increasingly restricted and banned, and composites companies and their customers are looking for more sustainable solutions according to the European Composites Industry Association (EuCIA) [81]. The composites industry is facing growing environmental pressures. As the industry continues to grow and the volume of FRPs used increases, so does both production scrap and EoL waste [81].

The three main EoL solutions of treating composite waste are landfill disposal, incineration, and recycling. The impact of each was well represented by Oliveux et al. in a 2015 article [82] and is shown in figure 24. Although landfills are the most common and cheapest technique for discarding the non-biodegradable FRP waste, it is creating a negative impact on the environment and ecosystem [79].
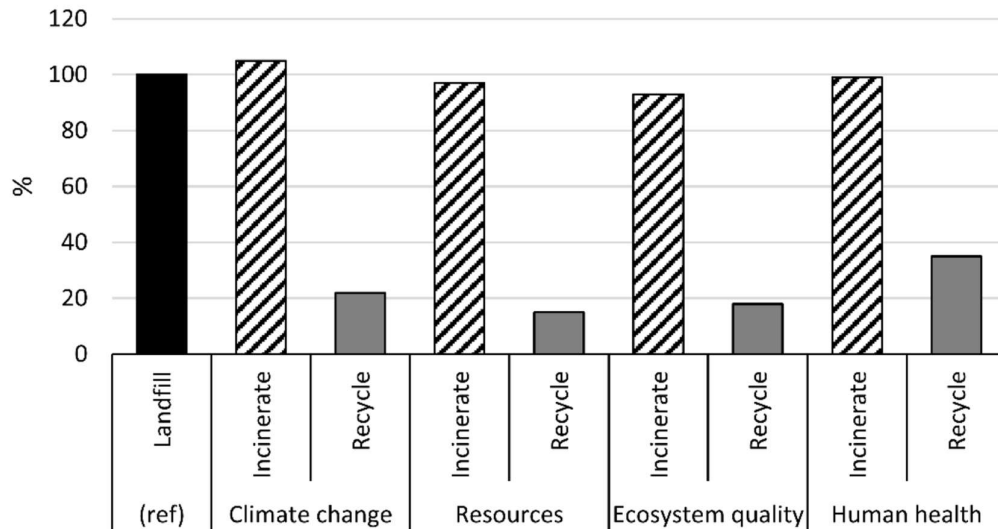
Impact comparison: landfill, incineration and recycling

Figure 24. The impact comparison of landfill disposal, incineration, and recycling [82].

Landfill

Landfill is a relatively cheap disposal route, but it is the least preferred waste management option under the European Union's (EU)Waste Framework Directive. Landfill of composite waste is already banned in Germany (in 2009) and other EU companies are expected to follow this route [69], [80]. However, globally still most of GF manufacturing waste is landfilled. Approx. 70% of reinforcement GF is used to manufacture thermoset based GFRPs, which also produces approx. 15% manufacturing waste [83]. Most of the production and EoL waste in the UK is landfilled, and up to 90% of the GFRP waste is landfilled [82]. In the Netherlands, under the third edition of the National Waste Management Plan landfilling of composite waste is banned "in principle". However, wind farm operators can benefit from an "exemption" if the cost of alternative treatment is higher than 200 €/t. According to a survey conducted by WindEurope [84], the cost of mechanically recycling wind turbine blades in the Netherlands ranges between 500–1000 €/t including onsite pre-cut, transport, and processing. Mechanical recycling itself costs between 150–300 €/t. Therefore, landfilling is still practiced [69].

Incineration

Incineration is a waste treatment process that is based on the combustion of organic substances contained in waste materials. It is another common method of disposal of FRP. However, in this process around 50% of the composite waste remains as ash and must be landfilled [80]. The cost for landfill and incineration is also expected to increase over the coming years. Many initiatives have looked at the mechanical recycling of glass fibre composites. In this route, the waste composite is broken up and then ground into small particles. The resulting mixture of fibre, polymer and additives is then re-used in other products. use as a filler in sheet and bulk moulding compounds (SMC/BMC) and in asphalt and concrete reinforcement [80].

Recycling

Energy demand involved in composite recycling methods is the following, sorted from the highest to the lowest: Chemical recycling (21–91 MJ/kg); Pyrolysis (24–30 MJ/kg); Microwave Pyrolysis (5–10 MJ/kg); Mechanical recycling (0.1–4.8 MJ/kg) [82]. Recycling of FRPs can be done without fibre/matrix separation, in this case the material can be chopped for example and be reused as a filler for other applications, in this case a part of the material's value is lost, due to the non-directional properties of the material finally obtained from the recycling process, however this is a relatively inexpensive process, as it relies on material chopping (mechanical recycling). Other recycling methods involve the separation of the matrix from the fibres. Such processes are more complex and expensive, but provide more value, as new directionally reinforced parts or structures can be made.

It is worth noting that out of the two main constituent phases (fibres and matrix), usually the fibres are the most valuable. Nevertheless, recycling the matrix material can still be advantageous, provided that the recycling process costs are lower than the cost of purchase for new material. This introduces another sub-categorization of recycling methods, the ones that enable re-use of the fibres and the ones that enable re-use of the matrix.

Currently the most common method in the industry for the recycling of FRPs is by pyrolysis. While not fully certain, according to Amaechi et al., it is not economically viable to recycle thermoset CFRPs using pyrolysis, while thermoset GFRPs are mostly considered [82]. ELG Carbon Fibre is the world's first commercial CF recycler [77]. ELG Carbon Fibre process (modified pyrolysis): initially involves metal removal and cutting of large structures down to sizes suitable for down-stream processing—shredding of laminates and prepregs. Then, for recovery via modified pyrolysis (resin is burned off). CF is then converted through milling, nonwoven mat production and pelletization. Feedstock is primarily unused prepregs, but the process also suits cured production waste and EoL materials [85]. In chemical approaches, often long-term heat treatment and/or high pressure are required. On the other hand, the pyrolysis approach, which is considered an environmentally unfriendly and high energy-consuming method, is usually a distractive method for the GFs recycling [86]. Samsung Venture Investment corporation has invested in Connora Technologies to help it commercialize its chemical recycling "Recyclamine recyclable epoxy thermoset technology", a green chemistry platform that provides a method of making and recycling composite waste materials and products [87].

Industrial Composite Recycling —Current Recycling End-of-Life Solutions

Industrial recycling applications—Higher Technology Readiness Level (TRL) technologies— which are already implemented in the recycling facilities are briefly discussed in this subchapter. Current EoL recycling solutions available industrially are only those options that have already reached high TRL and are summarized in this section. The in-detail description of respective composite recycling technologies and their detailed spectrum from low to high TRL, as well as the comparison of the techniques, are discussed in the next section. In figure 25 End-of-Life (EoL) scenarios of carbon fibre/glass fibre–reinforced composites are presented schematically.
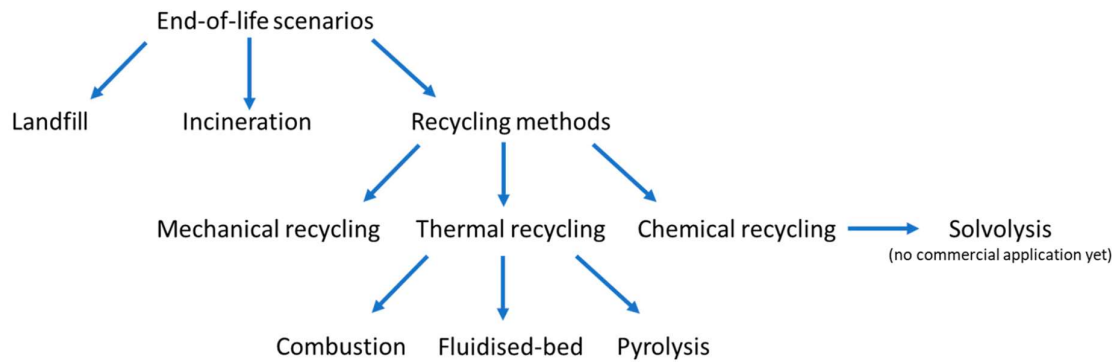
Figure 25. Representation of End-of-Life (EoL) scenarios of carbon fibre/glass fibre–reinforced composites.

Industrial Mechanical Recycling and Cement Kiln Method

Mixt Composites Recyclables (Tournon-sur-Rhône, France, ground GFs, used as reinforcement in asphalt, concrete, chipboards and rFRPs), Filon Products Ltd. (Burntwood, UK, ground GFRPs incorporated in their end products), Hambleside Danelow (Daventry, UK, ground GFRPs reused in their rFRPs, developed a process for mechanically recycling GRP to retain fiber length), Reprocover (Mechelen, Belgium, composite covers, street furniture, etc.), Fiberline-Zajons-Holcim (Middelfart, Denmark and Melbeck, Germany, cement kiln method), Eco-Wolf (Edgewater, FL, USA, grinding GFRPs and pro, uctionb of fibers for spray-up equipment), Procotex (Mouscron, Belgium, carbon, aramid, PEEK and natural fibers) and Apply Carbon (Laguidic, France, milled and cut carbon), Extreme EcoSolutions (Nijkerk, Netherlands, shredding and grinding GRPs to powder) [73], [82].

Industrial Thermal Recycling

ELG Carbon Fibre (West Midlands, UK, world's first commercial CF recycler, unsized milled and chopped fibres, modified pyrolysis), Materials Innovation Technologies MIT-RCF (Fletcher, NC, USA, fibre reclamation and use in preforms and finished parts), Karborek Spa (Martignano, Italy, milled and chopped CFs, 95% rCF composite multi-layered felts), CFK Valley Stade Recycling GmbH and carboNXT GmbH (Wischhafen, Germany, chopped and milled fibres), Hadeg Recycling Ltd. (Stade, Germany, short fibres mainly), ReFiber ApS (Roslev, Denmark), Japan Carbon Fiber Manufacturers Association (Ohmuta, Japan, pyrolysis and grinding), Firebird Advanced Materials (Raleigh, NC, USA, microwave-assisted pyrolysis), Formoso Technologies Group (Madrid, Spain, treatment ofbcomposite waste such as GF fabric, carbon fiber rolls, uncured prepregs and cured parts, recovery of fibers and oil for energy supply from the resins), Carbon Fibre Recycle Industry Co Ltd. (Kani Gun, Japan, thermal decomposition of CFRP waste by a self-combustion process) [73], [77], [82].

Industrial Chemical Recycling

Adherent Technologies (Albuquerque, NM, USA, 3-step process combining pyrolysis and solvolysis), Panasonic Electric Works Co. (Kadoma, Japan, hydrolysis, recovery of monomers and copolymers, recovery solid fractions such as fibres and fillers), SACMO (Holnon, France, solvolysis), Siemens AG

(Munich, Germany, solvolysis), Innoveox (France, solvolysis hydrothermal oxidation) [82]. Future Innoveox (Paris, France, promising methods also include the Vitrimer method— a very promising method for reusing fibre mats [88].

Recycling and recovery treatment methods SWOT

Today, the main technology for recycling composite waste is through cement co-processing, also known as the cement kiln route. Composite materials can also be recycled or recovered through mechanical grinding, thermal (pyrolysis, fluidised bed), thermo-chemical (solvolysis), or electro-mechanical (high voltage pulse fragmentation) processes or combinations of these. These alternative technologies are available at different levels of maturity and not all of them are available at industrial scale, as shown by the technological readiness levels (TRL) presented in the tables below for each existing treatment method [89], [90]. The processing methods also vary in their effects on the fibre quality (length, strength, stiffness properties), thereby influencing how the recycled fibres can be applied. The wind industry is pushing for the development and industrialisation of alternative technologies to provide all composite-using sectors with additional solutions for end of life. The following section presents recycling technologies currently in practice or under investigation for composite recycling and applicable for wind turbine blades. The recycling technologies, their strengths, and limitations as well as points of attention (related to health and safety) are listed for each process. The latter are expected to already be addressed accordingly by the industry and therefore don't require further statements [90].

Cement co-processing (Cement kiln route)

In cement co-processing the glass fibre is recycled as a component of cement mixes (cement clinker). The polymer matrix is burned as fuel for the process (also called refuse-derived fuel), which reduces the carbon footprint of cement production. Cement co-processing offers a robust and scalable route for treatment of composite waste. It also has a simple supply chain. Wind turbine blades can be broken down close to the place of disassembly thus facilitating transport to the processing facility. Although it is very promising in terms of cost-effectiveness and efficacy, in this process the fibre shape of the glass disappears and therefore cannot be used in other composites applications [90].
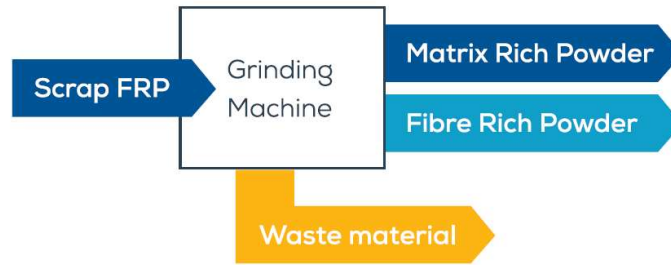
TRL	STRENGTHS	DISADVANTAGES	POINTS OF ATTENTION
9	• Highly efficient, fast and scalable • Large quantities can be processed • Capability to reduce CO_2 emissions of cement manufacturing by up to 16% • Slightly increasing energy efficiency of cement manufacturing • No ash left over	• Loss of original fibre's physical shape	• Pollutants and particulate matter emissions (although appropriate mitigation exists in compliance with the Industrial Emissions Directive) • So far only suitable for glass-reinforced composites

Figure 26. SWOT analysis of cement co-processing method.

Mechanical grinding

Mechanical grinding is a commonly used technology due to its effectiveness, low cost, and low energy requirement. It does however drastically decrease the value of the recycled materials. The recycled products, short fibres, and ground matrix (powder) can be used respectively as reinforcement or fillers. Because of the deterioration of the mechanical properties, the incorporation level of filler material is extremely limited in thermoset composite applications (less than 10%). For re-use of the fibres as reinforcement in thermoplastic applications, the variation in composition and potential contamination with resin particulates has a negative impact on reinforced thermoplastic resin manufacturing speed and thermoplastic resin quality. This could be minimised if the separating and dismantling processes were upgraded and could be suitable in cases where no more value retention is possible [90].
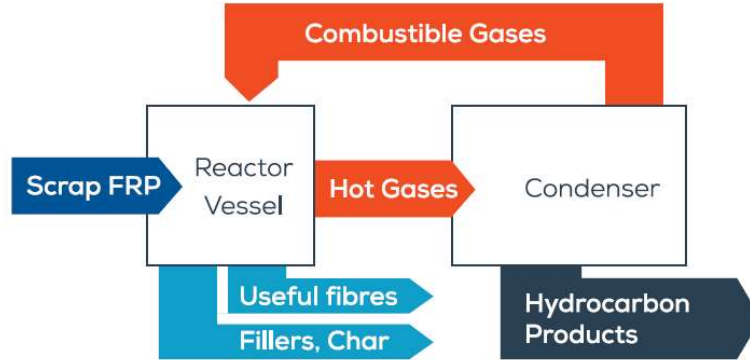
TRL	STRENGTHS	DISADVANTAGES	POINTS OF ATTENTION
Glass fibre: 9 Carbon fibre: 6/7	• Efficient and high throughput rates	• Not competitive (yet) with use of virgin raw materials • Quality of recyclates compromised due to the high content of other materials • Up to 40% material waste generated during grinding, sieving and processing • Consequently, large volume applications not (yet) developed	• Requires dedicated facilities with closed area to limit dust emissions

Figure 27. SWOT analysis of mechanical grinding method

Pyrolysis

Pyrolysis is a thermal recycling process which allows the recovery of fibre in the form of ash and of polymer matrix in the form of hydrocarbon products. Although it allows for the lowest value loss from industrial-scale technologies, there is still a loss of value. Matrices are turned into powder or oil, potentially useable as additives and fillers. The fibre surface is often damaged due to the high temperatures, resulting in a decrease in mechanical properties. Pyrolysis requires high investment and running costs [89], [90]. Economic viability depends on the scale and re-use that the matrix-obtained chemicals can have. To date, this recycling technology is only economically viable for carbon fibres. It is, however, not currently implemented at large scale since the volumes of carbon fibre reinforced composites are low. With the next generation of mega-turbines, the required weight reduction and mechanical properties will enhance the preferred use of carbon fibre composites and the market volume might grow accordingly.
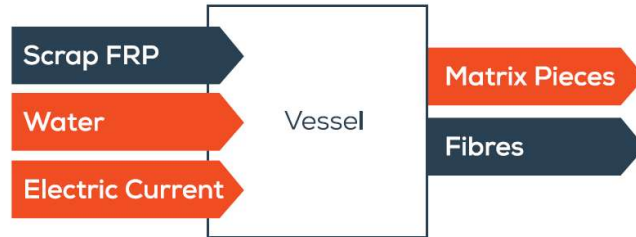
TRL	STRENGTHS	DISADVANTAGES	POINTS OF ATTENTION
Pyrolysis: 9 Microwave: 4/5	• The bi-products (Syngas and oil) can be used as energy source or as base chemicals/building blocks • Easily scaled-up • Microwave pyrolysis: Easier to control. Lower damage to the fibre • Already used at commercial scale for recycling carbon fibre composites	• Fibre product may retain oxidation residue or char • Loss of strength of fibre due to high temperature • Decreased quality of the recovered carbon fibres from original material (lowest value loss in comparison to other mature recycling technologies)	• Economically sound for carbon fibre recovery to date

Figure 28. SWOT analysis of pyrolysis method

High voltage pulse fragmentation

High voltage pulse fragmentation is an electro-mechanical process that effectively separates matrices from fibres with the use of electricity. However, only short fibres can be recovered from the process and obtaining quality fibres requires high levels of energy, an issue that could be overcome by operating at higher rates. Compared to mechanical grinding, the quality of the fibres obtained is higher; fibres are longer and cleaner [89], [90].
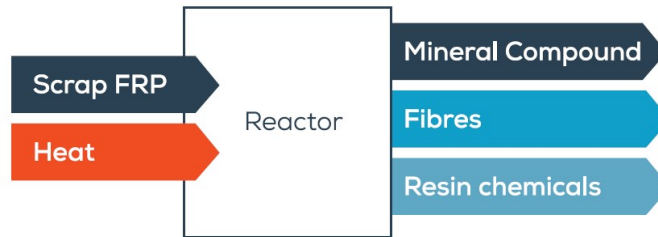
TRL	STRENGTHS	DISADVANTAGES	POINTS OF ATTENTION
6	• Potential to be scalable to treat large amounts of waste • Low investments required to reach the next TRL	• Only laboratory- and pilot-scale equipment are available • Decreased quality of the recovered glass fibres from original material	• Size of the available installations might be suboptimal to recycle the current stock of wind turbine

Figure 29. SWOT analysis of high voltage pulse fragmentation method.

Solvolysis

Solvolysis is a chemical treatment where solvents (water, alcohol and/or acid) are used to break the matrix bonds at a specific temperature and pressure. Solvolysis offers many possibilities due to a wide range of solvent, temperature, and pressure options. Compared to thermal technologies, solvolysis requires lower temperatures to degrade the resins, resulting in a lower degradation of fibres. Solvolysis with super-critical water seems to be the most promising technology since both fibres and resins can be retrieved without major impacts on their mechanical properties. Solvolysis is easily scalable but investment and running costs are high and it is still at a relatively low TRL [89], [90]. To date, only the carbon fibres are recycled through solvolysis. However, it is not currently implemented at large scale since the volumes of carbon fibre reinforced composites are low. With the next generation of mega-turbines, the required weight reduction and mechanical properties will enhance the preferred use of carbon fibre composites and the market volume might grow accordingly.
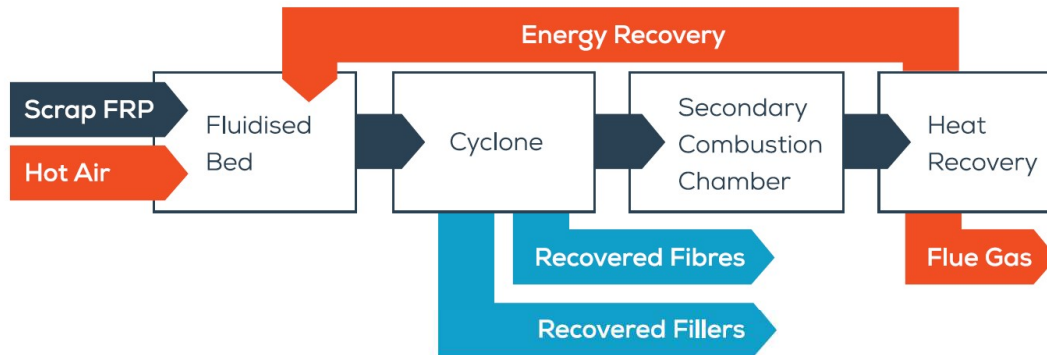
TRL	STRENGTHS	DISADVANTAGES	POINTS OF ATTENTION
5/6	• Recovery of clean fibres at their full length • Soup of resin chemicals produced which can be used as chemical building blocks • Low risk solvents are used such as alcohols, glycols and supercritical water	• High energy consumption due to high temperature and high pressure of some processes • Uses large volumes of solvents, although these are mostly recovered and reintegrated into the process • Decreased quality of the recovered carbon fibres from original material	• To date only the carbon fibres are recycled

Figure 30. SWOT analysis of solvolysis method.

Fluidised bed (Gasification)

The unique characteristic of this process is that it can treat mixed material (e.g., painted surfaces or foam cores), and therefore could be particularly suitable for end-of-life waste [89], [90].

TRL	STRENGTHS	DISADVANTAGES	POINTS OF ATTENTION
5/6	• More tolerant of contamination • Recovery of energy or potential precursor chemicals • High efficiency of heat transfer	• More degradation of fibres than solvolysis/pyrolysis	• Process-related emissions (although appropriate mitigation exists) • Scale-up still needs to be developed

Figure 31. SWOT analysis of fluidised bed (gasification).

Output material quality

The analysis and evaluation of the recovered material properties is related to the baselines defined in the previous sections and linked to the current technology readiness level of each process [90].
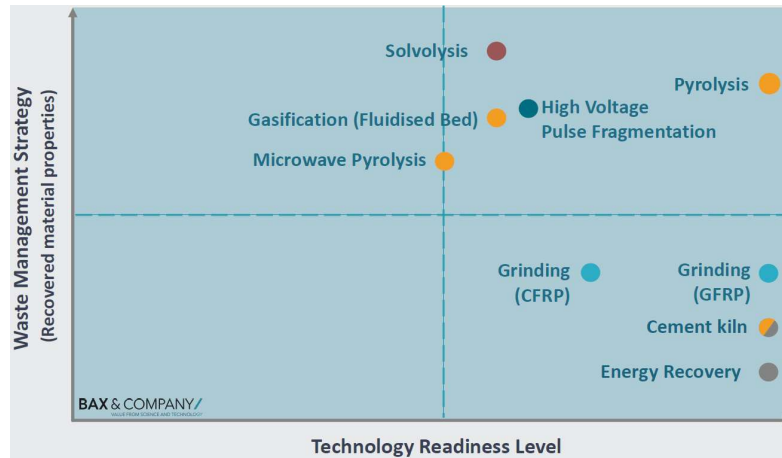
Figure 32. Recovered material properties through different recycling methods against the TRL.

Energy demand and GHG emissions

GHGs are mainly related to the energy demand (electricity and depending on the process also gas or coal) and in some cases to by-products (e.g. gasification: CO_2 is emitted during the process).

Figure 33. Energy demand and GHG emissions.

* The intensity of emissions depends on the energy source. Most processes use (at least partly) electricity, for which we consider the same mix.

Process related costs and material value

Process costs and material value vary significantly even among EU recyclers using the same process due to the influence of several varying process parameters such as: through-put rates/ capacity, temperature, pressure, and retention time in the reactor.
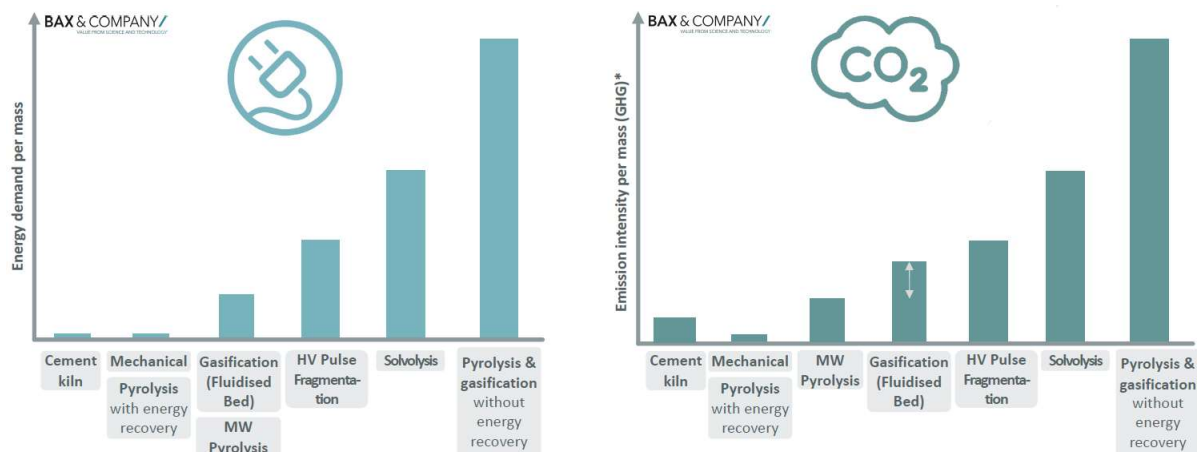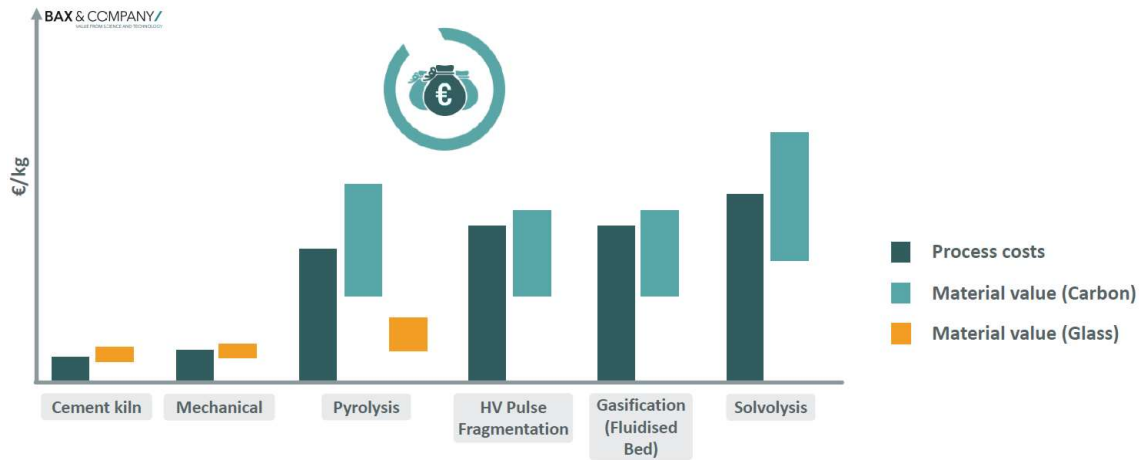

Figure 34. Process related costs and material value as a result from different recycling methods

The aforementioned highlight that while various technologies exist to recycle glass fibre and carbon fibre from wind turbine blades, these solutions are yet to be widely available at industrial scale and to be cost-competitive. In many cases, the recycled material cannot compete with the price of virgin materials. For example, the price of virgin glass fibre (1-2 €/kg) does not make the recovery of fibre as standalone product economically competitive. However, it is envisaged that the recovery of the whole composite materials into chemical building blocks will represent a viable route. This is based on the recovery of pyrolysis oils and of chemicals obtained through gasification, which is happening in other large volume sectors and value chains (i.e., plastic waste).

The size of the bars is indicative and varies among EU recyclers using the same process due to varying process parameters such as throughput rates/capacity, temperature/pressure and retention time in the reactor.

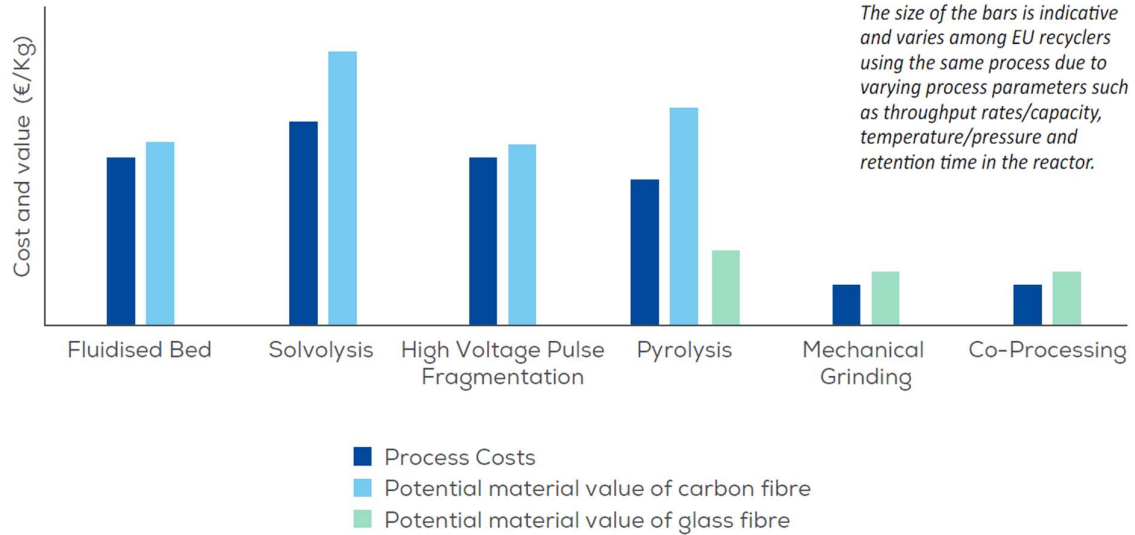Figure 35. Estimated relative costs and values of composite recycling technologies.

The best strategy for wind blades is the one that combines design, testing (according to latest standards to decrease repair and failure rates), maintenance, upgrades (e.g., reinforcement) and the appropriate recycling technology to ensure the maximal value of the material is retrieved throughout its lifetime. It should also systemically allow the re-use of materials for the same or similar purposes (e.g., allows polymer matrices to revert to monomers and avoids fibre damage during the process). Having a good understanding of the environmental impacts associated with the choice of materials during design and with the different waste treatment methods at end-of-life through life cycle assessments will also help define the appropriate strategy.

6   Economic Considerations

6.1   Introduction

Wind energy is recognised as to crucial sector in the future energy supply of the European Union and of the whole world. By 2020, around 180 GW of onshore and offshore wind power could be installed in the European Union; estimates from the European Commission [91] and the European Wind Energy Association [84]); meaning between 10 and 15% of the total EU electricity demand. Worldwide, wind energy will also supply a sizeable amount of electricity – around 16% in 2020, according to the forecasts of the Global Wind Energy Council [92]. Yet the factors that determine the economics of a wind energy farm are not well known to many, and there has been an intense discussion on the reasons behind the recent increase of its generation costs after 20 years of steady reduction.

6.2 Onshore Wind Energy

Onshore wind turbine technology has made significant advances over the past decade. Larger and more reliable turbines, along with higher hub heights and larger rotor diameters, have combined to increase capacity factors. In addition to these technology improvements, total installed costs, O&M costs and LCOEs have been falling as a result of economies of scale, increased competitiveness and maturity of the sector [93].

Onshore wind is now a mature technology, fully commercialised in numerous [94] countries together with an emerging global and regional supply chain, with increasing market expansion in large and smaller emerging economies such as China, India, Morocco and Egypt [94]. At the end of 2018, total wind energy installed capacity reached 540 GW worldwide, providing 5% of total global electricity generated [94]. Recently, in 2018, the levelized cost of energy (LCOE) of onshore wind energy was lower than conventional fossil fuel technologies in Germany [95], and globally had a capacity-weighted average of $0.056/kWh [96]. LCOE is widely used to measure and compare alternative sources of energy and is used by Governments to screen and evaluate policy decisions [97]. Within the analysis of technology innovation, it is important to deepen the understanding of dynamics leading to energy cost reduction in all its parts.

Today, virtually all onshore wind turbines are horizontal axis turbines, predominantly using three blades and with the blades "upwind". The largest share of the total installed cost of a wind project is related to the wind turbines. Contracts for these typically include the towers, installation, and delivery. Wind turbines now make up between 64% and 84% of the total installed costs of an onshore wind project [98]. Indeed, with declining installation costs, the contribution turbines make to the overall share of total installed costs is now trending towards the higher end of the range. The other major cost categories include the installation costs, grid connection costs, and development costs. The latter includes environmental impact assessment and other planning requirement costs, project costs, and land costs – with these representing the smallest share of total installed cost.

illustrates the evolution in average turbine rating and rotor diameter between 2010 and 2018 in some major onshore wind markets. Sweden, Germany, China, and Canada stand out, with increases of greater than 40% in both the average rotor diameter and turbine capacity of their commissioned projects, between 2010 and 2018. In percentage terms, the largest increase in turbine capacity was observed in Ireland (104%) followed by Denmark (71%). The largest increase in rotor diameter occurred in Canada (78%) followed by China (60%). Of the countries considered, on average for 2018, Denmark and Sweden have the largest turbine rating and rotor diameters, respectively, while India had the lowest turbine rating, and the United Kingdom had the lowest rotor diameter. Overall, in 2018 the country-level average capacity ranged from 1.96 MW to 3.59 MW, and rotor diameter from 100 metres (m) to 126 m.

Wind turbine prices reached their previous low between 2000-2002, with this followed by a sharp increase in prices. This was attributed to increases in commodity prices (particularly cement, copper, iron and steel); supply chain bottlenecks; and improvements in turbine design, with larger and more efficient models introduced into the market. However, due to increased government renewable

energy policy support for wind deployment, this period also coincided with a significant mismatch between high demand and tight supply, which enabled significantly higher margins for OEMs during this period.
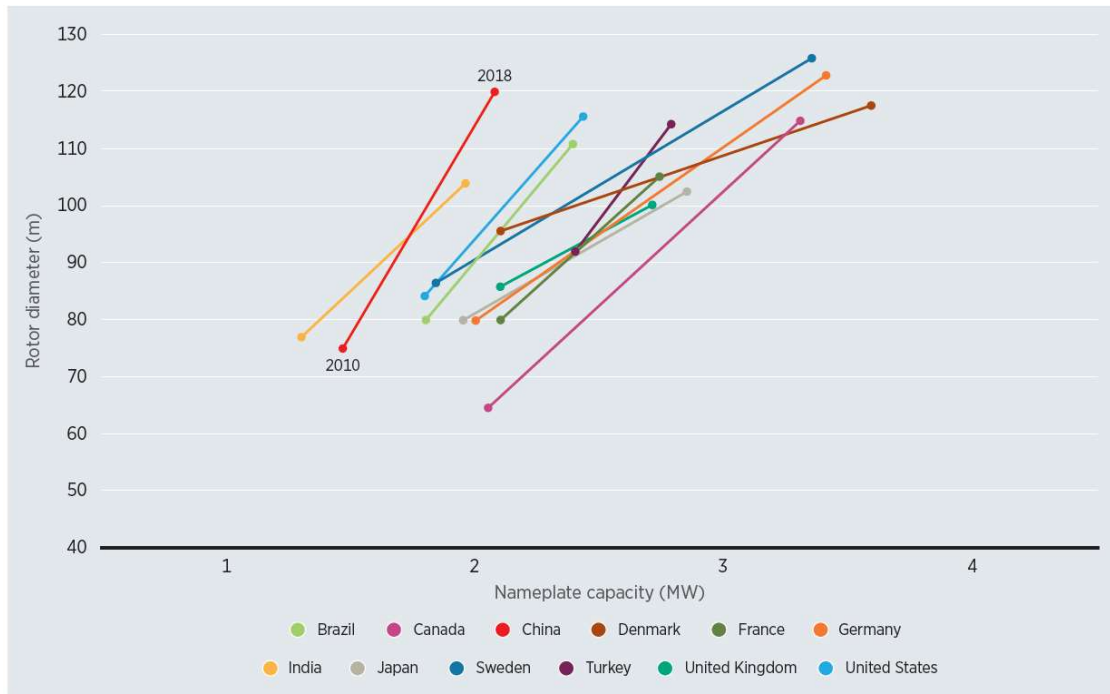
Figure 36. Weighted average rotor diameter and name plate capacity evolution, 2010-2018.

Highlights

- The global weighted-average LCOE of onshore wind fell 39% between 2010 and 2019 from USD 0.086/kWh in 2010 to USD 0.053/kWh in 2019. There was an 9% year-on-year reduction in 2019 [93].
- In 2019, 41 GW (75%) of the new onshore wind projects commissioned had an LCOE lower than the cheapest new source of fossil fuel-fired power generation [93].
- The cumulative capacity of onshore wind has increased more than threefold during the past decade, from 178 GW in 2010 to 594 GW in 2019 [93].
- The global weighted-average total installed cost has fallen by 24%, from USD 1 949/kW in 2010 to USD 1 473/kW in 2019, when it was down 5% on the 2018 value of USD 1 549/kW [93].
- The country/region weighted-average total installed cost for onshore wind in 2019 ranged from around USD 1055 to USD 2368/kW. China and India have weighted-average total installed costs between 21% to 55% lower than other regions [93].
- Average turbine prices fell below USD 850/kW in 2019. Prices in most regions, excluding China, have fallen by between 55% and 65% from their peaks in 2008 and 2009 [93].

- Technology improvements have resulted in an almost one-third improvement in the global weighted-average capacity factor, from 27% in 2010 to 36% in 2019 [93].

6.3   Purpose of the Technoeconomic Model

When evaluating any change to the design and/or fabrication of a wind turbine, it is critical that the designer evaluate the impact of these changes on the system cost and performance. The designer must consider several elements of this process: initial capital cost (ICC), balance of station (BOS), operations and maintenance (O&M), levelized replacement cost (LRC), and annual energy production (AEP). As wind turbines grow and become more sophisticated with increased size, the impact of design on these elements is not always clear. For example, increasing AEP may increase ICC. If one step does not balance out the other, proposed improvements may have a negative overall impact.

The levelized COE has been used to attempt to evaluate the total system impact of any change in design. This levelized COE is calculated using a simplified formula that attempts to limit the impact of financial factors, such as cost of money in wind farm development, so that the true impact of technical changes can be assessed.

6.4   The generation cost of wind energy

The key parameters that govern wind power costs are:

- **Capital costs**, including wind turbines, foundations, road construction and grid connection, which can be as much as 80% of the total cost of the infrastructure over its entire lifetime [99].
- **Variable costs**, the most significant being the operation and maintenance (O&M) of wind turbines, but also including other categories such as land rental, insurance and taxes or management and administration. Variable costs are relatively low and will oscillate around a level of 20% of the total investment [99].
- The **electricity** produced, which in turn depends on the local wind climate, wind turbine technical specifications, site characteristics and power generation reductions. The indicator that best characterizes the electricity-generating capacity of a wind farm is the capacity factor, which expresses the percentage of time that a wind energy farm produces electricity during a representative year [99].
- The **discount rate and economic lifetime** of the investment. These reflect the perceived risk of the project, the regulatory and investment climate in each country and the profitability of alternative investments [99].

It is important to differentiate between the costs of the wind farm in terms of capacity installed, total of capital costs, variable costs, and the cost of wind power per kWh produced, which considers the wind resource.

6.4.1 Capital costs

The capital costs of wind projects can be divided into several categories:

- the cost of the turbine itself which comprises the production, blades, transformer, transportation to the site and installation.
- the cost of grid connection, including cables, sub-station, connection, and power evacuation systems (when they are specifically related to and purpose-built for the wind farm)
- the cost of the civil work, including the foundations, road construction and buildings.
- other capital costs, including development and engineering costs, licensing procedures, consultancy and permits, SCADA (Supervisory, Control and Data Acquisition) and monitoring systems.

As explained in the previous sub-section, wind energy is a capital-intensive technology, so most of the outgoings will be made at this stage. The capital cost can be as much as 80% of the total cost of the project over its entire lifetime, with variations between models, markets, and locations. The wind turbine constitutes the single largest cost component, followed by grid connection.

- Grid connection costs. In the past, most wind farm projects have been connected to the distribution voltage grid (8–30 kV) through low to medium voltage transformers. However, it is becoming more common for wind farms to be connected to the transmission network, which results in higher costs.
- Civil works. The situation is more heterogeneous for this category. Some countries, like Spain report a gradual reduction, which they attribute to the economies of scale that arise when the number and size of the wind turbines per wind farm increases. However, in the United Kingdom [4] the infrastructure costs, including civil works, are expected to remain stable in rea terms up to 2020, whereas in other countries like France they are on the increase.
- Other capital costs. The elements that make up this category include development costs, land costs, health & safety measures, taxes, licenses, and permits, etc. They may be quite high in some areas due to stringent requirements, such as environmental impact assessments. The institutional setting, particularly spatial planning, and public permitting practices, have a significant impact on costs (as well as whether a wind farm is built).

6.4.2 Variable costs

Wind turbines, like any other industrial equipment, require operation and maintenance (O&M), which constitutes a sizeable share of the total annual costs – although the figure is substantially lower than for fossil fuel electricity generating technologies. In addition, other variable costs need to be incorporated to the analysis. The most important variable costs of a wind energy investment are:

- O&M, including provisions for repair and spare parts and maintenance of the electric installation.
- land and sub-station rental.
- insurance and taxes.
- management and administration, including audits, management activities, forecasting services and remote-control measures.

Variable costs are not as well-known as capital costs, and our survey found significant variations between countries, regions, and sites. Few turbines have reached the end of their lifetime, which would allow for a more thorough analysis in this respect. Certain costs can be estimated easily. For insurance and regular O&M, it is possible to obtain standard contracts covering a considerable portion of the wind turbine's total lifetime. Costs for repair and related spare parts are much more difficult to assess, as this information is not readily available.

The local wind resource is by far the most important factor affecting the profitability of wind energy investments and also explains most of the differences in the cost per kWh between countries and projects. Just as an oil pump is useless without a sizable oil field, wind turbines are useless without a powerful wind resource.

The correct micro location of each individual wind turbine is thus crucial for the economics of any wind energy project. In fact, it is widely recognised that during modern wind industry's infancy (1975–1985), the development of the European Wind Atlas Methodology was more important for productivity gains than advances in wind turbine design [100]. Wind turbines, whose size and characteristics are adapted to suit the observed wind regime, are sited after careful computer modelling, based on local topography and meteorology measurements.

The average number of full load hours varies from location to location and from country to country [101]. The range for onshore installations goes from 1700 to 3000 h/year (averaging 2342 in Spain, 2300 in Denmark and 2600 in the United Kingdom, to give some examples at national level). In general, good sites are the first to be exploited, although they can be in areas that are difficult to reach

7 Blade Factory Considerations

7.1 Summary of NREL Blade Cost Model

A technical report describing a detailed blade cost model for wind turbines in the range of 30-100m was developed by the National Renewable Energy Laboratory, a federally funded research and development facility sponsored by the department of energy in the US [102]. The model applies to multimegawatt wind turbine blades manufactured using vacuum-assisted resin transfer moulding, which is the most widely adopted manufacturing method for modern wind turbine blades. The model is implemented both in a large Excel file and in Python. The latter is freely available in the repository

of the Wind-Plant Integrated System Design and Engineering Model (WISDEM). WISDEM is a multidisciplinary analysis and optimization design framework developed at the National Renewable Energy Laboratory. This parametric blade cost model represents a valuable research tool to run design optimization studies for wind turbine blades and estimates both fixed and variable costs per blade for a given number of blades produced per year, cycle time, workforce and other key metrics. Variable costs consist of the costs for the materials, the labour, and the utilities. The fixed costs capture the equipment, tooling, building, maintenance, overhead, and capital. To estimate all these quantities, the number of labour hours and the cycle time (CT) required by the various manufacturing processes are carefully estimated. The fixed and variable costs are then used to construct a parametric virtual model of a blade manufacturing facility. The model is first presented with its approach and assumptions and then computes the costs of three blades, namely the 33-meter-long Wind Partnership for Advanced Component Technologies (WindPACT) study blade, the 63-meter-long International Energy Agency (IEA) Wind Task 37 land-based reference wind turbine blade, and the 100-meter-long SNL-100-03 blade developed at Sandia National Laboratories.

The model is applicable to blades made with a conventional structural-skin geometry, namely two straight spar caps, one or more shear webs, leading- and trailing-edge reinforcements, and an outer shell skin with a sandwich structure. Additionally, the model is valid for blades with mild sweep and prebend. As long as the blade curvature is not excessive, the manufacturing process is unchanged. Finally, the model assumes that spar caps, root inserts, and shear webs are pre-infused and then inserted into the low- and high-pressure skin moulds. The model loses validity for blades characterized by a more complex internal geometry, such as blades with tapered and/or pultruded spar caps, segmented blades, blades made with manufacturing methods different than VARTM, and so on. Blades that deviate from the assumptions of the model require modifications (possibly minor) to the model. The model was initially developed in a blade manufacturing facility to analyse the manufacturing process and identify inefficiencies in labour and cycle times. In a second step of development, the details of the models were developed for cost and manufacturing process modelling. The model involves many assumptions regarding the steps, the work rate for each step, how workers and teams are formed, and so on, and assumes that the key limiting step is the infusion step involving the moulds. These assumptions originate from real blade factories and have been calibrated such that the overall cost and cycle times match available empirical industry data. Originally implemented in a large Excel file, the model has now been implemented in a Python code and coupled to the Wind-Plant Integrated System Design Engineering Model (WISDEM) framework. WISDEM is a multiyear, multidisciplinary design, analysis, and optimization (MDAO) framework developed at the National Renewable Energy Laboratory (NREL) and freely available in an online repository on github.com/WISDEM. MDAO models have been increasingly adopted within the design of wind turbines. These methods offer the opportunity to run design optimization studies in an automatic manner, generating a multitude of results in a relatively limited amount of time. In addition, properly defined automatic design procedures ensure that all synergies and constraints between disciplines are taken into account at the initial stages of multiple design iterations. This represents undeniable progress compared to former methods, where single discipline experts performed the detailed design of each wind turbine component and only at a second stage integrated all of them together, iterating when necessary. The single iteration design relies on the expertise of the single designers, in which the existing couplings between disciplines can only be captured partially. MDAO aims at providing a valuable alternative. The blade cost model is fully coupled with RotorSE, the rotor design optimization model of WISDEM. This means that each blade cost execution can be called from RotorSE automatically. It is important to highlight that the Python code implementing this model consistently adopts the International System of Units. The Python code implementing the blade cost model works by reading in PreComp input files

that describe the outer blade shape and internal structure. PreComp is the standard cross-sectional analysis tool within WISDEM. The PreComp input files are typically generated by Numad, a three-dimensional finite element method pre-processing code implemented in MATLAB and developed at Sandia National Laboratories (SNL).

7.1.1 Limitations of the NREL Cost Model

The model should also be subject of improvements in several areas. To start, the price of foam and balsa wood has so far been assumed proportional to the area, however it is also proportional to the thickness, and that thickness is highly dependent on the location within the blade. The foam core kit will need further details in terms of the breakdown of costs to include machining of kerfs, design labour costs, and ideally a process flow for the core kit supply and further details pertinent to the contributions to layup. The list of consumables may also be extended, for example, with materials adopted during the finishing operations. Additionally, the model should support blade components manufactured via methods alternative to VARTM, such as pultrusion, and Additive Manufacturing, and should be able to estimate the costs of bonded root inserts, which are more and more commonly used, as well as segmented blades. A step of ultrasonic inspection could also be added. This is often performed on the bonding lines and should be part of the labour model as well as the equipment. Similarly, a step for remediation could be added to the labour model. The accuracy of tooling should be improved to include lifting apparatus and jigs and breaking down the tooling costs to include the hinges of the mould which are significant proportion of the mould cost. Further resolution to labour costs could include the time taken for parts of the workforce to migrate around the factory to perform the various tasks required. Finally, the virtual model of the factory could be made more sophisticated, first by allowing the cycle time to exceed 24 hours and estimating the consequences, and later to model and optimize teams of varying size for each of the manufacturing steps.

7.1.2 Cost Outputs of the current NREL Blade Model for the 15MW Reference Blade

The Standard NREL Blade cost model [102] was run using the reference blade design as defined in section 3. The blade length was 122 m, root diameter of 6.37 m, and it assumes 300 blades per year output from the factory. A new assumption is made, where the core material absorbs an additional 26% of the total resin mass, which is the percentage of extra resin uptake by the core materials as stated for the blades of the Levenmouth demonstrator turbine. The results are summarised in table 7.1 below with both the standard NREL model assumptions and for the increased mass associated with the costs of additional resin absorption by the core material. The breakdown of blade costs are given in the pie chart in figure 37.

Table 7.1 Cost comparison between conventionally infused reference blade, and increased mass core blade.

Cost Item	Conventional NREL IEA-15MW Costs (USD)	Percentage Of Total	Conventional NREL IEA-15MW +26% extra core resin Costs (USD)	Percentage Of Total
Material Costs	571,601	72.3	602,647	73.3
Consumables	17,243	2.2	17,243	2.1
Labour	97,376	12.3	97,376	11.8
Overhead Labour Costs	29,212	3.7	29,212	3.6
Utilities	10,020	1.3	10,523	1.3

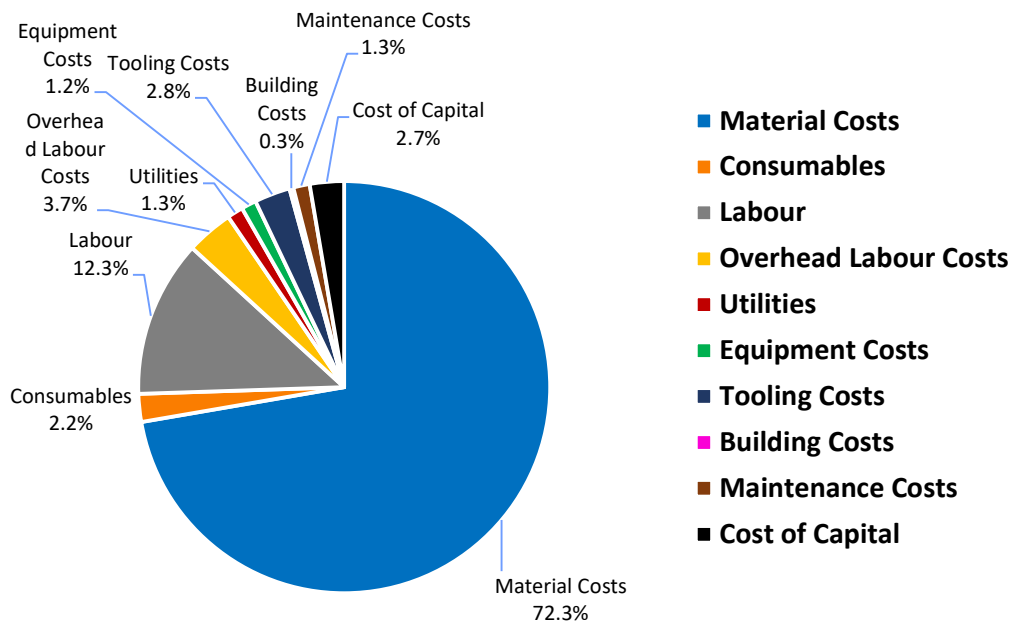|				
Equipment Costs	9183	1.2	9183	1.1
Tooling Costs	22,057	2.8	22,057	2.7
Building Costs	2491	0.3	2491	0.3
Maintenance Costs	10,192	1.3	10,192	1.2
Cost of Capital	21,261	2.7	21,523	2.6
BOM	588,844	74.5	619,891	75.4
OPEX	170,555	21.6	171,320	20.8
CAPEX	31240	4.0	31240	3.8
Total (USD)	*790,640*		*822,451*	
Blade Weight (kg)	*66,576*		*71,010*	

Figure 37. Breakdown of Blade Costs for Conventional IEA-15MW NREL Model.

The total cost of the reference blade from the conventional NREL model with no changes gives $790,640. The total for the NREL model with the assumption of resin absorption by the cores is $822,451. The difference can be attributed to the increase in resin mass required of the resin (4435 kg). This adds further to the material costs, and to a lesser extent the cost of utilities since a greater amount of energy is required to cure the resin. The other notable observation from the results is blade weight, which is increased due to the increase mass of the resin into the cores to 71010 kg. This is a significant assumption which should therefore be included in subsequent iterations of the NREL model application since the blade weight increases by 6.67% with this assumption whilst the overall blade costs increase by 4.02%.

7.2 LCA Analysis of the Standard Reference Blade

The new reference blade discussed in this report underwent LCA analysis with greater detail for mould costs, to include detailed material costs for the fabrication of the plug, and for the half-shell moulds.

The Bill of Materials, along with utility costs are also considered for this reference standard to which all manufacturing improvements will be based on.

This LCA study is primarily focused on giving the embodied carbon of a single wind turbine blade however it also shows the impact this blade has when utilised for an entire windfarm. As an offshore windfarm is an energy production product it is important to give results with respect to the energy produced, in this case, $kgCO_2e/MWh$. This value includes the sum of the CAPEX (Capital Expenditure), OPEX (Operational Expenditure and decommissioning divided by the lifetime output of the windfarm. These values are represented through the following:

- Capex – Total project development and construction of wind farm components

- Opex – Operations and Maintenance impact during operating life

- Decommissioning – Removal of the substructure, cable and wind turbine

- Net capacity factor – Electrical energy produced after losses

7.2.1 Assumptions of the LCA Model

The assumptions made for this project can be split into two groups:

1   The assumptions made with respect to a single blade:

- The polyester based materials which made up less than 1% of the blade material was assumed to have the same embodied carbon due to the lack of available data for the smaller very specific materials used

2   The assumptions made for the model windfarm which the blade is applied to:

- 1500MW Wind farm

- 100 Turbines, all 15MW

- Steel semi-submersible substructure selected

- Project life set as 30 years

- 3 HVAC substation included

- 1 HVDC substation included

- 66kV array cable used

- 220kV HVAC export cable

- 400kV HVDC export cable used

- All substation platforms substructures are jackets

- Hub height set at 150 metres

- Mean wind speed set to 10m/s

- Water depth set to 60 metres

- Distance to construction and O&M port set to 40km

- Standard CTV O&M strategy for current wind farms adopted

- No scour protection included

The limitations involved in this LCA were minimal as the focus was on the wind turbine blade where the full blade composition was available. The limitations worth highlighting are:

Blade material transportation distances have been ignored as the focus of this comparison is between the material and processes involved

Due to lack of data available for the decommissioning of offshore wind farms, basic assumptions were made from the installation expenditures of the platforms.

7.2.2   LCA Results

The results shown in Table 7.2 are separated out to show the construction of the blade itself and the blade to include the mould and the associated costs of the mould such as the material for the plug. The wind farm LCA result (with assumptions as shown in Table 7.3) also takes into account the total carbon CAPEX, OPEX, and decommissioning costs all divided by the lifetime output of the windfarm.

It is worth emphasising that whilst the contribution of consumables represents a fairly small contribution to the overall carbon cost, consumables currently represent a considerable amount of landfill waste. The total contribution from tooling is shown in Table 4.9 for the moulds themselves (with between 2 and 3 moulds per component, which is what is required to achieve 300 blades per year with a 48 hour cycle time) and Table for the mould plugs (for which only 1 plug is required per mould component).

Table 7.2. LCA results for the individual blade

Blade LCA Results		Units
Number of blades	300	[-]
Single Blade bill of materials Carbon Cost	394,156	tonnes CO2e
Single blade consumables carbon cost	4,426	$kgCO_2e$
Mould plug (for all blade components) carbon cost	819,257	$kgCO_2e$
Mould tooling (for all blade components) carbon cost	4,127,693	$kgCO_2e$
Energy usage during manufacture of single blade carbon cost	20,819	$kgCO_2e$
Total carbon cost for single blade	419,402	$kgCO_2e$

Total carbon cost for whole farm blades	**130,767,704**	kgCO$_2$e

Table 7.3 - Total windfarm LCA scenario and results

Other LCA Inputs & Results		Units
Turbine rating	15	MW
Capacity factor	60.5	%
Turbine availability	93.5	%
Turbine AEP	74.38	GWh
Wind farm AEP	7.438	TWh
Windfarm lifetime energy production	223.14	TWh
Windfarm capital/installation carbon cost	7.111	kgCO$_2$/MWh
Windfarm operational carbon cost	4.542	kgCO$_2$/MWh
Windfarm decommissioning carbon cost	0.345	kgCO$_2$/MWh
Wind farm LCA	12	kgCO$_2$/MWh

8   Manufacturing Process Improvements

8.1   Introduction

To better reduce blade costs and energy consumption, several hypothetical scenarios for process improvement are introduced and summarised, each of which will be further discussed in a second report in this series. However, for the purpose of completion here they will be briefly introduced in this section.

8.2   Variant 1: Standard Infused Blade with AM Core

To verify that AM can make a positive impact on blade manufacturing using novel AM cores, some cost modelling has been carried out. The NREL detailed cost model was implemented for a reference blade design described previously which has a 122 m length and rated at 15 MW. For the AM sandwich core case the NREL cost model has been modified to account for onsite factory production of cores using large format thermoplastic 3D printers.

8.2.1   Rationale for AM Cores in Blade Manufacture

The rationale to produce sandwich cores via thermoplastic Additive Manufacturing within a blade factory revolves around flexibility in the manufacturing process, but also the ability to produce cores which have greater conformity to the curvature of the mould, this could enable a reduction in the number of hinge points or kerfs. This is important since this enables potential for larger core sections which conform to the mould and reduces the numbers of kerfs and thus in turn reduces the total resin uptake. Secondly the resin flow can be better controlled via bespoke resin channels at the surface of the core material.

8.2.2 Key Model Assumptions

The majority of the blade manufacturing process could be kept the same, with only the core materials replaced with material created using thermoplastic additive manufacturing (AM). This could still have advantages over the conventional blade manufacturing process, as conventional core materials absorb a considerable amount of resin during the infusion process, leading to an increase in their density, and material costs as well as overall blade weight. They are also scored with a grid pattern to allow them to conform with the shape of the mould, and these slots tend to act as initiation points for blade damage in the field, eventually leading to delamination of the skins from the core material. The AM manufactured cores could be watertight and could be pre-fabricated to the shape and curvatures of the mould, so they would not need to be scored to such an extent.

A parametric cost model has been derived from the NREL cost model described in section 7, which assumes all conventional blade manufacturing techniques are deployed. However, in this case a new variant of blade is envisaged. This involves upper-level costing within the context of a parametric blade factory model derived from NREL, but which uses large platform thermoplastic extrusion additive manufacturing to produce the core material within the blade factory as well as a print farm approach where a number of desktop printers carry out the printing operation of single tiles.

Assumptions are omitted where they remain the same as for the un-modified NREL parametric model. The main feature of the modification is that the model calculates the number of large-format thermoplastic pellet 3D printers required to extrude a specified mass of thermoplastic pellets from the bill of materials using a specified deposition rate and rounds this up to the nearest integer.

For the large Area approach, the material cost per kg is based on the Arnite AM2001 pellet feedstock material system and is approximately 9.4 USD/kg. The deposition rate for the large area AM model is taken as 50kg/m^2 which is the deposition rate of the latest model of extruder by CEAD. The model uses the CEAD Flexbot system parameters since these are known values from the machine specifications. The number of robot cells is given by the equation below:

$$N_{Cells} = \left\lceil \frac{m_{core} * (1 + Scrap\ Rate)}{Deposition\ Rate * CT * (1 - Average\ Downtime)} \right\rceil$$

Secondly for the print farm approach, the number of cells are equivalent to the number of printers, and the deposition rate is assumed to be the as advertised nominal volumetric value of 6600 mm^3 converted to 0.547 kg/hr assuming a density of PET of 1.38 g/cm^3 for the E3D Supervolcano hot end [103] which is capable of much greater deposition rates compared with the standard desktop printers. Secondly for the print farm approach, the PET is assumed to be $6/kg for dry pellet feedstock, this is due to the fact that a filament production line can produce filament within the factory floor and so this is added into the model for the print farm approach only.

The number of print cells are expected to directly contribute to additional utility costs via the additional floor space required for the extra machines required for printing.

$$Power\ Consumption = \frac{Floor\ Space * 250\frac{kW}{sqm}}{Production\ Days * 24hr}$$

$$Floor\ Space = Machine\ Working\ Area * Number\ of\ Robot\ Cells$$

The Machine Working Area for the large area approach assumes the current dimensions of the AM robot cell based at the ORE Catapult Blyth site and measures 5.9 m x 8.7 m for the robot and extruder, plus the additional 3.5 m x 4.5 m for the operator booth giving a total of 67.1 m^2. This part of the model can be further improved with more accurate power consumption figures and then added to the overall blade utilities.

The equipment costs assume additional equipment investment due to the CAPEX of the AM cells.

$$Equipment\ Costs = \frac{Equipment\ Investment}{Equipment\ Life * \#Blades\ per\ year}$$

Where the additions of costs to the standard NREL manufacturing process from the AM cells is:

$$Equipment\ Costs = \frac{N_{Cells} * Purchase\ Value}{Equipment\ Life * \#Blades\ per\ year}$$

Here, a 15-year lifespan is assumed for the AM cell, and the Purchase value is taken as the list price of the CEAD Flexbot with the full spec to include the machining option in USD which amounts to $505,000.

The tooling costs are as is since this part of the process remains unchanged. The building costs are expected increase due to the additional footprint from the AM cells. The building investment space is computed as the product of the number of AM cells and the machine working area of 67.1 m^2. Floor costs is assumed to be 800 USD/m^2 as per NREL.

$$Building\ Costs = \frac{(Floor\ Space * Floor\ Costs)}{Building\ Life * \#Blades\ per\ Year}$$

There are additional maintenance costs due to the extra building investment, and extra equipment investment.

There are additions to the labour costs of running the AM cells and these are summarised. It is assumed that pre-processing and software setup takes 15 minutes per AM cell, with 15 minutes to cycle time. Also, that it takes two workers (on the recommendation of CEAD) 15 minutes to clean the nozzle, adding 15 minutes to the cycle time. It is assumed that it will take 1 worker 10 minutes to remove the part at the end of the print per AM cell, with 10 minutes of cycle time. After the print, it is assumed that the cooldown for each part will take 3 hours, where it can be left unattended. It is also assumed that it will take approximately 3 hours to machine the part to tolerance, however this is highly dependent on the core section size and geometry, if curved then special fixtures will be needed and the machining operation may take longer. Cleaning of the AM cell and upkeep is assumed to take 1 worker half an hour per AM cell, with a cycle time of half an hour.

Another key assumption of the model is that it may be assumed that the labour costs associated with the core kit placement can be halved due to larger cores which conform to the mould profile. Secondly for the conventional blade model it is assumed that an extra 26% by weight of resin is used which is absorbed by the traditional foam core, however in the AM core models it is assumed that the AM core does not absorb resin. This therefore could account for any reduced blade weight and lower material costs in the BOM for the AM core model.

The assumptions made in the AM core models such as zero resin uptake in AM cores, and 26% uptake in traditional foam cores, would need to be thoroughly investigated to determine these phenomena and to challenge these assumptions. Likewise, it would have to be proved that larger AM cores could be produced which match the infusion characteristics of conventionally infused foam cores.

For blade weight, where if it can be proved that there is substantially reduced resin absorption through infusion using additively manufactured core material, then there are weight savings which could be further explored. Since blade weight can be reduced by up to 6.67% assuming no resin absorption takes place.

At present the AM models produce an updated material cost per kg to include all the additional costs associated with the machine CAPEX and OPEX pertinent to the AM core fabrication only, which will then be added to the conventional NREL model as discussed in section 7 as inputs. The results will be presented in future work. The price per kg of material goes from $9.4/kg to $9.62/kg for the pellet form and from $6/kg to $6.98/kg for the PET for the print farm approach.

8.3   Variant 2: Standard Infused Blade with Reusable Bagging

Durable elastomeric custom produced bags could cut consumables and increase production rate. Manufacturers are always looking for opportunities to reduce costs where an increasing number of infusion suppliers are finding solutions to this.

Typically, the weights are around 8-10 kg per square meter and so at scale any reusable vacuum bag technology would need expensive lifting and handling equipment, along with careful consideration in storage method and storage space to optimise their lifespan.

A growing number of manufacturers as well as some of those in aerospace are beginning to find these advantages in reusable vacuum bag (RVB) technology. Proponents indicate that silicone elastomeric bags may be able to replace disposable bagging films. Advantages include improved part-to-part quality and greater shop safety and cleanliness. Likewise, they provide a way to cut down on consumables such as tacky tapes and reduce a shop's waste stream. However, RVBs will require additional capital expenditure and offer challenges that must be overcome prior to implementation, and they aren't always advantageous in every part process situation.

Each RVB system have their advantages and disadvantages, which fabricators would need to consider e.g. the relative ease of building and using the RVB, its tolerance for a specific resin chemistry and processing temperature, and, most importantly, the aggregate cost per square foot.

RVBs can be produced using synthetic or natural rubbers. The most common synthetics, include a broad range of silicones, however other elastomeric materials have been used in vacuum membranes,

for example forms of polyurethane, ethylene/propylene, polysulfide, fluorosilicone, nitrile and chloroprene.

Silicones are polymerised siloxanes, or polysiloxane, an inorganic/organic polymer. Thus, they consist of an inorganic silicon/oxygen backbone where organic groups (methyl, ethyl or phenyl), derived from petroleum distillates, are used. Formulated to exhibit rubber-like elongation, silicone rubber is a common RVB material. To be useful as RVB materials, silicones require in-situ polymerization via the addition of a catalyst which is typically platinum, but also tin, where their cure can vary with environmental conditions.

Silicone sheet materials, especially high-strength compounds that are postcured for higher heat resistance, have been used for decades as membranes, diaphragms and envelope bags in production tooling. Major suppliers of silicone sheet goods and liquid formulations include Wacker Chemical Corporation (Munich, Germany), Arlon Silicone Technologies (Bear, Del.), Dow Corning Corp. (Midland, Mich.), Shin Etsu Silicones of America (Tokyo, Japan), Mosites Rubber Co. (Ft. Worth, Texas) and ACC Silicones Europe (Amber House, Bridgwater, Somerset, U.K.).

Silicone bagging materials have moved from high-end autoclave applications to low-cost infusion applications, after suppliers began offering room-temperature vulcanizing (RTV), lower-viscosity, two-part, platinum-cured silicone formulations. These forms were stable, more user-friendly, have good properties and can be sprayed, poured or brushed into position to create a custom silicone bag for infusion.

Various approaches can be used to fabricate a custom RVB for low-temperature, out-of-autoclave cures, including seaming silicone sheet stock, however the fastest and most common method is to use a dedicated spray machine that employs either an atomizing spray head or a splatter-type head which generates a film directly on the mould. Multiple layers are built up to the desired RVB thickness, typically from around 1 mm to 10 mm. The working pot times, air assist velocity needed for spraying, spray equipment clean-up requirements and specifics like final bag thickness vs. weight and cure time vary by material type and supplier. Many different types of edge seal are available, and many are proprietary or based on patent-pending technology. The simplest seal for a frameless RVB is a half-round or V-shaped profile affixed to the lower tool's flat flange, which is then covered with the elastomer spray. After cure, the profile is pulled out, leaving a channel a few inches from the RVB edge.

Vacuum and resin ports are created by bonding port components to the bag or placing them at various desired locations, masking them against the spray and then spraying the silicone material over them. Resin flow channels can also be designed into the bag itself. When a vacuum is pulled through the ports and the perimeter channel, the RVB is pulled against the tool. However, there are also other methods of vacuum sealing.

Both silicone and natural rubber offer benefits for certain applications and have process and handling similarities, together with some uniquely individual characteristics. An important similarity is that epoxy resins will attack all types of RVBs, breaking them down at a faster rate than polyester or vinyl ester resins. It has been said that the silicone chemistry is formulated for tear strength and is an important criterion when selecting a bagging system and it can directly correlate to bag life. In terms of heat resistance, natural and silicone rubbers differ. There are autoclave-suitable silicone RVBs that can take temperatures as high as 240°C. Natural rubbers normally can't tolerate such high temperatures.

On the issue of weight, RVBs get heavy when they are fabricated for larger parts. Each supplier's material will vary in terms of coverage per pound of liquid, however an RVB for a 3m x 3m part can approximately weigh 30 kg or more, which is greater than one person could comfortably handle therefore logistics become more important. Designing edge frames and lifting points will become a requirement with oversize systems. This will in turn add further weight, and the requirement for heavier lifting equipment will result in greater CAPEX.

If silicones aren't properly processed, they can transfer material from the bag to parts, however that is less of an issue if the part isn't being finished or painted on the part surface. The use of barrier films, such as fluorinated ethylene propylene (FEP) release films, can prevent transfer from the bag to the surface. Also, silicone and natural-rubber membranes can be easily repaired when torn for example using overlaid doubler patch.

8.3.1 Sprayable Silicone Bags

Prairie Technology Group were the first organisation to patent a spray-on RVB in 2006 (U.S. Patent number 7014809B2). The concept involves a technique of creating a reusable flexible polymer bag or skin which utilises a spray (or swirl spray) application of a sprayable polymer, where the bag or skin is used as a bagging material to be used in the resin transfer moulding process (infusion or vacuum bagging process) for fabrication of glass or carbon fibre reinforced plastic parts.

A benefit of this technique is a viscosity low enough that the silicone can be atomized, instead of splattered, along with the propensity to adhere to itself upon application of successive layers either when previous layers have cured or uncured. Some vendors also rent out the equipment with operator training and could reduce CAPEX for short numbers of runs. Many edge seal designs can be offered.

Bags with thickness variations can be produced where the thick sections can act as pressure intensifiers for key regions of the part. Fabrics can be added for further reinforcement; however, it isn't a requirement, but it can help support placement of the vacuum channel and ports. Another recommendation for larger bag sizes, is to add hard anchor points along the bag margins, integrated with cloth reinforcement so that the RVB can be safely and easily lifted with an overhead crane or lifting system.

The costs of bagging consumables associated with the infusion process are estimated for a whole one-piece blade using the reference blade parameters, at an upper level only (Table 8.1). Some parameters of which are taken from the NREL model and others are added where lacking in the NREL model. The costs are then taken for each consumable and are calculated for various numbers of moulding pulls to determine a rough inflexion point by which reusable bagging material could become profitable. However, at this stage only the material cost of the silicon sprayable bagging is considered, no labour costs, or complex lifting jigs are yet considered at this stage. The costs of the consumables such as the tacky tapes and masking tapes are proportional to blade length, and the costs of the films and areal materials are proportional to the total blade areas of the reference blade, such as the shells and shear webs. The costs for each the silicone bag approach and conventional approaches are given in the below equations:

$$Total\ Cost\ Consumables\ _{Conventional} =$$

$$[Cost_{Masking\ Tape} + Cost_{Tacky\ Tape} + Cost_{Relea\quad Agent} + Cost_{Flow\ Medium} + Cost_{Bagging\ Film}$$
$$+ \ Cost_{Release\ Film} + Cost_{Tubing}] * Pulls$$

$$Total\ Cost\ Consumables\ _{Silicone\ Bag} =$$

$$[Cost_{Release\ Agent} + Cost_{Tubin}\ ] * Pulls + Cost_{Silicone\ material}$$

Table 8.1. Cost totals for upper level consumables for the Conventional case versus reusable bagging system with number of pulls.

Number of Pulls	Conventional Consumables Cost (USD)	Reusable Silicone Bag Costs (USD)
10	158,736	341,006
20	317,471	407,583
30	476,207	474,161
50	793,678	607,316
100	1,587,356	940,204

From the above table, at around 30 pulls, the total consumables costs associated with the bagging and infusion process reaches an inflexion point where the reusable silicone bag becomes more cost effective. Also, since the bagging material is deposited at 7 kg per square meter, and costs $19.8/kg, this is only a hypothetical scenario since the system would become much too heavy to handle without highly complex lifting equipment. There are many further things which merit consideration using the reusable silicone bag approach, such as labour, the CAPEX associated with the lifting equipment, the spray dispenser costs, and the storage requirements of the silicone bag to name a few. This will form a large part of further work in this area to better detail this in approach in terms of the cost effectiveness especially when combined with blade segmentation strategies.

8.4   Variant 3: Segmented Blade

The effect on blade segmentation will be investigated to determine to what effect it has on the cost and LCA of a blade. It is hypothesised that there is a nonlinear relationship with blade segmentation and costs since the greater the numbers of segments result in increasing assembly costs. However, between 2 or 3 segments could generate the benefits of lower mould and consumables costs whilst balancing this with the labour force required to perform the final assembly.

8.5   Variant 4: Thermoplastic Infusion Alternatives

Increasing demand for lightweight materials is a major driving force for the steady growth of the continuous fibre-reinforced polymer composite industry. In recent years, strict global targets demanding greater environmental responsibility have led to a shift in research focus to address the end-of-life challenges posed using thermoset matrices. Thermosets offer lower-cost processibility than thermoplastics, which historically required cost- and energy-intensive production methodologies. Consequently, despite their well-demonstrated recyclability, thermoformability and weldability, thermoplastics are yet to attain the same technological maturity as thermosets. In parallel to the increasing demand for fibre-reinforced polymer (FRP) composites, there is renewed interest in thermoplastic (TP) matrices across many sectors where their thermoset (TS) counterparts are

dominant. While it has long been established that TP matrices offer more favourable benefits than TS matrices in terms of recyclability, welding and thermoformability [104]–[106], their high-melt viscosities necessitate high processing temperatures and pressures, and thus, renders them cost-prohibitive and impractical for most sectors [107], [108]. Research efforts to address this have paved the way for the application of innovative *in situ* polymerisation methodologies to produce continuous fibre-reinforced TP composites. Early-generation reactive TP precursors such as cyclic butylene terephthalate (CBT) [109]–[111], caprolactam [112], [113] and laurolactam [114], [115] now facilitate the production of fibre-reinforced polybutylene terephthalate (PBT), polyamide-6 (PA-6) and polyamide-12 (PA-12) by liquid composite moulding, respectively. These materials do, however, require mould heating to achieve temperatures above 150◦C (PA-6 and PA-12) and 180◦C (PBT), which makes the fabrication of large-scale structures relatively challenging. This additional requirement for mould heating may be impracticable for the wind energy sector, for instance, where blade lengths continue to increase to meet growing global demand [116]. The study of bulk polymerisation of acrylic resins started in the 1940s, and only few studies were reported on the reactive processing of acrylic composites [117]. The growing interest in the field of TP-FRPs has led to the development of Elium®, a family of liquid TP acrylic resins, which are suitable for manufacturing large composite structures with continuous fibre reinforcement at room temperature via *in situ* polymerisation. With viscosities as low as 100 mPa s, these acrylic resins are considered more cost-effective than the aforementioned first-generation reactive resins. Moreover, their suitability for the production of large-scale components by resin infusion [118]–[120]; and their thermoformability and recyclability [121] have recently been demonstrated. The present article reviews the advancements to-date in the use of reactive acrylic resins as attractive solutions to the challenges associated with traditional thermosetting and thermoplastic matrices for composite applications. A comprehensive summary of comparative analyses performed to-date alongside comparable thermosetting composites is also presented.

More specifically for this variant, the ATOM method will be used to assess different material options and their effect on the bill of materials in terms of global warming potential. The main focus will be on thermoplastic resins, including Elium among other resins such as Infugreen (epoxy-based), and Recyclamine (amine-based).

9   Conclusions

This report aims to describe the current state-of-the-art in blade manufacturing and sets out a new reference dataset for both the cost and the Life Cycle Analysis (LCA) for a new blade design iteration intended for use as an educational tool for research into new trends. This report also sets out to show the cost breakdown for this 122 m blade design iteration both using the conventional NREL model as is, and to show any sensitivity of the model to new assumptions such as additional resin absorption into the sandwich cores. Furthermore, newer, more current input parameters are suggested to further improve the accuracy of the NREL cost model in terms of the Bill of Materials (BOM), and in the cost of consumables. Then suggestions are made in terms of how the manufacturing process could be further improved in the future. Model Aspects taken forward for future consideration must include:

- Greater emphasis on mould requirements and associated costs, currently the NREL model lacks any significant details around jigs lifting equipment, storage requirements, manufacturing costs of the mould (formation of the plug)
- Greater consideration required for factory layout and implications on process flows. For example, a large blade factory may require a labour force which needs time to move around the factory floors.
- Greater definition for the use of reusable bagging consumables to reduce wastage.

- More consideration into the implications of blade segmentation on the overall process flow and costs.

Future work will be carried out to further assess the viability of each of the variants described in section 8, along with improved LCA assessments for both the reference blade and the variants where applicable. For the variants, cost modelling will also have further details regarding the additively manufactured cores, with more accurate cost breakdowns. For the thermoplastic infusion alternative (variant 4), greater focus on how different sub-variants of fibre/resin combinations to include Elium (PMMA based), and Infugreen (epoxy-based), and Recyclamine (amine-based) resins affect the bill of materials from a material global warming potential standpoint will be investigated.

10 References

[1] T. Kåberger, "Progress of renewable electricity replacing fossil fuels," *Glob. Energy Interconnect.*, vol. 1, no. 1, pp. 48–52, 2018, doi: 10.14171/j.2096-5117.gei.2018.01.006.

[2] and E. B. Tony Burton, David Sharpe, Nick Jenkins, *Wind Energy Handbook*. Wiley, 2001.

[3] L. Mishnaevsky *et al.*, "Materials for Wind Turbine Blades : An Overview," pp. 1–24, 2017, doi: 10.3390/ma10111285.

[4] "Automated filament winding aids segmented blade production | CompositesWorld." https://www.compositesworld.com/articles/automated-filament-winding-aids-segmented-blade-production (accessed Jun. 08, 2021).

[5] "TPI Composites Blade Manufacturing Process - YouTube." https://www.youtube.com/watch?v=jpRudTUIyfM (accessed Mar. 21, 2022).

[6] M. S. Koefoed, "Modeling and Simulation of the VARTM Process for Wind Turbine Blades," no. 50, 2003.

[7] "Tooling up for large wind turbine blades - Renewable Energy Focus." http://www.renewableenergyfocus.com/view/1149/tooling-up-for-large-wind-turbine-blades/ (accessed Sep. 07, 2021).

[8] T. Intregralblade, "Siemens unveils 75 m wind turbine blade," *Reinf. Plast.*, vol. 56, no. 4, pp. 30–31, 2012, doi: 10.1016/s0034-3617(12)70078-4.

[9] G. Gardiner, "Modular design eases big wind blade build." https://www.compositesworld.com/articles/modular-design-eases-big-wind-blade-build (accessed Nov. 05, 2021).

[10] L. M. Jr and P. Brøndsted, "Statistical modelling of compression and fatigue damage of unidirectional fiber reinforced composites," *Compos. Sci. Technol.*, vol. 69, no. 3–4, pp. 477–484, 2009, doi: 10.1016/j.compscitech.2008.11.024.

[11] "The still-promised potential of basalt fiber composites | CompositesWorld." https://www.compositesworld.com/articles/the-still-promised-potential-of-basalt-fiber-composites (accessed Jun. 28, 2021).

[12] L. Nijssen, *Fatigue Life Prediction and Strength Degradation of Wind Turbine Rotor Blade Composites Fatigue Life Prediction and Strength Degradation of Fatigue Life Prediction and Strength Degradation of Wind Turbine Rotor Blade Composites The work described in this . .*

[13] "New polyurethane rotor blade helps wind turbines last longer - cefic.org." https://cefic.org/a-solution-provider-for-sustainability/chemistrycan/driving-the-circular-economy/new-polyurethane-rotor-blade-helps-wind-turbines-last-longer/ (accessed Jun. 28, 2021).

[14] H. W. Zhou *et al.*, "Carbon fiber/carbon nanotube reinforced hierarchical composites: Effect of CNT distribution on shearing strength," *Compos. Part B Eng.*, vol. 88, pp. 201–211, 2016, doi: 10.1016/j.compositesb.2015.10.035.

[15] M. R. Loos, J. Yang, D. L. Feke, and I. Manas-Zloczower, "Enhanced fatigue life of carbon nanotube-reinforced epoxy composites," *Polym. Eng. Sci.*, vol. 52, no. 9, pp. 1882–1887, Sep. 2012, doi: 10.1002/pen.23145.

[16] S. Boncel, A. Kolanowska, A. W. Kuziel, and I. Krzyz, "Carbon Nanotube Wind Turbine Blades : How Far Are We Today from Laboratory Tests to Industrial Implementation ?," 2018, doi: 10.1021/acsanm.8b01824.

[17] A. Kumar, K. Matt, and S. Strong, "Development of Novel Self-Healing Polymer Composites for Use in Wind Turbine Blades," vol. 137, no. September, pp. 1–5, 2015, doi: 10.1115/1.4029912.

[18] "Core for composites: Winds of change | CompositesWorld." https://www.compositesworld.com/articles/core-for-composites-winds-of-change (accessed May 05, 2021).

[19] E. A. Published by Bella Weetch, "Diab to enhance wind turbine blades using SABIC technology | Energy Global." https://www.energyglobal.com/special-reports/04022021/diab-to-enhance-wind-turbine-blades-using-sabic-technology/ (accessed Jul. 02, 2021).

[20] Gurit Ltd, "Composite materials for Wind Energy," 2019, [Online]. Available: www.gurit.com.

[21] J. Jonkman, S. Butterfield, W. Musial, and G. Scott, "Definition of a 5-MW Reference Wind Turbine for Offshore System Development." .

[22] C. Bak *et al.*, "The DTU 10-MW Reference Wind Turbine," 2013.

[23] P. Bortolotti *et al.*, "IEA Wind TCP Task 37: Systems Engineering in Wind Energy - WP2.1 Reference Wind Turbines," *IEA Wind TCP Task 37*, no. May, 2019, [Online]. Available: https://www.osti.gov/biblio/1529216-iea-wind-tcp-task-systems-engineering-wind-energy-wp2-reference-wind-turbines%0Ahttp://www.osti.gov/servlets/purl/1529216/.

[24] E. Gaertner, J. Rinker, L. Sethuraman, B. Anderson, F. Zahle, and G. Barter, "IEA Wind TCP Task 37: Definition of the IEA 15 MW Offshore Reference Wind Turbine," pp. 1–44, 2020, [Online]. Available: https://github.com/IEAWindTask37/IEA-15-240-RWT.

[25] K. Dykes *et al.*, "Introducing WISDEM: An Integrated System Modeling for Wind Turbines and Plant," 2015.

[26] J. Rinker *et al.*, "Comparison of loads from HAWC2 and OpenFAST for the IEA Wind 15 MW Reference Wind Turbine," *J. Phys. Conf. Ser.*, vol. 1618, no. 5, 2020, doi: 10.1088/1742-6596/1618/5/052052.

[27] C. Bottasso, P. Bortolotti, A. Croce, and F. Gualdoni, "Integrated aero-structural optimization of wind turbines," *Multibody Syst. Dyn.*, vol. 38, Dec. 2016, doi: 10.1007/s11044-015-9488-1.

[28] P. Bortolotti, A. Kapila, and C. L. Bottasso, "Comparison between upwind and downwind designs of a 10 MW wind turbine rotor," *Wind Energy Sci.*, vol. 4, no. 1, pp. 115–125, 2019, doi: 10.5194/wes-4-115-2019.

[29] S. Scott, P. Greaves, P. M. Weaver, A. Pirrera, and T. MacQuart, "Efficient structural optimisation of a 20 MW wind turbine blade," *J. Phys. Conf. Ser.*, vol. 1618, no. 4, 2020, doi: 10.1088/1742-6596/1618/4/042025.

[30] T. Macquart, V. Maes, D. Langston, A. Pirrera, and P. M. Weaver, "A New Optimisation Framework for Investigating Wind Turbine Blade Designs," *Adv. Struct. Multidiscip. Optim.*, no. June, pp. 2044–2060, 2018, doi: 10.1007/978-3-319-67988-4_151.

[31] C. C. By, "Scott , S ., Macquart , T ., Rodriguez , C ., Greaves , P ., Mckeever , P ., Weaver , P ., & Pirrera , A . (2019). Preliminary validation of ATOM : an aero-servo-elastic design tool for next generation wind turbines . Journal of Physics : Preliminary v," 2019.

[32] "GitHub - NREL/ROSCO: A Reference Open Source Controller for Wind Turbines." https://github.com/NREL/ROSCO (accessed Feb. 02, 2022).

[33] BS EN IEC 61400-1, "BS EN IEC 61400-1:2019-Wind energy generation systems. Design requirements," p. 176, 2019, Accessed: Feb. 02, 2022. [Online]. Available: https://www.en-standard.eu/bs-en-iec-61400-1-2019-wind-energy-generation-systems-design-requirements/.

[34] T. MacQuart, S. Scott, P. M. Weaver, and A. Pirrera, "Piecewise linear aeroelastic rotor-

tower models for efficient wind turbine simulations," *J. Phys. Conf. Ser.*, vol. 1618, no. 4, 2020, doi: 10.1088/1742-6596/1618/4/042033.

[35]   S. J. Scott, "Optimal Aeroelastic Tailoring of Wind Turbines," University of Bristol, 2021.

[36]   B. Schafer, "CUFSM - Cross-section elastic buckling analysis v5.04," 2019. available: https:// www.ce.jhu.edu/cufsm/.

[37]   P. Chaviaropoulos *et al.*, "PI-based assessment (application) on the results of WP2-WP4 for 20 MW wind turbines," *INNWIND Deliv.*, no. September, 2017.

[38]   A. Puck and H. Schürmann, "Failure analysis of FRP laminates by means of physically based phenomenological models," *Fail. Criteria Fibre-Reinforced-Polymer Compos.*, vol. 3538, no. 96, pp. 832–876, 2004, doi: 10.1016/B978-008044475-8/50028-7.

[39]   D. I. Chortis, N. A. Chrysochoidis, and D. A. Saravanos, "Damped structural dynamics models of large wind-turbine blades including material and structural damping," *J. Phys. Conf. Ser.*, vol. 75, no. 1, 2007, doi: 10.1088/1742-6596/75/1/012076.

[40]   O. Stodieck, J. E. Cooper, and P. M. Weaver, "Interpretation of Bending/Torsion Coupling for Swept, Nonhomogenous Wings," *J. Aircr.*, vol. 53, no. 4, pp. 892–899, Dec. 2015, doi: 10.2514/1.C033186.

[41]   S. Scott *et al.*, "Effects of aeroelastic tailoring on performance characteristics of wind turbine systems," *Renew. Energy*, vol. 114, pp. 887–903, 2017, doi: 10.1016/j.renene.2017.06.048.

[42]   K. Svanberg, "A Class of Globally Convergent Optimization Methods Based on Conservative Convex Separable Approximations," *SIAM J. Optim.*, vol. 12, pp. 555–573, Jan. 2002, doi: 10.1137/S1052623499362822.

[43]   G. Marsh, "Tooling up for large wind turbine blades," *Reinf. Plast.*, vol. 51, no. 9, 2007, doi: 10.1016/S0034-3617(07)70281-3.

[44]   C. A. S. Hill and J. Dibdiakova, "The environmental impact of wood compared to other building materials," *Int. Wood Prod. J.*, vol. 7, no. 4, pp. 215–219, Oct. 2016, doi: 10.1080/20426445.2016.1190166.

[45]   G. Finnveden *et al.*, "Recent developments in Life Cycle Assessment," *J. Environ. Manage.*, vol. 91, no. 1, pp. 1–21, Oct. 2009, doi: 10.1016/J.JENVMAN.2009.06.018.

[46]   A. Haapio and P. Viitaniemi, "A critical review of building environmental assessment tools," 2008, doi: 10.1016/j.eiar.2008.01.002.

[47]   A. Forsberg and F. von Malmborg, "Tools for environmental assessment of the built environment," *Build. Environ.*, vol. 39, no. 2, pp. 223–228, Feb. 2004, doi: 10.1016/J.BUILDENV.2003.09.004.

[48] J. C. Bare, P. Hofstetter, D. W. Pennington, and H. A. Udo de Haes, "Life cycle impact assessment workshop summary. Midpoints versus endpoints: The sacrifices and benefits," *Int. J. Life Cycle Assess.*, vol. 5, no. 6, pp. 319–326, 2000, doi: 10.1007/BF02978665.

[49] M. Z. Hauschild *et al.*, "Identifying best existing practice for characterization modeling in life cycle impact assessment," *Int. J. Life Cycle Assess. 2012 183*, vol. 18, no. 3, pp. 683–697, Sep. 2012, doi: 10.1007/S11367-012-0489-5.

[50] O. Jolliet and A. Brent, "Final Report of the LCIA Definition Study, Life Cycle Impact Assessment Programme of The Life Cycle Initiative Development of a method to optimally size micro-grids based on meta-heuristic optimization algorithms View project Environmental process modelin."

[51] "Welcome - EuCIA Eco Impact Calculator." .

[52] M. A. J. Huijbregts *et al.*, "Is cumulative fossil energy demand a useful indicator for the environmental performance of products?," *Environ. Sci. Technol.*, vol. 40, no. 3, pp. 641–648, Feb. 2006, doi: 10.1021/ES051689G/SUPPL_FILE/ES051689GSI20051130_064936.PDF.

[53] R. Fay, G. Treloar, and U. Iyer-Raniga, "Life-cycle energy analysis of buildings: a case study," *http://dx.doi.org/10.1080/096132100369073*, vol. 28, no. 1, pp. 31–41, 2010, doi: 10.1080/096132100369073.

[54] M. K. Dixit, J. L. Fernández-Solís, S. Lavy, and C. H. Culp, "Need for an embodied energy measurement protocol for buildings: A review paper," *Renew. Sustain. Energy Rev.*, vol. 16, no. 6, pp. 3730–3743, Aug. 2012, doi: 10.1016/J.RSER.2012.03.021.

[55] P. G. Hammond, C. Jones, E. F. Lowrie, and P. Tse, "A BSRIA guide Embodied Carbon The Inventory of Carbon and Energy (ICE)."

[56] L. F. Cabeza, C. Barreneche, L. Miró, J. M. Morera, E. Bartolí, and A. Inés Fernández, "Low carbon and low embodied energy materials in buildings: A review," *Renew. Sustain. Energy Rev.*, vol. 23, pp. 536–542, Jul. 2013, doi: 10.1016/J.RSER.2013.03.017.

[57] Y. Jiao, C. R. Lloyd, and S. J. Wakes, "The relationship between total embodied energy and cost of commercial buildings," *Energy Build.*, vol. 52, pp. 20–27, Sep. 2012, doi: 10.1016/J.ENBUILD.2012.05.028.

[58] M. K. Dixit, J. L. Fernández-Solís, S. Lavy, and C. H. Culp, "Identification of parameters for embodied energy measurement: A literature review," *Energy Build.*, vol. 42, no. 8, pp. 1238–1247, Aug. 2010, doi: 10.1016/J.ENBUILD.2010.02.016.

[59] Y. S. Song, J. R. Youn, and T. G. Gutowski, "Life cycle energy analysis of fiber-reinforced composites," *Compos. Part A Appl. Sci. Manuf.*, vol. 40, no. 8, pp. 1257–

1265, Aug. 2009, doi: 10.1016/J.COMPOSITESA.2009.05.020.

[60] "ENERGY BEST PRACTICE ENERGY BEST PRACTICE ENERGY BEST PRACTICE ENERGY BEST PRACTICE GUIDEBOOK."

[61] U. States Department of Energy, "Bandwidth Study on Energy Use and Potential Energy Saving Opportunities in the Manufacturing of Lightweight Materials: Glass Fiber Reinforced Polymer Composites," 2017.

[62] T. Suzuki and J. Takahashi, "PREDICTION OF ENERGY INTENSITY OF CARBON FIBER REINFORCED PLASTICS FOR MASS-PRODUCED PASSENGER CARS," *Ninth Japan Int. SAMPE Symp.*

[63] C. J. Rydh and M. Sun, "Life cycle inventory data for materials grouped according to environmental and material properties," *J. Clean. Prod.*, vol. 13, no. 13–14, pp. 1258–1268, Nov. 2005, doi: 10.1016/J.JCLEPRO.2005.05.012.

[64] J. Bachmann, C. Hidalgo, and S. Bricout, "Environmental analysis of innovative sustainable composites with potential use in aviation sector—A life cycle assessment review," *Sci. China Technol. Sci. 2017 609*, vol. 60, no. 9, pp. 1301–1317, Aug. 2017, doi: 10.1007/S11431-016-9094-Y.

[65] S. Kara and S. Manmek, "COMPOSITES: CALCULATING THEIR EMBODIED ENERGY 2 PREFACE."

[66] R. A. Witik, J. Payet, V. Michaud, C. Ludwig, and J. A. E. Månson, "Assessing the life cycle costs and environmental performance of lightweight materials in automobile applications," *Compos. Part A Appl. Sci. Manuf.*, vol. 42, no. 11, pp. 1694–1709, Nov. 2011, doi: 10.1016/J.COMPOSITESA.2011.07.024.

[67] R. K. Rankine, J. P. Chick, and G. P. Harrison, "Energy and carbon audit of a rooftop wind turbine:," *http://dx.doi.org/10.1243/09576509JPE306*, vol. 220, no. 7, pp. 643–654, Oct. 2006, doi: 10.1243/09576509JPE306.

[68] J. Wang, S. Q. Shi, and K. Liang, "Comparative Life-cycle Assessment of Sheet Molding Compound Reinforced by Natural Fiber vs. Glass Fiber."

[69] "WindEurope–Cefic–EuCIA. Accelerating Wind Turbine Blade Circularity. White Paper.," 2020.

[70] P. Belton, "What happens to all the old wind turbines? - BBC News." .

[71] "IATA - Aircraft Decommissioning." .

[72] C. V. Amaechi, C. O. Agbomerie, E. O. Orok, and J. Ye, "Economic Aspects of Fiber Reinforced Polymer Composite Recycling," *Encycl. Renew. Sustain. Mater.*, pp. 377–397, Jan. 2020, doi: 10.1016/B978-0-12-803581-8.10738-6.

[73]   S. Job, "Recycling composites commercially," *Reinf. Plast.*, vol. 58, no. 5, pp. 32–38, Sep. 2014, doi: 10.1016/S0034-3617(14)70213-9.

[74]   Y. Liu, M. Farnsworth, and A. Tiwari, "A review of optimisation techniques used in the composite recycling area: State-of-the-art and steps towards a research agenda," *J. Clean. Prod.*, vol. 140, pp. 1775–1781, Jan. 2017, doi: 10.1016/J.JCLEPRO.2016.08.038.

[75]   G. Marsh, "What's to be done with 'spent' wind turbine blades?," *Renew. Energy Focus*, vol. 22–23, pp. 20–23, Dec. 2017, doi: 10.1016/J.REF.2017.10.002.

[76]   P. Liu and C. Y. Barlow, "Wind turbine blade waste in 2050," *Waste Manag.*, vol. 62, pp. 229–240, Apr. 2017, doi: 10.1016/J.WASMAN.2017.02.007.

[77]   C. V. Amaechi, C. O. Agbomerie, A. Sotayo, F. Wang, X. Hou, and J. Ye, "Recycling of Renewable Composite Materials in the Offshore Industry," *Encycl. Renew. Sustain. Mater.*, pp. 583–613, 2020, doi: 10.1016/B978-0-12-803581-8.11445-6.

[78]   "Johnson to ban gas car sales by 2030 in UK 'green revolution.'" .

[79]   S. Gharde and B. Kandasubramanian, "Mechanothermal and chemical recycling methodologies for the Fibre Reinforced Plastic (FRP)," *Environ. Technol. Innov.*, vol. 14, p. 100311, May 2019, doi: 10.1016/J.ETI.2019.01.005.

[80]   A. Jacob, "Composites can be recycled," *Reinf. Plast.*, vol. 55, no. 3, pp. 45–46, May 2011, doi: 10.1016/S0034-3617(11)70079-0.

[81]   A. Jacob, "Recycling composites," *Reinf. Plast.*, vol. 55, no. 3, p. 3, May 2011, doi: 10.1016/S0034-3617(11)70037-6.

[82]   G. Oliveux, L. O. Dandy, and G. A. Leeke, "Current status of recycling of fibre reinforced polymers: Review of technologies, reuse and resulting properties," *Progress in Materials Science*, vol. 72. Elsevier Ltd, pp. 61–99, Jul. 2015, doi: 10.1016/j.pmatsci.2015.01.004.

[83]   J. Thomason, P. Jenkins, and L. Yang, "Glass Fibre Strength—A Review with Relation to Composite Recycling," *Fibers 2016, Vol. 4, Page 18*, vol. 4, no. 2, p. 18, May 2016, doi: 10.3390/FIB4020018.

[84]   "WindEurope - the voice of the wind energy industry." .

[85]   M. Holmes, "Recycled carbon fiber composites become a reality," *https://doi.org/10.1016/j.repl.2017.11.012*, vol. 62, no. 3, pp. 148–153, Nov. 2021, doi: 10.1016/J.REPL.2017.11.012.

[86]   O. Zabihi *et al.*, "A Sustainable Approach to the Low-Cost Recycling of Waste Glass Fibres Composites towards Circular Economy," *Sustain. 2020, Vol. 12, Page 641*, vol. 12, no. 2, p. 641, Jan. 2020, doi: 10.3390/SU12020641.

[87] "Samsung invests in recyclable composites," *Reinf. Plast.*, vol. 59, no. 2, p. 70, Mar. 2015, doi: 10.1016/J.REPL.2015.01.026.

[88] W. Alabiso and S. Schlögl, "The Impact of Vitrimers on the Industry of the Future: Chemistry, Properties and Sustainable Forward-Looking Applications," *Polym. 2020, Vol. 12, Page 1660*, vol. 12, no. 8, p. 1660, Jul. 2020, doi: 10.3390/POLYM12081660.

[89] "ETIPWind (2019) How wind is going circular: blade recycling.," 2019. .

[90] "Accelerating Wind Turbine Blade Circularity | WindEurope." .

[91] L. Mantzos and p Capros, "EUROPEAN ENERGY AND TRANSPORT Scenarios on energy efficiency and renewables," 2006.

[92] "GLOBAL WIND 2006 REPORT ," *GLOBAL WIND ENERGY COUNCIL* . .

[93] "Renewable Power Generation Costs in 2019," */publications/2020/Jun/Renewable-Power-Costs-in-2019*.

[94] "Renewable Energy Statistics 2019," */publications/2019/Jul/Renewable-energy-statistics-2019*.

[95] C. Kost, S. Shammugam, V. Jülch, H.-T. Nguyen, and T. Schlegl, "LEVELIZED COST OF ELECTRICITY RENEWABLE ENERGY TECHNOLOGIES," 2018.

[96] "Renewable Power Generation Costs in 2018," */publications/2019/May/Renewable-power-generation-costs-in-2018*.

[97] J. Aldersey-Williams and T. Rubert, "Levelised cost of energy – A theoretical justification and critical assessment," *Energy Policy*, vol. 124, pp. 169–179, Jan. 2019, doi: 10.1016/j.enpol.2018.10.004.

[98] "Renewable Capacity Statistics 2018," */publications/2018/Mar/Renewable-Capacity-Statistics-2018*.

[99] M. I. Blanco, "The economics of wind energy," *Renewable and Sustainable Energy Reviews*, vol. 13, no. 6–7. Pergamon, pp. 1372–1382, Aug. 2009, doi: 10.1016/j.rser.2008.09.004.

[100] L. Petersen, " In Search of the Wind Energy Potential," *J. Renew. Sustain. Energy*, 2017, doi: 10.1063/1.4999514.

[101] "Full Load Hour - an overview | ScienceDirect Topics," *Offshore Wind Farms*, 2016. .

[102] P. Bortolotti *et al.*, "A Detailed Wind Turbine Blade Cost Model," 2019. Accessed: Apr. 14, 2021. [Online]. Available: www.nrel.gov/publications.

[103] "E3D Launches SuperVolcano HotEnd Boasting 11x the Volumetric Throughput of V6 | All3DP." https://all3dp.com/4/e3d-announces-launch-supervolcano-hotend-offering-

11x-volumetric-throughput-v6/ (accessed Feb. 28, 2022).

[104] J. Hinkley, N. Johnston, and T. O'Brien, "Interlaminar Fracture Toughness of Thermoplastic Composites," *Adv. Thermoplast. Matrix Compos. Mater.*, pp. 251-251–13, Dec. 1989, doi: 10.1520/STP24606S.

[105] N. H. Nash, T. M. Young, P. T. McGrail, and W. F. Stanley, "Inclusion of a thermoplastic phase to improve impact and post-impact performances of carbon fibre reinforced thermosetting composites — A review," *Mater. Des.*, vol. 85, pp. 582–597, Nov. 2015, doi: 10.1016/J.MATDES.2015.07.001.

[106] K.-Y. Kim, L. Ye, and K.-M. Phoa, "Interlaminar Fracture Toughness of CF/PEI and GF/PEI Composites at Elevated Temperatures," *Appl. Compos. Mater. 2004 113*, vol. 11, no. 3, pp. 173–190, May 2004, doi: 10.1023/B:ACMA.0000026586.12629.7E.

[107] J. Howes, A. Loos, and J. Hinkley, "The Effect of Processing on Autohesive Strength Development in Thermoplastic Resins and Composites," *Adv. Thermoplast. Matrix Compos. Mater.*, pp. 33-33–17, Dec. 1989, doi: 10.1520/STP24593S.

[108] E. Akca and A. Gursel, "A review on the matrix toughness of thermoplastic materials," *Period. Eng. Nat. Sci.*, vol. 3, no. 2, Aug. 2015, doi: 10.21533/PEN.V3I2.52.

[109] H. Parton and I. Verpoest, "In situ polymerization of thermoplastic composites based on cyclic oligomers," *Polym. Compos.*, vol. 26, no. 1, pp. 60–65, Feb. 2005, doi: 10.1002/PC.20074.

[110] C. Yan, L. Liu, Y. Zhu, H. Xu, and D. Liu, "Properties of polymerized cyclic butylene terephthalate and its composites via ring-opening polymerization," *https://doi.org/10.1177/0892705717697774*, vol. 31, no. 2, pp. 181–201, Mar. 2017, doi: 10.1177/0892705717697774.

[111] T. Abt and M. Sánchez-Soto, "A Review of the Recent Advances in Cyclic Butylene Terephthalate Technology and its Composites," *http://dx.doi.org/10.1080/10408436.2016.1160820*, vol. 42, no. 3, pp. 173–217, May 2016, doi: 10.1080/10408436.2016.1160820.

[112] S. Pillay, U. K. Vaidya, and G. M. Janowski, "Effects of moisture and UV exposure on liquid molded carbon fabric reinforced nylon 6 composite laminates," *Compos. Sci. Technol.*, vol. 69, no. 6, pp. 839–846, May 2009, doi: 10.1016/J.COMPSCITECH.2008.03.021.

[113] K. van Rijswijk, J. J. E. Teuwen, H. E. N. Bersee, and A. Beukers, "Textile fiber-reinforced anionic polyamide-6 composites. Part I: The vacuum infusion process," *Compos. Part A Appl. Sci. Manuf.*, vol. 40, no. 1, pp. 1–10, Jan. 2009, doi: 10.1016/J.COMPOSITESA.2008.03.018.

[114] P. Ó Máirtín, P. McDonnell, M. T. Connor, R. Eder, and C. M. Ó Brádaigh, "Process

investigation of a liquid PA-12/carbon fibre moulding system," *Compos. Part A Appl. Sci. Manuf.*, vol. 32, no. 7, pp. 915–923, Jul. 2001, doi: 10.1016/S1359-835X(01)00005-7.

[115] L. Zingraff, V. Michaud, P. E. Bourban, and J. A. E. Månson, "Resin transfer moulding of anionically polymerised polyamide 12," *Compos. Part A Appl. Sci. Manuf.*, vol. 36, no. 12, pp. 1675–1686, Dec. 2005, doi: 10.1016/J.COMPOSITESA.2005.03.023.

[116] "Thermoplastic Wind Blades: To be or not? | CompositesWorld." .

[117] K. van Rijswijk and H. E. N. Bersee, "Reactive processing of textile fiber-reinforced thermoplastic composites – An overview," *Compos. Part A Appl. Sci. Manuf.*, vol. 38, no. 3, pp. 666–681, Mar. 2007, doi: 10.1016/J.COMPOSITESA.2006.05.007.

[118] R. E. Murray, D. Swan, D. Snowberg, D. Berry, R. Beach, and S. Rooney, "Manufacturing a 9-meter thermoplastic composite wind turbine blade," *32nd Tech. Conf. Am. Soc. Compos. 2017*, vol. 1, no. December, pp. 29–43, 2017, doi: 10.12783/asc2017/15166.

[119] "Elium® resin: a disruptive innovation in the world of composites?" .

[120] R. E. Murray *et al.*, "Structural validation of a thermoplastic composite wind turbine blade with comparison to a thermoset composite blade," *Renew. Energy*, vol. 164, pp. 1100–1107, Feb. 2021, doi: 10.1016/J.RENENE.2020.10.040.

[121] D. S. Cousins, Y. Suzuki, R. E. Murray, J. R. Samaniuk, and A. P. Stebner, "Recycling glass fiber thermoplastic composites from wind turbine blades," *J. Clean. Prod.*, vol. 209, pp. 1252–1263, 2019, doi: 10.1016/j.jclepro.2018.10.286.

CATAPULT
Offshore Renewable Energy

GLASGOW

ORE Catapult
Inovo
121 George Street
Glasgow
G1 1RD

+44 (0)333 004 1400

BLYTH

National Renewable
Energy Centre
Offshore House
Albert Street, Blyth
Northumberland
NE24 1LZ

+44 (0)1670 359555

LEVENMOUTH

Fife Renewables Innovation
Centre (FRIC)
Ajax Way
Leven
KY8 3RS

+44 (0)1670 357649

GRIMSBY

O&M Centre of Excellence
ORE Catapult, Port Office
Cleethorpe Road
Grimsby
DN31 3LL

+44 (0)333 004 1400

ABERDEEN

Subsea UK
30 Abercrombie Court
Prospect Road, Westhill
Aberdeenshire
AB32 6FE

07436 389067

CORNWALL

Hayle Marine Renewables
Business Park
North Quay
Hayle, Cornwall
TR27 4DD

+44 (0)1872 322 119

PEMBROKESHIRE

Marine Energy Engineering
Centre of Excellence (MEECE)
Bridge Innovation Centre
Pembrokeshire Science
& Technology Park
Pembroke Dock, Wales
SA72 6UN

+44 (0)333 004 1400

CHINA

11th Floor
Lan Se Zhi Gu No. 15
Ke Ji Avenue,
Hi-Tech Zone
Yantai City
Shandong Province
China

+44 (0)333 004 1400

LOWESTOFT

OrbisEnergy
Wilde Street
Lowestoft
Suffolk
NR32 1XH

01502 563368